UNIVERSITY OF LIVERPOOL

Development and comparison of hepatic spheroids and electrospun scaffolds for use in high throughput screening applications

Thesis submitted in accordance with the requirements of the University of Liverpool for the degree of Doctor in Philosophy by

Jonathan David Temple

September 2022

Acknowledgments

I would like to thank my supervisors for their time and support throughout my PhD. Dr Raphaël Lévy for his support in Liverpool and Dr Gary Allenby for his support whilst at the industrial partner. I would also like to thank Dr Rob Workman for his guidance whilst I was at the industrial partner.

My friend and colleague Dr Dominic Byrne deserves a special mention as, although it is not his field, he was an extremely valuable mentor both in the lab and outside. He supported me through easy and tough times and I am extremely grateful to him. Of the same note Dr Anne Herrmann was also a huge help when producing the stable cell lines and working with the luciferase assays.

My final and most influential thanks is to my fiancée Laura, she has supported me throughout the whole process and has had to help me through the highs and the lows. I would have not completed this PhD had it not been for her amazing attitude and continued support.

Abstract

Spheroid models are the current gold standard for the use of 3D liver cultures for high-throughput screening due to their ability to be cultured for longer time periods than 2D cells, their simple production and limited cost. However, as spheroids grow over a certain size (~300 µm), they compact in the centre resulting in a region where no nutrients or oxygen can reach. This means that reagents for imaging or biochemical assays are also unable to penetrate to these cells resulting in a loss of information. As the spheroid grows, the hypoxic core also expands making screening and toxicity testing inaccurate, especially over time, as large amounts of necrosis and apoptosis are already present.

Growing cells on porous 3D scaffolds offers a potential solution to these problems. Here we compare one type of scaffold (randomly orientated electrospun Mimetix® Poly-L-lactic acid) with 3D spheroid cultures. The 4 µm diameter fibres create pore sizes of 15-30 µm giving the scaffold an overall porosity of 80%, allowing nutrients, reagents and gases better penetration to the cells in 3D.

The comparison of two very different 3D cultures is rarely performed as it is difficult to accurately normalise between the cultures, making determining the most *in-vivo* like 3D cell culture an extremely difficult task. Traditional cell counting techniques do not transfer well into 3D so most research utilise proxy measures such as total protein to estimate the number of cells and use this to normalise between cultures, conditions and time points. Here we assess the accuracy of some of these cell number proxies and find that using a stable HepG2 cell line that expresses luciferase as the most accurate.

Using this stable HepG2 we compare the health and function of these cells grown in 2D, 3D spheroids and 3D scaffolds. The hypothesis of this work was to determine if culturing cells in scaffold cultures overcame the issues faced by 3D spheroid cultures and is a collaborative effort between the University of Liverpool and Aurelia Bioscience and was funded by the BBSRC. The scaffold material

was purchased from the Electrospinning company. We demonstrate that the scaffold cultures improve both the viability and function of the cells compared to those in spheroids and demonstrate the potential of these scaffolds for high-throughput screening assay.

Publications, awards and presentations

PUBLICATIONS

PUBLISHED

Temple, J., Velliou, E., Shehata, M., & Lévy, R. (2022). Current strategies with implementation of three-dimensional cell culture: the challenge of quantification. Interface Focus, 12(5). https://doi.org/10.1098/RSFS.2022.0019

IN PREPARATION

Temple, J., Velliou, E., Gupta2, P., Lévy, R. Addressing the challenges of biochemical analysis faced by 3D cells cultures

AWARDS

3DBioNet Conference (September 2020) - Overview of the challenges and opportunities of 3D Cell Culture - First place speaker award

3DBioNet Conference (January 2020) - Overview of the challenges and opportunities of 3D Cell Culture - Second Place Poster Award

NLD DTP Conference (June 2018) - Development of 3-dimensional cell cultures for integrated modelling of liver cells and tissues - First Place Speaker Award

University of Liverpool, CCI Imaging Award (December 2017) – First place

PRESENTATIONS

UCL 3D models for cancer Conference (July 2021) – Talk - “Evaluation of spheroid and scaffold-based liver cultures for the development of a reliable model for the prediction of drug hepatotoxicity”

ELRIG, drug discovery conference (February 2021) - Poster Presentation - “Development and comparison of hepatic spheroids and electrospun scaffolds for use in high content screening applications”,

3DBioNet Conference (September 2020) – Talk - “3D cell culture: With great power comes great responsibility”

3DBioNet Conference (January 2020) - Poster Presentation - “Development and comparison of hepatic spheroids and electrospun scaffolds for use in high content screening applications”,

ACTC Conference (December 2018) – Talk - “Imaging of 3D cell cultures: challenges and opportunities”

NLD DTP Conference (June 2018) – Talk - “Development of 3-dimensional cell cultures for integrated modelling of liver cells and tissues”

Abbreviations

ATP	Adenosine triphosphate
ADR	Adverse drug reactions
BSA	Bovine serum albumin
CO_2	Carbon dioxide
CYP	Cytochrome P450
DILI	Drug-Induced Liver Injury
DMSO	Dimethyl sulfoxide
DMEM	Dulbecco's Modified Eagle Medium
DNA	Deoxyribonucleic acid
ECM	Extracellular matrix
ELISA	Enzyme-linked immunosorbent assay
FBS	Fetal bovine serum
g	Grams
GAPDH	Glyceraldehyde-3-Phosphate Dehydrogenase
H&E	Hematoxylin and eosin
HMEC	Human Mammary Epithelial Cells
IPSC	Induced pluripotent stem cells
kD	kilo Daltons
L	Litre
LDH	Lactate dehydrogenase
LOT	Liquid-overlay technique
LSEC	Liver sinusoidal endothelial cells
µ-	Micro
m-	Milli
M	Molar
Min	Minute
MW	Molecular weight
NPC	Non-parenchymal cells
O_2	Oxygen
PBS	Phosphate buffered saline
PDMS	Polydimethylsiloxane
PCR	Polymerase chain reaction
PEI	Polyethylenimine
RFP	Red fluorescent protein
RO	Reverse osmosis
rpm	revolutions per minute
RT	Room temperature
S	Seconds
SDS	Sodium dodecyl sulfate
TBST	Tris-Buffered Saline with 0.05 % Tween20
TMRM	Tetramethylrhodamine, Methyl Ester, Perchlorate
ULA	Ultra-low adherence
2D	Two dimensional
3D	Three dimensional

Chapter 1 - Introduction

Chapter 2 – Materials and methods

Chapter 3 - Optimisation of spheroid and scaffold culture

Chapter 1 - Introduction

1.1 Introduction

For the last four decades, 2D cell culture has been the basis for a large array of scientific research (Paul, 1970). It enables the study of cells under controlled conditions, outside of their natural environment and offers a high degree of tunability. The problem however, is that cells *in-vivo* do not grow in a two-dimensional state and it is clear that this difference has effects on cell signalling and fate (Haycock, 2011). 3D cell culture therefore offers a platform where cells can be grown to better mimic their natural environment leading to more physiological responses.

One of the main advantages of 3D cell culture is the potential exposure of the whole cell surface to relevant biochemical cues. This better allows the activation of signalling pathways as well as other cellular process such as transcriptional expression and apoptosis (Haycock, 2011). It enables cells to behave akin to those in *in-vivo* conditions in terms of cellular communication, cellular functions and the development of the extracellular matrix (ECM). 3D cultures, produce a more accurate representation of the cellular composition of tissues permitting the study of tumour characteristics such as dormancy, hypoxia and anti-apoptotic behaviour. 3D cell culture also enables cells to adopt a polarity, like *in-vivo*, something that is only partially achievable in 2D (Bissell et al., 2002; Kleinman et al., 2003; Suparna, 2014).

Drug-induced liver injury (DILI) is a major concern for both the pharmaceutical and health industries and is the major reason for drug withdrawal as well as preventing drug approval. Current *in-vitro* models only predict between 60-70% hepatotoxins while animal models are only predicting around 50% (Olsen & Whalen, 2009; Serras et al., 2021; Vorrink et al., 2018; Xu et al., 2008). The main reasons for this poor prediction include low liver functionality as well as lower drug metabolising enzyme expression. It is therefore important to develop a liver model that improves these factors to a level akin to those *in-vivo*. 3D cell culture has shown promising advances in this area, due to its

ability to better represent the *in-vivo* environment, including maintaining the hepatic properties of primary cells, improving cytochrome p450 enzyme levels and improving the prediction of hepatotoxicity (Kammerer, 2021; Shinozawa et al., 2021; Westerink & Schoonen, 2007).

1.2 The Liver

The liver is a vital organ, situated in the abdominal-pelvis region, weighing approximately 1.5 kg (around 1.4 kg in females and 1.8 kg in males). It has a number of important functions including bile formation, metabolism of compounds (xenobiotics, cholesterol, ammonia, bilirubin, carbohydrates fatty acids and lipoproteins), storing glycogen and vitamins, producing a number of hormones and urea and albumin synthesis (Bacon et al., 2006; Kuntz & Kuntz, 2008).

The liver consists of two lobes, separated by the falciform ligament with the right being the larger of the two. It receives 80% of its blood from the portal vein via the spleen and intestines and the other 20 % from the hepatic artery; they along with bile ducts make up a portal triad (Krishna, 2013; Sibulesky, 2013). Each of the liver lobes is made up of around one million functional units called lobules or hepatic acini which are hexagonal in shape with a portal triad located at every corner (Godoy et al., 2013; Sibulesky, 2013). Sinusoids, which are capillaries with permeable pores, connect the portal triads to the hepatic central vein at the core allowing highly oxygenated blood and nutrient rich blood to mix and supply the cells. These pores are between 0.1 µm and 0.3 µm allowing molecules like gases, proteins, toxins and hormones to diffuse towards the hepatocytes for processing. This structure also results in the formation of an oxygen gradient as the oxygen is consumed and gives the lobules three defined zones, zone 1 (periportal), zone 2 (midzonal) and zone 3 (pericentral); with the hepatocytes in each zone having different liver functionality (Figure 1.1) (Cox et al., 2020; Godoy et al., 2013). It is for this reason that many researchers in the field utilise 3D spheroid models as they naturally mimic the zonation of the lobules.

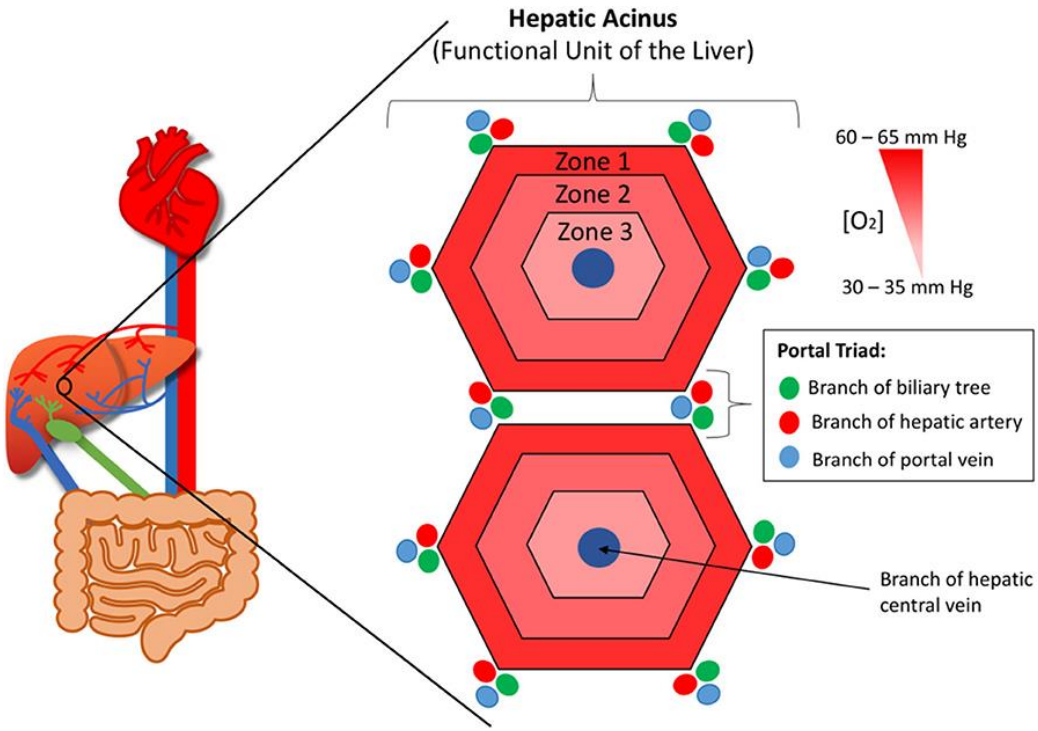

Figure 1.1. Schematic of the functional lobule of the liver demonstrating the position of the portal triad and the zonation of each unit. At each corner of every lobule is a portal triad consisting of branches of the biliary tree, hepatic artery and portal vein and at the centre of the lobule is a branch of the portal vein. This structure creates an oxygen gradient across the lobule with zone 1 having the highest concentration and zone 3 the lowest (Cox et al., 2020).

1.2.1 Liver cells and their functions

The liver is primarily made up of four cell types: hepatocytes, liver sinusoidal endothelial cells (LSEC), Kupffer cells and stellate cells (Figure 1.2). Hepatocytes are the parenchymal cells of the liver and make up 60% of the total cell number; carrying out the majority of the metabolic functions (Bacon et al., 2006; Kuntz & Kuntz, 2008). They are functionally polarised with different transporters expressed between the basolateral membrane and the apical membrane. They line the liver sinusoids and are connected to capillaries on either side allowing them to control the movement of substances in and out of the blood. They express tight junctions and bile canaliculi, removing toxins and other unwanted substances and excreting them into the bile duct. They also express most of the circulating plasma proteins including albumin and protease inhibitors, releasing them into the blood (Cox et al., 2020; Godoy et al., 2013). Their polarised nature also allows them to control homeostasis

of several important molecules meaning they express a variety of enzymes, including those involved in phase I and phase II metabolism whilst also regulating molecules such as vitamins A and D, haem, glucose/glycogen and cholesterol (Bacon et al., 2006; Gissen & Arias, 2015; Godoy et al., 2013; Underhill & Khetani, 2018).

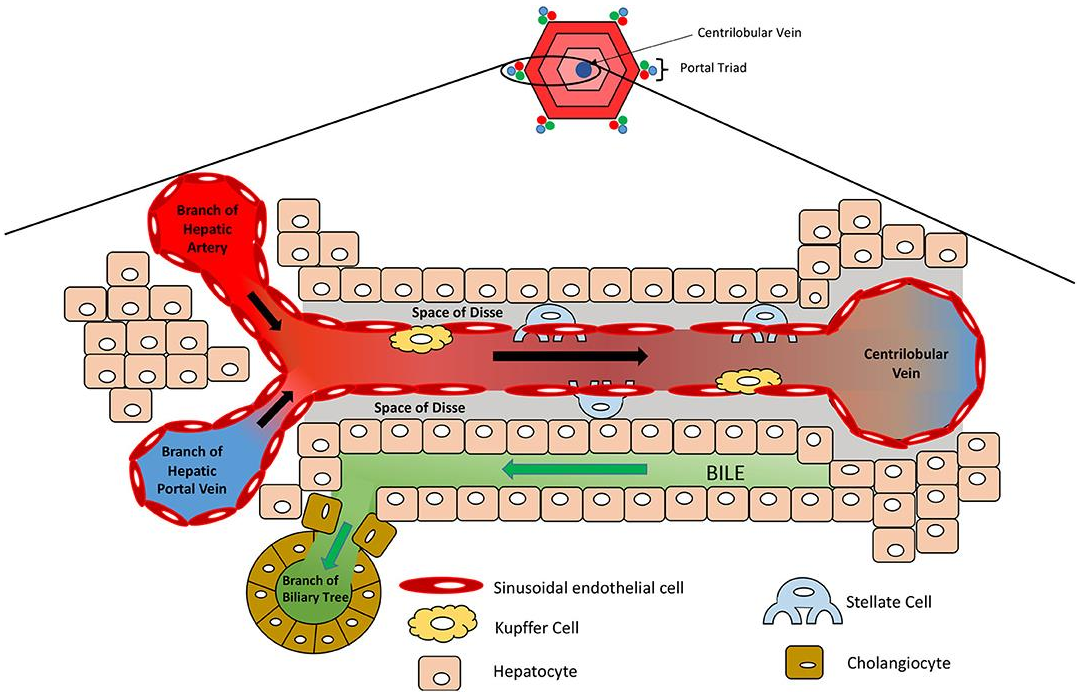

Figure 1.2 Microanatomy of liver sinusoid. Blood enters from the hepatic artery and portal vein, which is both oxygen and nutrient rich supplying nutrients and waste compounds to the cells of the liver for processing (Cox et al., 2020).

LSEC are the second largest cell population in the liver (19%). They line the capillaries and regulate substances between the blood and the liver. They play important roles in the receptor-mediated clearance of foreign compounds, regulate inflammation and immune response (Godoy et al., 2013; Kmieć, 2001; Limmer & Knolle, 2001). Kupffer cells are the resident macrophage in the liver making up 15% of the population found in the micro-vessels of the sinusoids. They have functions in engulfing bacteria and cell debris as well as in liver regeneration (Bacon et al., 2006; Wheeler, 2003). The fourth cell type, Stellate cells, make up around 6% of the cell population. These cells are

quiescent in the healthy liver with their main function being the storage of vitamin A. Once activated however, are involved in the formation of scar tissue during fibrosis (Bacon et al., 2006; Kordes et al., 2009).

1.2.2 Sources of liver cells used in *in-vitro* research

There are many cell types that are used for *in-vitro* liver studies, including primary hepatocytes, HepG2/C3A, HepaRG and induced pluripotent stem cells (Table 1.1). The gold standard for liver studies, primary hepatocytes, can be difficult to obtain, difficult to expand in culture and are often acquired from diseased livers making them less reliable when this is the case (Cho et al., 2008). They also lose hepatic function over 24-72 hours when cultured in 2D, reducing sensitivity and making repeat dose studies unreliable (Godoy et al., 2013; Xu et al., 2008). Animal hepatocytes are more readily available however differences between metabolism and pharmacokinetics make their use unreliable for the testing of human hepatotoxins (Godoy et al., 2013).

Adult somatic cells can be reprogrammed into Induced pluripotent stem cells (iPSCs) with the overexpression of key reprogramming genes, including OCT4, SOX2, NANOG, KLF4 and LIN28. Utilising specific cell culture media, supplements and growth factors somatic cell can be differentiated into any cell type of the ectoderm, endoderm or mesoderm whilst offering a limitless supply of cells. The problem, however, is that many of the liver models using these cells have low levels of phase I and phase II enzymes (Guguen-Guillouzo et al., 2010; H. Liu et al., 2010; Medine et al., 2013). Technical advances in differentiation protocols as well as organoid culture systems have improved the ability of iPSC for liver modelling, however, differences in drug metabolism are still a limiting factor (Sampaziotis et al., 2015; Wong et al., 2018).

Embryonic stem cell derived hepatocytes are another attractive platform to study liver biology, however, like iPSCs lack critical *in-vivo* characteristics such as cell polarity, which plays an important role in the functionality of hepatocytes.

HepG2 cells are extremely well characterised and have been used in many liver studies due to their robust morphological and functional differentiation. HepG2 cells display polarity, particularly when grown in trans wells or 3D cultures, and are able to carry out biotransformation of xenobiotic compounds and have no p53 mutations which enables them to activate DNA damage response, induce growth arrest and initiate apoptosis. When compared with primary human hepatocytes the expression of genes involved in cell cycle regulation, transcription, transportation and signal transduction were higher in HepG2, however, they show lower levels of transcription of genes related to cell death, lipid metabolism and xenobiotic metabolism (Gomez-Lechon et al., 2008; Guo et al., 2011). HepaRG, although not as well characterised as the HepG2 cells, have been shown to have polarised expression of drug transporters, high metabolic activity and high level of Phase I and Phase II drug metabolising enzymes (Aninat et al., 2006; Kanebratt & Andersson, 2008; Le Vee et al., 2013). However, HepaRG have demanding culture requirements including extended culture in the presence of DMSO to cause differentiation into the hepatocyte-like phenotype (Klein et al., 2014).

Table 1.1 Comparison of different liver cell sources used *in-vitro*.

	Advantages	**Disadvantages**
Human liver cell lines (Gerets et al., 2012; Sirenko et al., 2016)	Good availability Easy to expand Well characterised	Low drug enzyme activity Different expression of key genes/proteins
Stem cell-derived hepatocyte like cells (Gao & Liu, 2017; Hay et al., 2008; Takayama et al., 2014)	Good availability Enables personalised medicine Can establish disease models	Difficult/incomplete hepatocyte differentiation Lack of standardised differentiation protocols
Primary hepatocytes (Bell et al., 2018)	Similar to *in-vivo* expression Possible to cryo-preserve	Short viability in 2D Lack of human tissue availability Cryo-preservation recovery can be difficult and effect function
Co cultures of hepatocytes and non-parenchymal cells (Lazzari et al., 2018; Messner et al., 2013; Proctor et al., 2017)	Improved hepatocyte functionality More akin to *in-vivo* environment Allows the study of more disease states	Increased complexity Seeding and cell ratio issues Lack of standardisation

1.3 Drug-induced liver injury

Adverse drug reactions (ADR) are a major concern for both the pharmaceutical and health industries, by preventing drug approval and causing drug withdrawal. ADRs are grouped into 6 types, classified as A-F. Type A ADR are caused by the primary pharmacology of the drug making them common and relatively predictable. Types B-F, however, although less frequent, do have increased complexity and can be the result of several different factors. Type B for example are unrelated to the therapeutic action of the drug and type E only occur after the removal of the drug. This results in difficulties predicting and treating these forms of ADR (Edwards & Aronson, 2000).

Drug-induced liver injury (DILI) is a common adverse drug reaction that is accountable for around 50% of acute liver failure (Cox et al., 2020; Norris et al., 2008). Risk factors for DILI include drug dosage, drug lipophilicity, the extent to which the drug is metabolised and even genetic predispositions to DILI for specific drugs. There is also mixed evidence to support the effect of individual traits such as age, sex and chronic liver disease in the development of DILI (Leise et al., 2014).

DILI is the leading cause for the removal of drugs from the market as well as hindering drug approval during pre-clinical testing, costing pharmaceutical industries both time and money. It is therefore essential to have accurate and reliable *in-vitro* and *in-vivo* models for the detection of ADR early in drug development. Current gold standard in vitro models can only detect 60-70% of human hepatotoxins with animal models only predicting around 50% (Olsen & Whalen, 2009; Serras et al., 2021; Vorrink et al., 2018; Xu et al., 2008). 3D cell culture models offer huge potential here as they offer a model that is more akin to *in-vivo* with an improved ability to predict hepatotoxicity. However, the main limitation is a lack of standardisation along with high variability. It is also unclear which system is best for which application as this depends dramatically on the intended purpose and desired readouts.

1.4 3D cell culture

The importance of 3D cell culture techniques to mimic *in-vivo* conditions has been known since the 1980s but it has not been until the last decade with the advancement of both understanding, biomaterial development and technology that the field has taken off (Bissell et al., 1982; Simian & Bissell, 2017). The increase in research has led to a variety of 3D culture systems that have been developed to make cell cultures more representative of physiological conditions including spheroids; sandwich cultures and cells growing on hydrogels or polymer scaffolds; most of which can be made dynamic by incorporation into bioreactors or put under flow. Growing cells is a key activity of most research laboratories across the world and 2D cell culture is still the benchmark for most fields

including pharmaceutical testing (Adcock et al., 2015; Asthana et al., 2018; Chim & Mikos, 2018; Totti et al., 2017). This is in part due to the lack of established robust and reproducible protocols and the difficulties in attaining accurate biochemical readings and images in 3D culture systems. The huge variation in both size and structural and biochemical complexity between different 3D systems (Figure 1.3) further complicates the task of comparing their performance in replicating the physiological environment.

1.4.1 Types of 3D cell cultures

The 3D cell culture technologies can be broadly grouped into scaffold-free and scaffold-based. The former relies on low adherence surfaces to encourage cells in suspension to aggregate through techniques including hanging drop, low adherence round bottom wells, and rotating cultures. These cultures self-organise, produce and organise their own extracellular matrix (ECM) just like *in-vivo* tissues and form extensive cell-to-cell contacts making them akin to the avascular *in-vivo* environment of organs including; the heart, liver, eye and pancreas (Lazzari et al., 2018; Polonchuk et al., 2017; Tong et al., 1990; Usui et al., 2018). The culturing of scaffold-free cultures is a simple and cheap process, even possible using Petri dishes (Del Duca et al., 2004; Knight & Przyborski, 2015) whilst being scaleable, enabling the mass production of spheroids of a uniform and controllable size for high-throughput applications. Scaffold free culture can also be readily analysed using microscopic techniques and finally can form a single spheroid per well removing the need to harvest after formation as well as making further analysis easier (Haycock, 2011; Knight & Przyborski, 2015; Tung et al., 2011). They do, however, offer little structural support or porosity to the cells for the diffusion of nutrients and oxygen. This hinders the use of these spheroids as oxygen has been reported to only diffuse 100-150 µm through tissue, therefore any spheroid above 300 µm is likely to have a hypoxic core (Asthana & Kisaalita, 2012). Whilst this hypoxic core may be problematic in larger spheroids, as the core expands and eventually becomes necrotic, this gradient of oxygen concentration mimics the oxygen gradient found in the liver lobules. Therefore, if the size of the spheroids can be controlled,

then growing liver cells in spheroids naturally recapitulates the liver *in-vivo* environment making them a powerful *in-vitro* model.

This problem of porosity can be resolved by growing the cells on specialist scaffolds that mimic the extracellular matrix of the tissues. Scaffold-based cultures, including hydrogels and polymer scaffolds, utilise a physical network to mimic the ECM of the tissue; providing a substrate for cells to interact with. These may be fabricated from synthetic or natural materials and are customisable in terms of shapes, size, and biomolecular cues to best mimic the structure of in-vivo tissue.

A stepping stone between 2D and 3D, sandwich cultures have been established for three decades (Dunn et al., 1989) whereby a 2D cell layer is placed between thin layers comprised of ECM proteins. They provided an early demonstration of the benefits of more complex culture systems, for example, hepatocyte activity and function were much more analogous to hepatocytes *in vivo* (Dunn et al., 1992; Jones et al., 2012; LeCluyse et al., 1994; Qiao et al., 2021).

Similar in architecture to sandwich cultures, hydrogels are water-swollen networks of crosslinked polymers, typically ECM components that completely suspend the cells in ECM offering them a 3D environment. These gels can be natural or synthetic, with natural hydrogels formed of proteins and ECM components such as collagen, chitosan or Matrigel (Kleinman & Martin, 2005; Pineda et al., 2013; Reis et al., 2012). They are known to be biocompatible, non-immunogenic and have been shown to enhance multiple cellular activities (Kleinman & Martin, 2005; Kuss et al., 2018; Nahmias et al., 2006). Synthetic gels are often composed of materials such as poly(ethylene glycol) (Kloxin et al., 2009; Phelps et al., 2012) or polyacrylamide (Pelham & Wang, 1997; Wen et al., 2014) which boast simple chemistry and robust manufacturing, whilst being highly customisable for further applications.

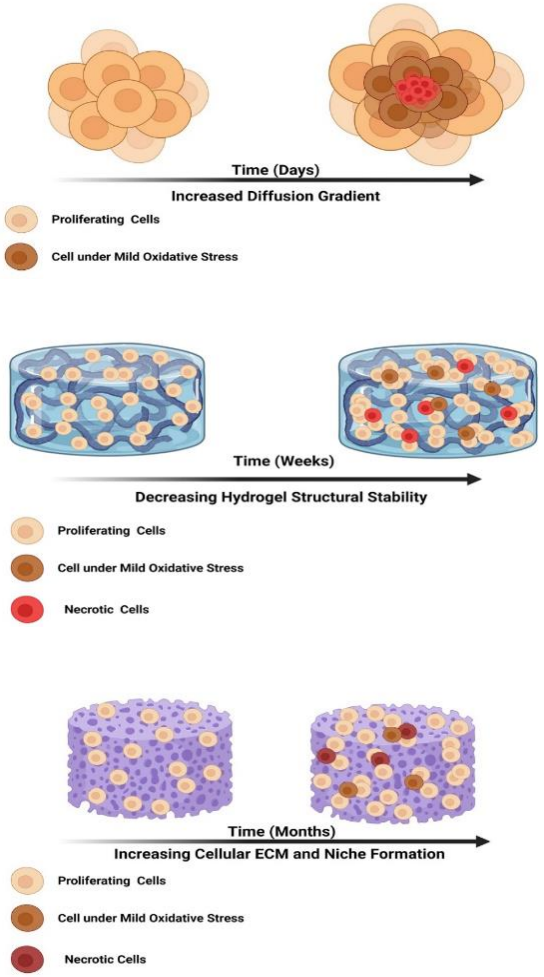

Figure 1.3. The heterogeneity of cells cultured in different 3D systems: Spheroids, Hydrogels and Scaffolds. Created using BioRender.

Polymer scaffolds can be made from both natural or synthetic materials and depending on their composition replicate different features of tissue ECM including internal organisation and mechanical stiffness. Polymeric scaffolds are fabricated through various methods such; as gas foaming, electrospinning, lyophilisation and 3D printing. Depending on the polymer and fabrication method selected, a variety of scaffolds with different internal organisation, pore size, geometry and overall elasticity can be generated. Typically, natural polymers lead to softer scaffolds and synthetic polymers to scaffolds with higher stiffness, including sponge-like structures. Overall, the versatility of biomaterials and fabrication techniques enables the generation of a wide range of structures with controlled properties that can mimic different tissues and diseases (Choi et al., 2010; Fierz et al.,

2008; Lee et al., 2008; Lewis et al., 2018; Munaz et al., 2016; Murphy et al., 2010; Salerno et al., 2010; Wishart et al., 2021). Polymer scaffold cultures potentially also offer being easier to manipulate and image whilst offering the potential for co-cultures, another area that has shown great promise in bettering the predictive capabilities of liver models (Kostadinova et al., 2013).

To improve these 3D cultures, both scaffold-free and scaffold cultures can be incorporated into bioreactors. Bioreactors exist in several designs; including spinning flasks, rotating walls, perfusion systems, capillary fibres and chip devices. They all aim to overcome one of the main limiting factors of other 3D culture systems, nutrient and gaseous exchange. The cells in these systems are typically under sheer stress, allowing a high mass transfer rate to be achieved throughout the cultures (Chung et al., 2006; Griffith & Swartz, 2006; Gutierrez & Crumpler, 2008). Bioreactors have been successfully implemented for a variety of cell types including; heart, muscle, liver, embryonic stem cells and mesenchymal stem cells (Burdick & Vunjak-Novakovic, 2009; Christoffersson et al., 2016; Cimetta et al., 2009; Figallo et al., 2007; Khodabakhshaghdam et al., 2021; Soldatow et al., 2013); whilst showing great potential in the toxicity testing of potential therapeutic drugs (Chao et al., 2009; Freyer et al., 2018; Novik et al., 2010).

Further to these different 3D cultures, to accurately study normal/disease phenotypes and heterogeneity, many are turning towards more complex 3D systems. The advances of culturing mini organs outside of the body have made it possible to use 3D culture techniques as an alternative to *in-vivo* models. These mini organ cultures, termed 'organoids', originate from a variety of sources including neonatal tissues, pluripotent/induced pluripotent stem cells, tissue biopsies and adult stem cells. The resulting organoids self-organise and recreate the physiology of organs, as well as accurately represent clinical diseases in remarkable detail (Huch & Koo, 2015).

Organoids initially were used to model tissue development and stem cell fate. Genes of interest were marked or removed, and the resulting organoids followed in real time to identify lineage specifications and cell fates (Clevers, 2016; Engel et al., 2020; Fusco et al., 2019; Lancaster &

Knoblich, 2014). Today organoids can be used in many experimental approaches developed for cell lines. The ability to use organoids, especially derived from human tissues, for an array of applications including; disease modelling, regenerative medicine, drug discovery and personalised medicine, has received widespread attention.

With such huge differences in geometry and complexity, analysing and comparing these models is daunting and complicated. Yet, systematic benchmarking of these approaches is a necessity or the field risks stagnation, where new systems are developed for the sake of novelty rather than for the potential benefits they bring to the understanding and modelling of biology. It is also a necessity as these cultures come with experimental hurdles, from reproducible culture protocols to monitoring detailed biochemical information and high-quality cell imaging. Overall, for an accurate establishment of 3D cultures as pre-clinical models for drug or therapy screening, several challenges need to be overcome, particularly with respect to readouts from these systems. Some practical challenges that are generally faced in 3D cultures include: (i) Difficulty in extracting the cells from different biomaterial-based 3D constructs due to classic dissociation techniques being inefficient and are highly influenced by the structural complexity of the culture. (ii) Diffusional limitations and gradient formations of nutrients, gases, reagents, dyes and antibody solutions, which can lead to inaccurate results and problems with imaging. (iii) The inability to account for the number of cells within the culture as normal cell counting methods rely on obtaining a single cell suspension and other proxy measures may be influenced by the transition from 2D to 3D. A good overview of the challenges faced is demonstrated within the SWOT (strengths, weaknesses, opportunities and threats) analysis performed by Carragher *et al.*, (2018). Although specific to high-content analysis, all points are relevant to the field of 3D cell culture.

1.4.2 Hepatic 3D cell models suitable for high-throughput studies

High through-put screening is commonly used in the pharmaceutical industry for toxicity testing with the ideal cell culture being one that is simple and easy to culture yet reliable and fit for purpose.

These cultures can be subjected to a combination of imaging and biochemical analysis upon compound treatment to predict toxicity on a large scale.

Hepatic 3D cell cultures have shown improved hepatic capacity, increased sensitivity and accuracy to drug toxicity, attracting lots of interest in the field (Bell et al., 2018; Messner et al., 2013). The problem, however, is reliability and accuracy, along with the reduced ability to measure multiple readouts; hence why 2D primary hepatocyte cell cultures are still the gold standard for hepatotoxin testing in the pharmaceutical industry. With a large variety of 3D cell cultures now described in the scientific literature, not all are applicable to high throughput studies due to culture times; expense and complexity (Figure 1.4).

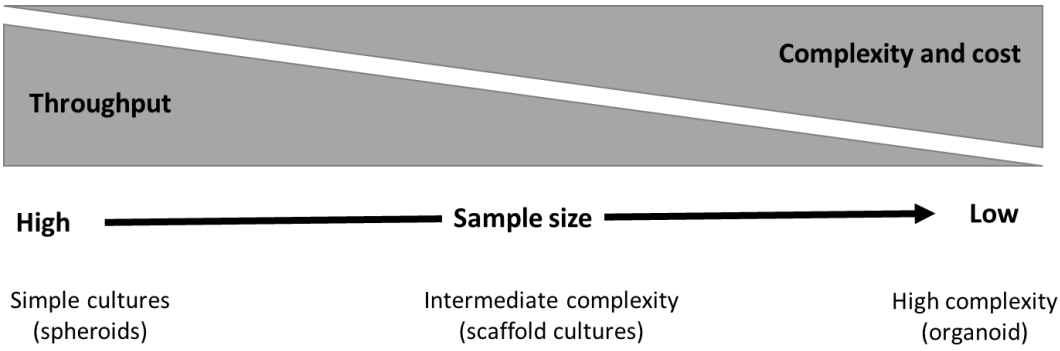

Figure 1.4. The balance between 3D model complexity with cost and throughput, representing the trade of between in-depth modelling of the *in-vivo* environment and speed.

Sandwich cultures are a bridge between 2D and 3D cultures as cells are cultured between two layers of extracellular matrix (ECM). Hepatocytes grown in sandwich cultures regain their natural polarity and develop proper basolateral and apical transporter expression along with expression of bile canaliculi. This makes them important models for hepatic clearance and bile acid related hepatotoxicity studies (Chatterjee et al., 2014; Yang et al., 2016; Zeigerer et al., 2017). The major limitation of these cultures, however, is that over time they develop cholestasis and bile canaliculi damage and therefore they are only a valuable tool for short-term studies (Bell et al., 2018; Zeigerer et al., 2017).

The most popular 3D culture for high throughput screening is spheroids due to their cheap and easy culture protocols, particularly in plate/well format. Once cultured they can be utilised in the well and rarely require manipulation. It is also possible to perform microscopic imaging whilst in the well by using clear bottom plates.

Spheroid cultures show increased urea, albumin and apolipoprotein B secretion, improved sensitivity to hepatotoxins and improved expression of genes related to drug, lipid and glucose metabolism (Bell et al., 2016; Bell et al., 2018; Mandon et al., 2019; Takahashi et al., 2015). Due to their improved hepatic function 3D liver spheroids have shown promise in studies of liver function, liver disease, such as cholestasis and viral hepatitis, and elucidating drug targets (Bell et al., 2016) .

Non-parenchymal cells can also be easily incorporated into spheroid cultures during initial seeding, further improving the model as they also have a key role in liver injury, improving the predictability of the models (Leite et al., 2016; Proctor et al., 2017).

The limitation of spheroid cultures is that the penetration of compounds, either drugs or biochemical reagents, is dramatically hindered due to their compact nature. Light penetration is also hindered, limiting the ability to extract all the information from the sample using high-content imaging.

Scaffold cultures offer a solution to this due to their increased porosity. They, like spheroids, have been shown to improve hepatic however, offer the potential to eliminate the diffusion limitations associated with spheroid cultures (Bate et al., 2021; Lewis et al., 2018; Schutte et al., 2011). Scaffold culture, however, is typically more expensive and time consuming and it can be difficult to populate scaffold material with cells (Asthana et al., 2018). Scaffold cultures can also face similar issues of light and compound penetration depending on their thickness and material, so it is important these factors are considered when deciding on the appropriate scaffold culture.

Other, more complex 3D cultures such as organoids and organ-on-a-chip devices are typically either too expensive or time consuming to culture for high throughput applications even though they may better predict hepatotoxicity. This, however, is likely where the field will move, possibly on a smaller scale, with some researchers like Shinozawa et al., (2021) already demonstrating the ability of using organoids in 384 well plate format for hepatotoxin testing.

1.4.3 Making the transition from 2D to 3D

(From published review article - Temple et al., 2022)

Is 3D better than 2D? Whilst this is often a starting argument, in the absence of a standardised criterion to distinguish 2D from 3D, it is useful to step back and consider the aim that our scientific community is trying to achieve: improve culture systems by making them more representative of the physiological environment. With this in mind, "2D" is a shorthand for traditional cell culture on petri dish whilst "3D" is any alternative culture system that gets us closer to that aim. This allows us to focus, not on the fraught question of whether a proposed system is 2D or 3D, but the extent to which it is representative of physiological or the pathological environment it is trying to recapitulate (Table 1.2). The comparison between models can then study cellular processes and tissue specific criteria such as; biomechanics, transport of small molecules, cell-to-cell interactions, ECM production and response to pharmacological agents. We suggest that such clarity of purpose in the development of new culture systems would help with side-by-side comparisons and reduce the risk that the field becomes inundated with systems that are ill defined and difficult to compare.

Table 1.2 The variability of key characteristics of cells growing in different environments.

	"2D" = growing on a flat surface (glass, plastic)	"3D" = anything more physiological than "2D"	Organoids	*In-vivo*
Diffusion	Unrestricted	Limited by culture system	Limited – no vascularisation	Vascularisation
Cell-to-cell interactions	Minimal – Side by side interactions	Increased number of interactions	Increased however similar to "3D"	Extensive
Cell physiology	*In vitro*	Highly variable depending on the culture type	Comparable to *in-vivo*	-
Cell shape	Long and flat	More akin to *in-vivo*	Comparable to *in-vivo*	Governed by location and function, highly variable
Proteome/Genome	Basic expression	Improved expression of key proteins and genes	*In-vivo* levels	-

3D cultures have shown potential in a variety of fields including the development of new drugs/drug classes, which require stringent testing and benchmarking. The *in-vitro* models used to test drugs, therefore, must be biologically relevant and highly robust. 3D cell culture demonstrated potential to make the process more effective and efficient at the pre-clinical level to reduce animal research, prevent wasted clinical trials and high attrition rates. However, this promising area of application has not seen rapid and extensive uptake of 3D into drug discovery and drug safety evaluation pipelines. This is explained in part by the tight regulation in the pharmaceutical industry but also the characterisation challenges associated with these systems.

Organoids also have shown great potential in the study of human biology and disease due to their ability to self-organise, allowing them to recapitulate the physiology and architecture of organs in great detail. Organoids are therefore, a powerful tool enabling in depth and real-time monitoring of cancer, infectious diseases and inheritable genetic disorders however, they also face the same difficulties of standardisation and quality control as other 3D cultures whilst having further complications of expense and starting material (Garcez et al., 2016; Berkers et al., 2019; Driehuis et al., 2019; Fusco et al., 2019; Engel et al., 2020).

1.4.4 3D culture methods – Challenges and good practice (From published review article - Temple et al., 2022)

"2D" cell culture is a relatively simple, cheap and robust process with a variety of culture vessels available depending on the intended purpose of the cultures, along with the quantity of cells required. The technique is easy to learn and is non-time consuming with the main consideration being to avoid contamination. They also face no issues regarding the diffusion of nutrients and gases to the cells as they are grown in a monolayer.

Scaffold free cultures are also viewed by many as both simple and cost effective but, are not without extra considerations. For example, hanging drop techniques are simple and cheap in that they can be cultured using petri-dishes. This process, however, is fiddly and can result in the loss of all samples, if knocked or inverted incorrectly, along with being time consuming when setting up, changing media and collecting samples.

Although tricky, hanging-drop techniques allow for defined size control unlike ultra-low attachment plates and bioreactors, which can result in spheroids of varying sizes. These two techniques, however, allow for easier long-term cultures and at greater numbers, without as high a risk of losing

all of the spheroids. It is therefore worth bearing in mind the advantages of the different culture methods depending on the spheroids intended purpose.

Aside from these issues, scaffold free cultures also face difficulties when trying to produce co-cultures that accurately mimic the natural architecture of *in*-vivo tissue. This is due to issues in controlling the final location of the different cell types, unlike scaffold-based cultures where the different cell types can be seeded periodically. It is difficult to add cells to spheroids in a layer-based system as they are likely to only attach to the top side of the spheroid as the bottom is inaccessible and agitation can be tricky, particularly in hanging-drop cultures.

Utilising any of these scaffold-free methods, the user also faces issues with collection and handling due to their small size and poor mechanical stability, particularly when compared with scaffold-based systems that are often easier to visualise by eye and can potentially be handled physically by tweezers etc.

Unlike other scaffold free 3D cell cultures organoids are mainly cultured in Matrigel® and are subjected to a variety of different growth factors for the differentiation of stem cells or tissue fragments into the desired organ. This approach, in its modern form, was first described by Sato *et al.*, (2009) and is the primary protocol used in the field. These protocols for organoid establishment and quality control, however, are not standardised across different labs which can lead to variability and difficulties with reproducibility. Meaning that it is vital to confirm, using either microscopy or biochemical analysis, that the organoids are in fact what was intended. Organoids are also relatively expensive when compared with culture methods for traditional cell lines and other model organisms like fly or worms, whilst also facing potential difficulties when obtaining starting material.

Culture of cells on scaffolds is a more complicated process as cells need to penetrate the scaffold whilst ensuring a homogeneous cell distribution within the whole matrix. In Hydrogel scaffolds such penetration is less of a problem: they involve creating cell/gel suspensions, which once crosslinked

hold the cells in a 3D environment in a more homogeneous manner. Other polymeric scaffolds including porous foams, fibrous or tubular scaffolds rely on seeding through addition of a cell suspension with the anticipation that the cells will diffuse and eventually migrate into the scaffold, often called the 'drop-on' method (Brown et al., 2018; Danti et al., 2013; German & Madihally, 2019b; Rajendran et al., 2017; Ruoß et al., 2018). This approach however, is often subject to lower cell attachment, penetration and poor and/or less homogeneous scaffold cellularisation, with most cells landing and remaining on the top of the scaffold (Asthana et al., 2018; Murphy et al., 2010). This is problematic as the cell layer prevents the diffusion of nutrients and reagents to the cells that reside inside the scaffold culture. Furthermore, cell growth takes place locally in 'pockets' of the scaffold and not in a consistent manner. It is therefore important to investigate and characterise the cell interactions and distribution within the scaffold material.

One way of improving the cell suspension penetration is seeding in dynamic flow and/or with rotation. However, in general the investigation of the cell seeding and cell diffusion/migration into scaffolds is an area which lacks standardisation. Many published articles include schematic diagrams, which illustrate the process of scaffold fabrication, but few include the specifics of the culturing process. The latter is particularly important, especially as the cell seeding methods/protocols can be scaffold specific and there is no unique approach to ensure 'optimal' cell seeding. Consequently, the lack of cell seeding and culturing protocols in publications can make it difficult for readers to understand and appreciate the experimental approach, particularly in cases where little microscopic analysis is performed (Tasnim et al., 2016). Wu *et al*, (2019) is an example of good practice with inclusion of informative schematics for both scaffold fabrication and cell culture. This approach clarifies the design of the culture system as well as how cells respond and organise themselves within the material (Figure 1.5) (Wu et al., 2019). Such detailed practice is beneficial to other researchers attempting to reproduce or build on the research as one of the commonly encountered difficulties is seeding or cell distribution after attempting to follow culture methods which lack detailed experimental methodologies and characterisation.

Unlike 2D cultures, where plates and flasks are made from standardised tissue culture plasticware, scaffold cultures also face increased variability when using non-commercial, and even to some extent commercial, materials due to non-standardised processes. This can lead to challenges for repeatability and especially reproducibility across different labs. Even hydrogels, such as Matrigel, can face issues with batch-to-batch variation potentially effecting results and differences between cultures (Hughes et al., 2010).

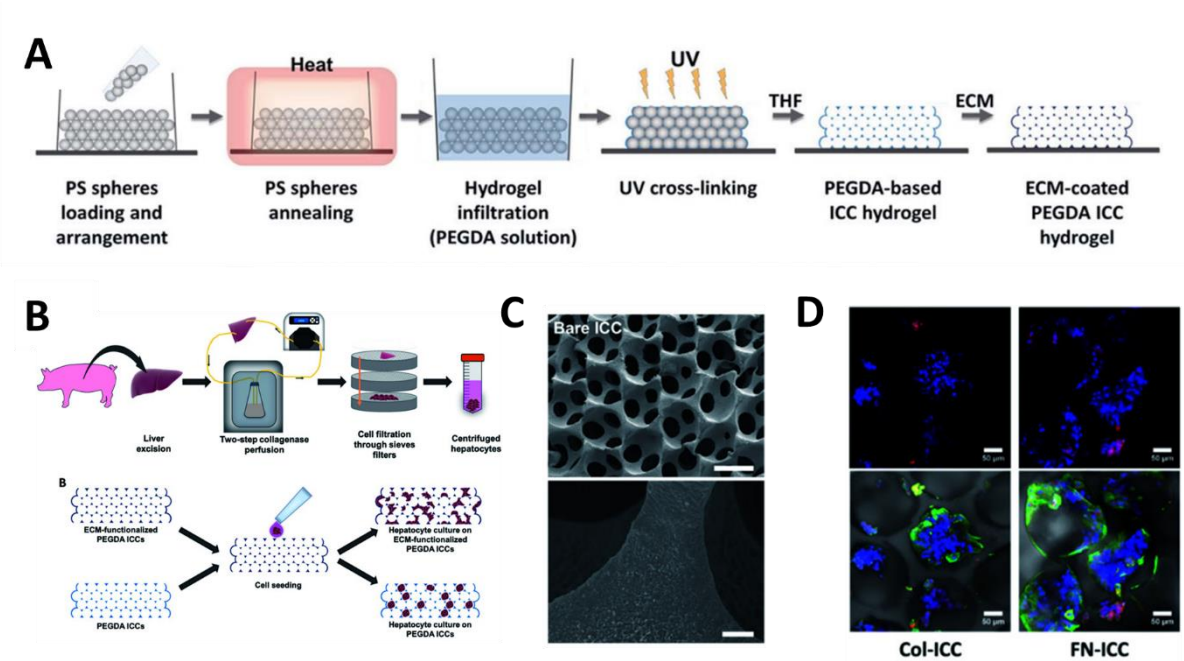

Figure 1.5. Poly(ethylene glycol) diacrylate (PEGDA) inverted colloidal crystal (ICC) scaffolds prepared by Wu *et al.* (2019). Their figures explain the fabrication off the ICC scaffolds (A) as well as how cell seeding was achieved (B). SEM imaging of the scaffold shows that the structure indeed looks like the schematic in figure (C) and immuno-fluorecence imaging is used to visualise how cells are binding and growing within the structure (D).

Detailed information on the culture method is important as multiple factors will influence the model, for example, cell seeding concentration, culture length and the technique used for cell seeding. Work by Raghavan *et al.* (2016) highlighted that even different spheroid formation techniques affect the end culture. They compared spheroids cultured using three methods: hanging

drop, liquid overlay on ultra-low attachment plates and liquid overlay on ultra-low attachment plates with rotation mixing. Results demonstrated that the spheroids differ in terms of cellular organisation and morphology, internal diffusion of nutrients and drugs, ECM deposition and chemosensitivity. It is, therefore, likely that smaller variations in protocols would also results in such differences.

With the increased complexity of 3D culture systems and experimental procedures comes additional technical challenges and experimental optimisation. Technical difficulty with 3D cultures, particularly how they are manipulated and handled, is often omitted and yet such crucial information is integral to experimental and data reproducibility. Inclusion of detailed step-by-step protocols is, therefore, something that should be standard practice throughout the field.

1.4.4 Biochemical analysis: the complications of 3D (From published review article - Temple et al., 2022)

As Petri dish based 2D cell culture has been the gold standard for the past six decades all current characterisation and analysis protocols are tailored to analysing cells in this format (Paul, 1970). Some biochemical assays have been adapted to 3D, but their application is hindered by the increased complexity in both morphology and functionality of the cultures as highlighted by Fang and Eglen (2017). Difficulties arise due to the hindered diffusion and the entrapment of gases, nutrients, waste and reagents within the systems, along with difficulties when quantifying and normalising between samples (Asthana & Kisaalita, 2012; Griffith & Swartz, 2006; Gupta et al., 2019; Shanbhag et al., 2005; Sirenko et al., 2015; Zustiak et al., 2010). For example, spheroid cultures are widely used due to their simplicity and cheap production cost, but they offer little structural support making them difficult to manipulate and handle, whilst having low porosity for the diffusion of nutrients, gases and assay reagents to the cells. Oxygen can only diffuse through 100-150 µm of tissue, therefore any spheroid above 300 µm is likely to have a hypoxic core (Asthana & Kisaalita, 2012; Griffith & Swartz, 2006). As nutrients and assay reagents are far larger than oxygen their diffusion in tissue will be significantly hindered. This will undoubtedly hamper larger cultures such as

spheroids over a particular size or scaffolds with low porosity; both in terms of getting nutrients in and waste products out but also for assays which rely on a substrates reaching and being taken up by the cells (Adcock et al., 2015; Totti et al., 2017). Organoids, even with their smaller size relative to spheroids, will also experience these issues of diffusion as they are typically grown in a complete matrix like Matrigel, which reduces their permeability.

Even for scaffolds with macro-porosity, after a certain time period, cells form dense and/or large clusters, which can block the pores and lead to uneven distribution and/or diffusional limitations when attempting *in-situ* characterisation assays. For example, for macroporous polyurethane (PU) foam type scaffolds which support growth of pancreatic cancer cells, Totti *et al.*, (2018) has shown little to no differences between different conditions, such as ECM coatings of the scaffolds, when assessing the culture with MTS. In contrast, sectioning, immunostaining and imaging revealed clearer differences between conditions. Similarly, Gupta *et al.*, (2019) were able to identify differences in viability and/or apoptosis in polymer scaffolds following drug and irradiation screening with advanced microscopy and imaging, in comparison to MTT which was unable to capture differences for different culture conditions. It is therefore important that before beginning analysis of any 3D cultures researchers consider which analytical approach is most appropriate for what they want to study and also how best to normalise across different cultures and conditions. Furthermore, it is important to consider that classical, gold-standard approaches followed in 2D cultures, cannot necessarily be implemented in 3D. For example, when conducting irradiation screening, the gold standard in 2D is the conduction of clonogenic assays for the development of survival curves post-treatment. Hamdi *et al.*, (2015) highlight the impossibility of extracting cells from spheroids for clonogenic assays and alternatively suggest *in-situ* approaches for post-treatment characterisation. Such readouts are new and/or differ from standard 2D practice. The field, therefore, needs to consider the most appropriate assay, as what has been validated and accepted for 2D is not always applicable for 3D, depending on the culture type.

To be meaningful, allow statistical analysis and cross-comparison biochemical measurements need to be normalised, for example, luminescence data expressed as 'arbitrary unit value per cell'. However, unlike 2D cultures, counting the exact number of cells in a 3D system is a challenging task. Very few researchers in the field count cells in the traditional manners using microscopy, due to an inability to visualise all the cells within the culture, or using an automated cell counter, as cells can be entrapped within the culture or cannot be collected into a single cell suspension. The issue is varied across 3D cultures as the more complex the internal organisation and chemistry, the more challenging it can be for cell extraction protocols to be successful.

To account for these technical challenges, many researchers report the use of a proxy reading, such as total protein/DNA, to give an estimation of the number of cells within the 3D culture system. These readings theoretically give an accurate estimation of the number of cells, however, they are hindered by reduced reagent diffusion along with some readings, such as luminescence, being affected by the thickness or opaqueness of the culture. Although it is the 3D nature of these cultures that give them enhanced functionality and performance it is also what is causing many of the complications of the associated measurements.

Several proxy measurements are implemented, the simplest being the use of a so called 'housekeeping' marker as an indicator of the number of cells. The expression of a protein or gene of interest is reported in relation to a house keeping gene or protein, such as GAPDH or β-actin. In theory, these markers are constitutively expressed and are required for the maintenance of basic cellular function expression so their levels remain unchanged between cultures and conditions (Eaton et al., 2013; Liu et al., 2017; Wu et al., 2019). Often published as standard practice, this method does not face the same problems as other proxy measurements, such as total DNA/protein concentration, because it is an internal control (the detected levels of both the house keeping protein/gene and the protein/gene of interest and are affected equally by diffusion and entrapment

within samples). However, the problem with this approach is that the expression of both the DNA levels and the protein levels of these housekeeping genes can change, even in 2D, depending on a number of factors including experimental treatment, tissue origin, donor variation, hypoxia and numerous chemical factors including insulin (Aldridge et al., 2008; Bustin, 2000; Eaton et al., 2013; Kuang et al., 2018; Suzuki et al., 2000).

If factors such as hypoxia affect the levels of housekeeping genes/proteins in 2D, then manipulating cells into 3D and other effects associated with some 3D cultures, including being under flow and experiencing shear stress, are likely to also affect their levels. In these cases, using such markers could equally lead to inaccurate measurements between conditions/cultures, particularly when comparing cells cultured in 2D vs 3D, or even between the same 3D cultures if the geometries of the cells are different. This point is highlighted well in the case of β-actin which is a commonly used housekeeping gene. When cells are cultured in 3D, compared with 2D, the expression of components that make up the cell cytoskeleton are altered, seemingly dependent on the tension exerted upon the cells (Walker et al., 2020). Work by Pruksakorn *et al,* (2010) found that when HepG2 cells are cultured in a scaffold-based 3D culture the expression of cytoskeleton proteins, including β-actin increased when compared with the same cells in 2D. They demonstrate that in these cells the culture geometry has a direct, positive effect on the levels of the house keeping gene. Conversely, Zhou *et al*, (2017) demonstrate that when mesenchymal stem cells are cultured in a 3D spheroid the levels of β-actin decreased dramatically leading to a long-lasting effect on the actin cytoskeleton. They note that it is only the expression of the cytoplasmic β-actin that is reduced, not that of nuclear β-actin expression, and conclude that it is the re-arrangement of the actin cytoskeleton that is largely responsible for the impact of 3D culture on cell size and morphology. A slight decrease in the levels of β-actin was also reported by Kim *et al*, (2018) when they cultured the colorectal cancer cell line, SW48, using a 3D soft agar matrix vs 2D. Interestingly, they also reported a dramatic increase in the levels of GAPDH, another commonly used housekeeping marker, compared with the same cells in 2D. This is disconcerting as although Zhou *et al*, (2017) found a large

decrease in the level of β-actin, they show that the levels of GAPDH were unchanged between 2D and 3D. The fluctuation in the levels of these housekeeping markers between cells cultured in 2D and 3D is, therefore, highly variable and appears dependent on both cell and culture type. These examples highlight that the use of these housekeeping genes, which is standard practice in 2D, is not necessarily translatable to cells cultured in 3D and should be considered carefully if utilised.
This method is however may be suitable when comparing similar 3D cultures to one another, for example, when comparing alike spheroids cultured under different conditions. Alike scaffold cultures, however, may face different levels of these genes due to their higher levels of heterogeneity across samples. It may be possible to prove that levels of certain housekeeping proteins/genes are unaffected between some 3D cultures and 2D or that new housekeeping markers could be identified.

To overcome the challenge of differences in gene expression, the quantification of total protein can be implemented as an alternative approach. Work by Eaton *et al.* (2013) demonstrates that using total protein is a more reliable control for quantitative fluorescent western blotting. The use of total protein or total DNA as a representation of the number of cells in the culture assumes that any change in the expression across different conditions or cultures is negligible at this level. This methodology has been implemented for a long time for different assays from normalising urea and albumin production (Bokhari et al., 2007; Dunn et al., 1989; Lazar et al., 1995; Sellaro et al., 2010; Tasnim et al., 2016; Vu et al., 2016) to normalising cytochrome p450 activity (Chitrangi et al., 2017; Wang et al., 2015). Although well characterised and commonly used, this approach is not without its pitfalls; making assumptions that all the cells within the sample have been completely lysed and the internal components released from the culture for measurement. This is problematic due to the likely variation in the levels of diffusion of both lysing agents into 3D cultures as well as the subsequent protein/DNA released, both in spheroid and scaffold cultures. One approach is to firstly homogenise the cultures prior to lysis however, although possible with spheroids it is not always applicable to scaffold-based cultures, particularly those large in size. Scaffold based cultures also

face complications of protein/DNA retention within scaffold models, which could occur as result of binding of protein/DNA to the scaffold material or entrapment (Shanbhag et al., 2005; Zustiak et al., 2010). Like in the case of the housekeeping markers, it is well known that the expression of many proteins/genes differ significantly when comparing cells in 2D and 3D (Bell et al., 2018; Kumar et al., 2008; Li et al., 2008). It is, therefore, not unreasonable to suspect that there may also be measurable differences in total DNA/protein expression between samples with the exact same number of cells caused by their culture method. This would mean that using this total protein/DNA as a proxy for cell number for normalisation could be inaccurate when comparing 2D and 3D, although, like the housekeeping markers, should be adequate when comparing similar culture methods.

Attempts have been made to increase accuracy and reproducibility of using total protein/DNA. Yan *et al,* (2015) demonstrate the use of a standard curve where total DNA was plotted against cell number. The curve was generated by measuring the DNA concentrations from lysates for which the number of cells is known. This idea was first outlined by Feng *et al*, (2010) although they do not use it for normalisation. Whilst this approach provides readouts as per number of cells, it faces the same issues of diffusion and DNA-scaffold binding. It is possible this approach is less accurate, assuming cells grown in 2D were used to make their standard curves. Additionally, standard curves have also been used for the prediction of cell number through the use of viability (Sarkar et al., 2017; J. Wang et al., 2016) and proliferation (Kumari et al., 2016) but both would face the same issue of diffusion and binding as Yan *et al,* (2015). Viability and proliferation, however, are not often used to estimate cell number, presumably as they can be directly affected by culture geometry as well as being readouts for other assays such as drug toxicity screening(Bokhari et al., 2007; Lan et al., 2010).

The traditional way in which to normalise across different models and conditions is to count the exact number of cells, without the use of a proxy measurement, ensuring that any measurable difference is down to the functionality of the cells. For 3D cultures this is more difficult because cell counters and microscopy techniques do not translate well into 3D. Both require all the cells within

the culture to be trypsinised and resuspended into a single cell suspension, something that is easily achieved in 2D due all the cells being on a single, planar surface and accessible by the dissociation solution. However, in 3D it is difficult to ensure all cells are removed from the culture and are in a single cell suspension, due to extensive cell-to-cell or cell-matrix interactions leading to clumping and entrapment. Despite this, these cell counting methods are still implemented by some researchers in the field (Dubiak-Szepietowska et al., 2016; Shah et al., 2018).

It is concerning that, when cell numbers are reported, it is sometimes unclear how it was measured. Using the seeding number of cells (Feng et al., 2010; Tasnim et al., 2016; Wu et al., 2019) would surely be a significant cause of error as it would assume not only that all cells are taken up into the 3D system but also that there is no change in cell number during the culture time or variation between conditions. Some papers even normalise their albumin and urea readings to cell number without giving any information on how this cell number was calculated (Liu et al., 2017; Liu, Wang, et al., 2016; Liu, Wei, et al., 2016; Yaqing Wang et al., 2018). Often researchers will normalise per well or to a control well, which is effectively normalising to seeding concentration and has the same pitfalls (Basu et al., 2018; Baze et al., 2018; Foster et al., 2019; Ogihara et al., 2017; Ott et al., 2017; Shin et al., 2018). Four of these studies use 3D spheroid cultures, which in theory should remain consistent in size and cell number if the seeding concentration is the same. However, although more reproducible than other culture types they are not without variation as can be seen in Ogihara *et al.'s* (2017) figure 2, possibly due to variation in seeding number or variation in growth making normalising this method less accurate (Das et al., 2016; Mehesz et al., 2011; Raghavan et al., 2016).

Similarly, to other 3D cultures, organoids face the same issues of normalisation as mentioned above. They do, however, face further complications as they are heterogeneous in both size and cell population which leads to complications when trying to measure quantifiable readouts, particularly if normalising by counting the number of organoids which is common in the field (Chumduri et al., 2021; Flanagan et al., 2021; Van Neerven et al., 2021).

1.5. Imaging techniques – Light-sheet microscopy

Fluorescence imaging is a powerful and informative technique but light scattering, diffraction and absorption limit the ability to image deep within the model to extract all the available information. Depending on the illumination method/type of microscope the field of illumination can be very different. This affects both the resolution of the image due to out of focus light and the speed of acquisition (Table 1.3).

Table 1.3. Comparing different microscope modalities

Microscope	Resolution	Imaging depth	Speed and throughput	Photo-bleaching
Wide field	200 nm	< 100 µm	High	High
Confocal	200 nm	< 100 µm	High	High
Light-sheet	200 nm	< 350 µm	Slow	Low
Multi-photon	60 nm	> 500 µm	Slow	Low
References: (Doi et al., 2018; Graf & Boppart, 2010; Jorand et al., 2012; Miller et al., 2017; T. Riss & Trask, 2021)				

Previously, to obtain detailed information in thicker samples would require embedding and slicing into thin sections but this method is not only time consuming, but only allows a small section of the samples to be imaged whilst also potentially damaging the 3D architecture of the sample. With the advancement of the field of microscopy it is now possible to optically section live 3D samples using light-sheet microscopy (Figure 1.6).

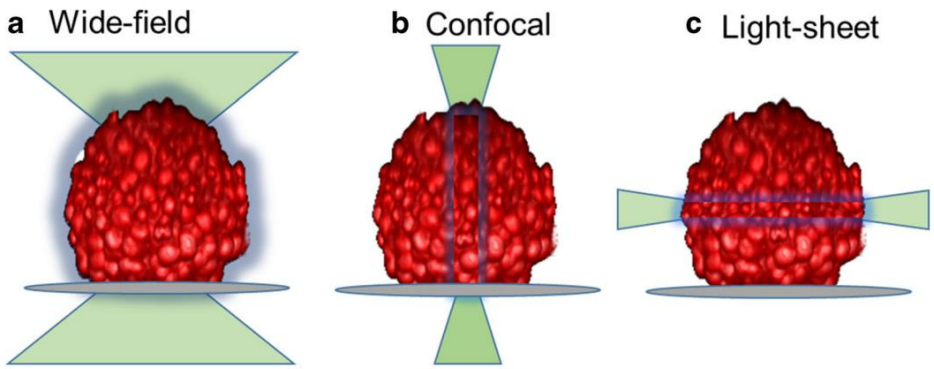

Figure 1.6. Schematic comparing the illumination fields of three light microscope modalities. The area of illumination is large for wide-field microscopy compared to confocal which illuminates using a single laser point by point. Light-sheet microscopy illuminates a whole slice of the sample allowing lots of information to be captured simultaneously (Riss & Trask, 2021).

Light-sheet microscopy or Single plane illumination microscopy (SPIM) uses a single, focused sheet of light to illuminate the sample, plane by plane, increasing both speed, reducing photobleaching and phototoxicity whilst having a wide-field of view (Logan et al., 2018; Nature methods, 2015; Stefaniuk et al., 2016; Zeiss, 2022). This gentle illumination allows the imaging of live samples without inducing too much stress on the cells making it perfect for imaging 3D samples over long periods (Figure 1.7).

Figure 1.7. Demonstration of light-sheet illumination on a 3D sample using the Zeiss Z.1 light-sheet microscope. The sample is mounted in a column of low percentage agarose that enables the sample to be held in position for imaging (Zeiss, 2022)

Light-sheet microscopes can image large samples, even whole (animal) organs depending on the sample chambre size. In Liverpool's Centre for Cell Imaging, I used the Zeiss Z.1 light-sheet microscope which can image samples up to ~1 cm in diameter by mounting the sample in a column of low percentage agarose. The main benefit of this microscope compared with other light-sheet microscopes is that the sample is rotatable through 360 ° allowing imaging from all angles. This allows multiple images to be taken and numerically fused together, into a 3D image, to improve image resolution and quality.

In recent years light-sheet microscopy has been modified to allow for high-throughput imaging of 3D cultures allowing researchers to take advantage of its wide field of view and quick imaging, however, losing the ability to image from multiple angles. Utilising a capillary under flow, samples are pushed through a light-sheet and imaged; unfortunately the ability to image samples in a multi-well format is extremely challenging and has not yet been achieved (Bernardello et al., 2022; Logan et al., 2018).

1.5.1 Imaging: A powerful tool (From published review article - Temple et al., 2022)

Microscopic imaging of 3D systems is a powerful tool that can give a detailed insight into what processes are taking place and to what extent within these systems. Imaging allows a more detailed understanding of the morphological and functional adaptations that the cells undergo when they are cultured in 3D. It allows the visualisation of cell distribution throughout the culture and how cells are binding and growing within scaffold materials (Lewis et al., 2018; Yan et al., 2015), validating whether cells are truly growing in 3D, identification of late stages of differentiation, visualisation and semi quantification of functional markers (Kyffin et al., 2019; Messner et al., 2018) and even toxicity testing (Sirenko et al., 2016) (Figure 1.8). Furthermore, obtaining a spatial distribution of the cells in 3D constructs, enables the correlation of cell behaviour (proliferation, clustering, secretion of markers, oxidative stress/hypoxia or nutrient stress) to specific structural or biochemical properties

of the 3D system. It also allows for mapping/screening of heterogeneity, the latter being critical not only for the validation, understanding and control of 3D cultures, but also for the accurate recapitulation of 3D tissues *in vitro*. Heterogeneity, naturally occurs in healthy and diseased tissues *in vivo* (and it certainly does not occur in traditional 2D cultures), therefore, capturing it and understanding it in 3D is of vital importance.

Imaging cells in 3D can be achieved through; physical or optical sectioning and its importance was noted as early as 1914 (Thyng, 1914). The former involves the mechanical sectioning of the sample to allow imaging deep within the model at high resolution. Although high in resolution and without the hinderance of dye penetration, physical sectioning techniques have limitations; they don't allow real time imaging due to the sample requiring embedding and mechanical sectioning can result in the loss of structure (Bassim et al., 2012; Shearer et al., 2016; Verhertbruggen et al., 2017). Protocols can also be long, time-consuming, and arduous and require sophisticated data reconstruction software.

Optical sectioning offers the potential for quick and non-destructive, three-dimensional imaging of subcellular structures within 3D models. Optical sectioning has been made easier with the development of new technologies like spinning disk and multi-photon microscopy along with light-sheet technologies, allowing greater imaging speed and depth as well as allowing single-plane illumination. These techniques permit imaging of samples in real-time without the risk of damage or distortion from embedding and sectioning. Optical sectioning, however, faces other complications that arise mainly due to the penetration of both light and reagents. Huang *et al.*, (2021) highlight well the different imaging techniques available for imaging 3D cultures and discuss both the penetration depth and resolution of each.

Light penetration will greatly depend on the method of illumination along with opacity and the level of light scattering within the culture; factors that vary across tissues and models (Ash et al., 2017;

Hama et al., 2011). Laser-scanning confocal microscopy (LSCM) for example, can penetrate to a depth of ~150 μm through brain tissue, however, two-photo microscopy can penetrate more than 500 μm (Costa et al., 2019; Hama et al., 2011). Various techniques exist including classic laser-scanning confocal (LSCM), multi-photon and light-sheet illumination, each with different levels of penetration, scattering, bleaching, photo-toxicity and background illumination due to out of plane light. The wavelength of the light used will also have an effect, with red light penetrating further than others (Ash et al., 2017; Zhao & Fairchild, 1998). Light penetration within 3D samples can be improved using clearing, which aims to increase the transparency of the sample and to match the refractive index of the molecules within the tissue to one another. Costa *et al.*, (2019) give a detailed overview of the different clearing methods and their advantages and limitations. Clearing, however, is only applicable to fixed samples and will only work on biological tissue so will have little effect on cultures using electrospun scaffolds or other such solid matrices.

The main problem with imaging 3D cultures, however, is attaining quantitative data and usually requires the ability to control across samples using cell number. As stated previously oxygen diffusion through tissue is around 150 μm, the diffusion of fluorescent markers and antibodies will be less due to their increased size. The diffusion of these markers is a limiting factor, often more so than light penetration, and will again depend on the 3D model being investigated. The issue here is that without the ability to visualise the whole cell population it is impossible to attain accurate and reliable data from the whole culture. One solution to this is to just measure from an imageable section, however, due to the natural heterogeneity of most 3D cultures this could lead to unreliable results. Another solution is the use of reporter cell lines that would, therefore, remove the issue of reagent diffusion particularly if using an imaging technique with good light penetration, like multi-photon or light-sheet, and if using cleared samples. Research is also being undertaken in label-free imaging, however, it is still in its infancy for use in 3D applications (Gong et al., 2021; Kallepitis et al., 2017; Ounkomol et al., 2018; You et al., 2018). The issue with these techniques, is that without labels to highlight a specific organelle or molecule it is hard to distinguish or study the object of

interest. Raman imaging offers a solution here but is difficult to use on 3D cultures due to issues with background signals and poor z-axis resolution caused by overlapping signals. Work by Sirenko *et al*, (2016) utilised nuclei staining with Hoechst 33342 as a measure of cell number to normalise compound toxicity, this is one of the few examples in the literature of fluorescent imaging being used quantitatively rather than qualitatively. This approach is informative as the assay can be multiplexed with other stains used simultaneously to study the cellular pathway the compound effects. The major problem with counting cell number this way, as highlighted by Sirenko *et al*, (2016), is that it is very difficult to quantify all of the cells in the 3D system due to problems with light and dye diffusion. They noted how there is a large difference between cells counted and the number of cells seeded making it difficult to quantify accurately, however, was a step in the right direction. Interestingly, there has not been much advancement with quantitative fluorescent imaging likely still due to penetration issues in 3D cultures. Therefore, techniques like Raman imaging are exciting as they could bypass these limitations.

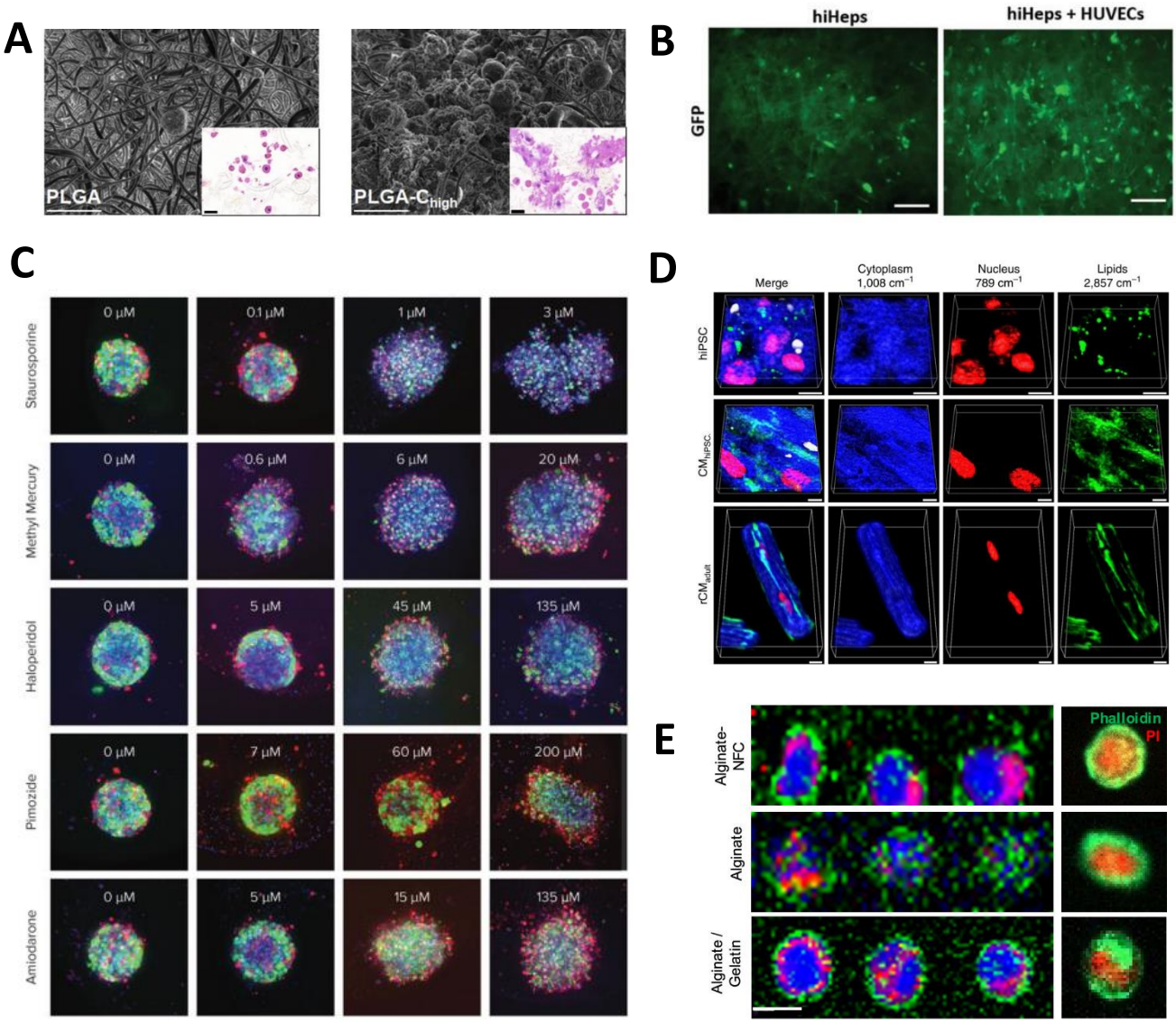

Figure 1.8. The varying degrees of imaging in the field. A- Electron microscope images demonstrating in high-detail how cells integrate with the electrospun fibres (Brown et al., 2018a). B – Fluorescent imaging shown purely to demonstrate that the cells populate the scaffold and to track growth (Yaqing Wang et al., 2018b). C – Quantitative fluorescent imaging of toxicity in spheroids for different drugs (Sirenko et al., 2016). D – Volumetric Raman imaging of cells growing in a hydrogel where the researchers were able to quantify the level of different cell components (Kallepitis et al., 2017). E – Ramen imaging of spheroids to visualise the distribution of different cell components (Marzi et al., 2022).

Imaging is informative yet, little to no quantitative measurements are performed using image analysis in 3D cultures, with most imaging work performed only to check cell distribution and binding. This is likely to be the result of microscope and software availability, feasibility of imaging, the papers intended purpose as well as the factors mentioned above. Often proof that the cells are growing or binding within the culture is all that is required for publication. The quality of imaging is also variable, with some studies imaging using basic confocal or even wide-field imaging. The level of investigation again depends on the need and something that is likely down to cost and availability.

Unfortunately, lots of information is being lost when complete analysis of the models is not being undertaken and the inclusion of detailed microscope work, particularly if in 3D, is invaluable in understanding what is going on between different systems, especially when studying co-cultures or demonstrating a new culture system.

1.6 Project objectives

The focus of this work is to compare two 3D liver cell models for high-throughput applications by testing the health and functionality of the cells. The hypothesis of this work is that the 3D scaffold cultures offer cells a healthier environment to grow, compared with 3D spheroid cultures, whilst enabling long culture lengths and allowing the cells to adapt into a 3D structure, improving their functionality. The scaffold cultures also offer further advantages over spheroid cultures due to their robust structure and customisable properties, which would enable them to easily be utilised in high-throughput and automatable processes, something that is of particular interest to the industrial partner.

Objective 1 - To establish robust and efficient protocols for the culture of 3D spheroids and scaffolds for use in high-throughput screening assays.

Objective 2 – Assess the current methods of normalisation in the field to allow accurate comparisons between cultures, conditions, and time points.

Objective 3 – Compare the models regarding health, function, and application in high-throughput screening studies with a focus on long culture times.

Objective 4 – Improve the models in their ability to recapitulate the *in-vivo* environment.

Chapter 2 - Materials and methods

2.1. Materials

All materials were acquired from ThermoFisher unless otherwise stated - https://www.thermofisher.com/uk/en/home.html.

2.2. Tissue Culture

2.2.1 2D cell culture

HepG2 cells (ECACC 85011430) were sourced from Sigma-Aldrich (https://www.sigmaaldrich.com/GB/en/product/sigma/cb_85011430) and were expanded before being stored at – 196 °C at passage 9. They were thawed at room temperature until fully thawed. HepG2 cells were cultured in t75 flasks and maintained in DMEM with 10 % FBS and 2 % L-Glutamine at 37 °C and 5 % CO_2 in a humidified atmosphere. The cells were passaged every 2-3 days or when they reached 70 % confluency. Cell media was removed, and the cells were washed twice with PBS. The PBS was removed before the cells were treated with 5 mL Versene (EDTA solution) for 10 minutes inside the incubator. 5 mL supplemented DMEM was added, and the cell suspension was moved to a 50 mL flacon tube. The cells were spun down at 500 xg and resuspended in 10 mL of media before being syringed using a 20 G needle to create a single cell suspension. Different seeding densities were seeded to ensure a flask was always at 70 % on the day of experiment.

2.2.2. Cell Counting

Cell counting was performed using a Beckman Coulter counter as it displayed higher accuracy than automated cell counters. Briefly 1 mL of cell suspension was added to 19 mL of ISOTON II and an average of three readings were made. Percentage of live cells was measured using a Countess 3 (5 µL Trypan blue was mixed with 5 µL cell suspension and added to the chip).

2.2.3. Spheroid culture

Spheroids were cultured as described in section 3.3. Briefly Perfecta3D® hanging drop plates were set up adding PBS to the reservoirs and 45 µL to each of the 96 hanging drop wells. A single cell suspension was created as described in section 2.1.2. and counted. Only cultures with 95 % live cells or higher were used. The suspension was diluted to 50,000 cells per mL and 10 µL was added to each droplet. The spheroids were maintained in the droplet with 10 µL media changes every 2 to 3 days.

2.2.4. Scaffold culture

The scaffold material was purchased form The Electrospinning company consisted of electrospun Poly-lactic acid (PLLA) polymer (Mimetix®). The scaffold consists of fibres, 4 µm in diameter, which intertwine to give pores of 15-30 µm, with an overall porosity of 80%.

2.2.4.1. Scaffold preparation

2 cm x 2 cm x 50 µm sheets of scaffold were placed in a 6 cm dish and soaked in 70 % ethanol for 1 hour. The scaffolds were washed in sterile PBS before being cut using a sterile 1 mm biopsy punch (kai medical). The scaffolds were then placed in a sealed 1.5 mL Eppendorf and placed in the fridge at 4 °C until seeding.

2.2.4.2. Scaffold culture vessel manufacturing

The middle section of screw lids for 1.5 mL cryovials were removed using a soldering iron and excess plastic removed using a scalpel. The tubes were then autoclaved and placed top down in a 6 cm dish filled with 2 g of liquid PDMS in a sterile environment (Figure 3.14.). Once cured the lids were cut from the PDMS and soaked for 1 hour in 70 % ethanol, washed with PBS and left to air dry. They were then stored until use.

2.2.4.3. Scaffold seeding

Scaffolds were cultured as described in section 3.4. Briefly 1 mL of 175,000 cells / mL cell suspension was added to the cryovial. Scaffolds were added and the tubes sealed using PDMS lids. The tubes were then taped down, flat down, on the bed of the rocker at either end inside the incubator. After 4 days the cell suspension was removed, the tube and scaffold were washed twice with PBS and then resuspended in supplemented DMEM. The scaffolds were then moved to a 96 well ULA plate with 200 µL media using a p200 pipette with the end of the tip removed using a scalpel.

2.2.4.4 CELVIVO culture

The CELVIVO ClinoStar® was purchased directly from the manufacturer after a short demo period (https://celvivo.com/products/clinostar/). The ClinoReactor®s were set up according to manufacturer's instructions. Briefly, 25 mL of sterile water was added to the humidification chamber to hydrate the gel spheres and left in the fridge overnight. 5 mL of culture media was then added to the culture chamber and inserted into the ClinoStar® to wash and pre-wet the culture chamber. The media was removed and 10 mL of fresh media containing scaffolds was added. The scaffolds were set to rotate in the reactor whilst a cell suspension of 700,000 cells / mL was created. 2.5 mL of media in the chamber was replaced with 2.5 mL of cell suspension giving a cell concentration of 175,000 cells / mL. It was checked that air bubbles were present to aid in dispersing the scaffolds and avoiding clumping. The reactors were set at 35 rpm with a dispersal event every minute. After 2 days the cell suspension was removed, and the scaffolds were resuspended in media and placed back into the reactor until required. Media changes were performed every 2 days.

2.3. Stable Cell lines

HepG2 H2B-RFP (pHIV-H2BmRFP, addgene, plasmid #18982) and HepG2 H2B-RFP/Luciferase (pHIV-Luciferase, addgene, plasmid #21375) were created using a lentiviral transduction method.

Twelve 10 cm dishes were seeded with HEK293T cells at 1.5 x 10^6 and placed in an incubator at 37 °C and 5 % CO_2 overnight. The cells were 30-40 % confluent the next morning.

Lentiviral reagent containing a 4:2:1 ratio of vector:packaging:envelope was prepared, with 17 µg of total protein used per dish. The HEK293T cells were then transfected using polyethylenimine (PEI) at a ratio of 2:1 PEI:DNA in serum free DMEM. The PEI and serum free media were added together and vortexed slight before waiting 5 minutes. The DNA was then added to the PEI and media mix, vortexed slightly and left for 30 minutes. The transfection mix was then added dropwise to each dish, ensuring an even distribution across the dish, before being incubated at 37 °C and 5 % CO_2 for up to 15 hours before a media change was performed.

After three days the media was collected from 10 of the 10 cm dishes containing HEK293T cells and centrifuged at 1000 xg for 5 minutes before being filtered through a 0.45 µm PES filter. Ultracentrifugation was then performed following the protocol described by Kutner et al., (2009). Media containing virus was transferred to sterile ultracentrifuge tubes and 4 mL of a 20 % sucrose cushion was expelled beneath the media. All tubes with then weighed and ensured to be within . The tubes were spun at 4 °C for 2 hours at 21000 rpm. Viral particles were resuspended in 100 µl PBS per tube and combined. 600 µL of PBS containing viral particles was immediately added to HepG2 and HepG2 H2B-RFP cells in a t25 flask and left for 48 hours. The HepG2 cells were then expanded before being frozen for storage in liquid nitrogen.

2.4. Microscopic imaging

2.4.1 EVOS cell imaging system

The EVOS XL Core imaging system was used to quickly check scaffold seeding or visualise samples in the wells using the RFP filter and a laser intensity of 60 %.

2.4.2 Light-sheet imaging

2.4.2.1 Sample mounting

3D samples were collected and placed in an Eppendorf tube before being washed twice in PBS and resuspended in 100 µL of PBS. 100 µL of 3 % low gelling point agarose was added to the tube and mixed, avoiding disturbing the 3D culture. Using a 1.5 mL glass capillary (Green, supplied by Zeiss) the cultures were sucked up into the capillary and left to set. It was important to make sure that the cultures were in the centre of the capillary and that scaffold cultures were upright to ensure that the best imaging quality was recorded, this was achieved by rolling the capillaries between the index finger and thumb as the agarose set.

2.4.2.2 Image acquisition

3D cultures were mounted in the Zeiss Z.1 microscope and the chamber was filled with RO water. The agarose tube was expelled from the capillary into the RO water and aligned with the light-sheet. Various filter sets and laser wavelengths were used depending on the fluorophores. The most common being 405 nm and 488 nm lasers for excitation at 10 % laser power and an exposure time of 100 ms. Emitted light was collected through a 420-470 filter for Hoechst staining and 575-615 for RFP. A 10x illumination objective and 20x W Plan-Apochromat object were used for all image acquisition. Z-stacks were acquired at 2 µm steps and using dual side fusion and pivot scan settings to ensure all signal was recorded. Multi-view images were recorded at 8 angles, 45 ° apart. Hoechst 33342 stock solution (20 mM) was diluted 1:50 for nuclei staining.

2.4.3 Image processing

2.4.3.1. Multiview reconstruction in FIJI

8 angles light-sheet images were reconstructed using the ‘Multiview reconstruction’ plugin in FIJI. Briefly, .czi files were firstly resaved as HDF5 files before detecting interest points using difference of gaussian and 3D quadratic fit functions. Samples were downsized 2x in X and Y and 1x in Z and the

threshold was set until no artifacts were detected outside of the culture. The interest points from each angle were then compared to all other angles using the 'Register using interest point' function with a significance of 5. It was checked that all angles were aligned using the percentage of the interest point detected across adjacent angles and the plugin viewer. Once confirmed the fusion process was started.

2.4.3.2 Dot counting in IMARIS for nuclei counting

Fused image files were firstly converted to IMARIS files and visualised in IMARIS. Dot counting was performed using default creation parameters. The estimated XY diameter was set at 7 µm as this was the average nuclei of HepG2 cells measured in IMARIS (n=20). Finally, a quality filter was applied to ensure (60 – Max) a reduction in the number of false positives before the dot analysis was performed.

2.4.3.3 Surface analysis for spheroid area and volume measurements

Fused image files were firstly converted to IMARIS files and visualised in IMARIS. Surface analysis was performed using default creation parameters. The smooth surface details function was set to 5 µm and the threshold set (500 – Max) before running the analysis.

2.5. Luminescence readings

Maximum luminescence was recorded on multiple different plate readers and imagers discussed in section 4.2.3. D-Luciferin, Firefly (PerkinElmer #122799) was stored at a 15 mg/ml stock solution at -80 °C and thawed an hour before analysis. It was diluted 1:100 to a working stock of 150 µg/mL in supplemented DMEM. For analysis, cultures were placed in clear bottom, white wall, 96 well plates for plate readers and black wall, 96 well plates for the IVIS imager. The media was removed and 100 µL luciferin was added. This concentration means that the amount of luciferin is in a large excess to maintain signal, however, luminescence readings were taken as soon as the luciferin was added to

all the cultures. To avoid confusion when using luminescence assays like CellTitre-Glow® 3D, luminescence produced by the stable cell line is referred to as inherent luminescence.

2.6. Bradford assay for protein quantification

Samples were lysed by sonication in PBS to avoid detergents interfering with the assay. 200 µL Bradford Reagent was added per well of a 96 well plate. Standards of BSA in the range 0 - 0.5 mg/mL BSA were made up and 5 µL of samples were added to each well in triplicate along with test samples. The absorbance was then measured at 595 nm and protein concentrations were obtained from the standard curve.

2.7. Cell viability measurements using CellTitre-Glow® 3D

Cell viability was analysed using the CellTitre-Glow® 3D assay (Promega) according to the manufacturer's instructions. 100 µL of CellTitre-Glow®reagent was added to all three cultures in 100 µL of media. The plates were shaken on an orbital shaker for 10 minutes to induce lysis and left to incubate at room temperature for 20 minutes. Luminescence readings were then recorded using a plate reader. 100 µL CellTitre-Glow® 3D and 100 µL media was used as a blank.

2.8. Western blotting for expression of GAPDH

Samples were lysed in 20 µL sample buffer containing SDS and denatured at 80 °C before being analysed by SDS-PAGE on a 10 % acrylamide gel. The proteins were then transferred to a nitrocellulose blotting membrane for 2 hours and blocked using 5 % milk in TBST for 1 hour at room temperature. Membranes were probed with GAPDH primary antibodies at 1:1000 in 5 % milk in TBST overnight at 4 °C. Membranes were then washed three times with TBST before incubating with secondary anti-rabbit antibodies (1:1000) for 2 hours. The membranes were washed again in TBST before being treated with ECL and placed in a cassette with X-ray film. The film was then developed, and the bands visualised.

2.9. JESS analysis for protein expression

JESS analysis utilises capillary-based immunoassays with all assay steps from protein separation, immunoprobing, detection, and analysis being fully automated. The sample, separation matrix, stacking matrix, antibodies, and reagents are loaded automatically from a specially designed plate (Figure 2.1). Jess begins by aspirating the separation matrix and then the stacking matrix into each capillary. Next, the sample is loaded, and capillaries are lowered to make contact with running buffer. Voltage is applied to enable separation by molecular weight. Once the separation is complete, UV light immobilizes the proteins to the capillary wall. With proteins now immobilized and the matrix cleared of the capillary, JESS starts the immunoprobing process (ProteinSimple, 2023)

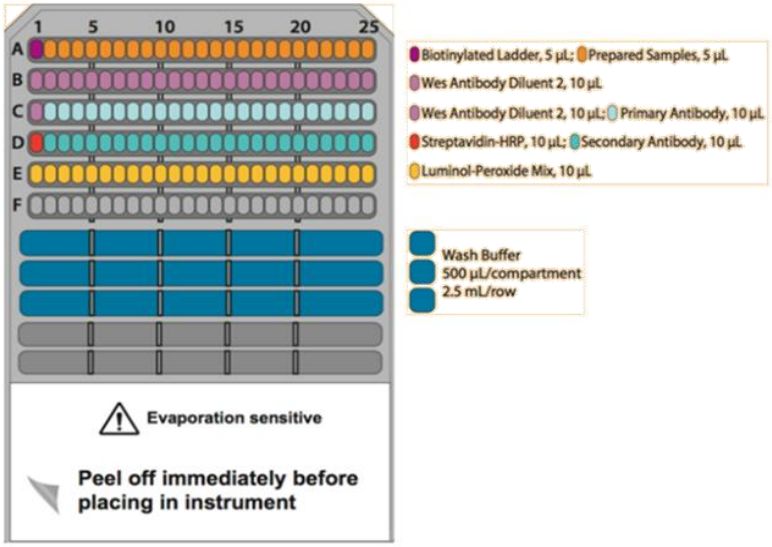

Figure 2.1. Plate set up for JESS analysis, plates were loaded whilst samples were thawed and denatured.

Samples were lysed using RIPA buffer and sonicated. JESS analysis was performed according to the manufacturer's instructions.

Briefly, standard pack reagents were prepared by adding 40 µL deionised water to make a 400 mM solution of the DTT (clear tube). Next 20 µL of 10X Sample buffer and 20 µL prepared 400 mM DTT were added to make the 5X Fluorescent Master Mix (Pink tube). 20 µL deionised water was added to

make the biotinylated ladder (green tube). Samples were then prepared by combining 1 part 5X Fluorescent Master Mix with 4 parts lysate in a microcentrifuge tub before being denatured at 95 °C for 5 minutes. Primary antibodies were diluted 1:50 with antibody diluent 2 and added to the plate. 200 µL Luminol-S and 200 µL Peroxide were combined and added to the plate. Once set up the plates were spun at low speed to remove bubbles and inserted into the JESS for running and analysis.

2.10. MTT assay

The MTT assay (Abcam #ab211091) was performed according to the manufacturer's instructions. Briefly, cultures were transferred to a 96 well plate and the media was aspirated off. 50 µL of MTT reagent and 50 µL serum-free media was added to each well, the blank was 50 µL of MTT reagent and 50 µL serum-free media, and left to incubate at 37 °C for 3 hours. After incubation, 150 µL of MTT solvent was added to each well, wrapped in foil and placed on an orbital shaker for 15 mins. Absorbance was then measured at 590 nm using a plate reader.

2.11. LDH assay

The LDH assay was performed according to the manufacturer's instructions. The culture media of all test cultures was changed at the same time, the day before the assay. 100 µL of cell media was taken from each culture and 100 µL of freshly prepared reaction media was added before wrapping the plate in foil and incubating at room temperature for 25 minutes. The absorbance was then measured at 490 nm.

2.12. Caspase activity measurements using Caspase-Glow® 3/7 3D

Levels of apoptosis were analysed using the Caspase-Glow® 3/7 3D assay (Promega) according to the manufacturer's instructions. 100 µL of Caspase-Glow® 3/7 3D reagent was added to all three cultures in 100 µL of media. The plates were shaken on an orbital shaker for 5 minutes to induce

lysis and left to incubate at room temperature for 25 minutes. Luminescence readings were then recorded using a plate reader. 100 µL CellTitre-Glow® and 100 µL media was used as a blank.

2.13. Lipid metabolism measurements using Cholesterol/Cholesterol Ester-Glo™

The levels of lipid metabolism were analysed using the Cholesterol/Cholesterol Ester-Glo™ assay (Promega) according to the manufacturer's instructions. The media was removed from all cultures and washed twice with PBS before 50 µL of Cholesterol lysis solution was added. The plates were shaken on an orbital shaker for 5 minutes and left to incubate at 37 °C for 25 minutes. 50 µL of Cholesterol detection reagent was added and the plates were shaken on an orbital shaker for 1 minute, wrapped in foil and left to incubate for 1 hour. Luminescence readings were then recorded using a plate reader. 50 µL of Cholesterol lysis solution, 50 µL Cholesterol detection reagent and 100 µL media was used as a blank.

2.14. Albumin production measured using ELISA

The ELISA was performed according to the manufacturer's instructions (Abcam #ab108788). Cultures were washed with cold PBS and spun down at 1500 rpm for 10 minutes before being resuspended in ice-cold lysis buffer (PBS, 1% Triton X-11 and protease inhibitor cocktail). Samples were then incubated on ice for 1 hour, spun down at 13000 rpm at 4 °C and the supernatant collected.

Albumin standards were prepared and 50 µL was added to the pre-coated microplate strips, along with culture samples before being incubated for 1 hour. The plate was washed 5 times with 200 µL wash buffer and incubated with 50 µL biotinylated albumin antibody for 30 minutes. The plate was washed again as described above and incubated with 50 µL SP conjugate for 30 minutes. The plate was washed as described above, 50 µL Chromagen substrate was added, and the strips were wrapped in foil and incubated for 25 minutes. Finally, 50 µL stop solution was added and the absorbance was read at 450 nm using a plate reader. The albumin concentration in the samples was calculated using values obtained from the standard curve.

Chapter 3 – 3D culture and image protocol development

3.1. Introduction

The industrial partner, Aurelia Bioscience, has interest in utilising electrospun Poly-lactic acid (PLLA) polymer (Mimetix®), created by The Electrospinning company, for high-throughput applications. This electrospun polymer is formed into a fibrous matrix which mimics the micro-environment of the ECM. The scaffold consists of fibres, 4 µm in diameter, which intertwine to give pores of 15-30 µm, with an overall porosity of 80%. The goal was to develop a better understanding regarding the comparison between spheroids and electrospun scaffold cultures. Aurelia Bioscience currently utilise spheroid cultures for compound and toxicity screening assay, however, are interested in potentially replacing the current spheroid models with another 3D cell culture that does not experience the same analytical issues, caused by problems with diffusion in and out of the culture.

The scaffolds are highly customisable using staining or incorporating particles like quantum dots making them easy to visualise and image. Unstained, Rhodamine 6G stained and quantum dot incorporated scaffold material (which emits at 600 nm) was purchased, to allow a variety of different fluorophore combinations to be utilised (Figure 3.1.). All three varieties of the scaffold also contain iron particles within the strands making them magnetic. The magnet properties allow them to be handled easily, particularly for media changes or changing assay solutions, whilst offering potential for automation in the future.

The objective of this chapter was to optimise a simple and easy culture protocol for both culturing and imaging the two different 3D cell culture models. With the primary focus of developing a cell culture protocol for binding cells to the scaffold material that was automatable and transferable into high-throughout applications.

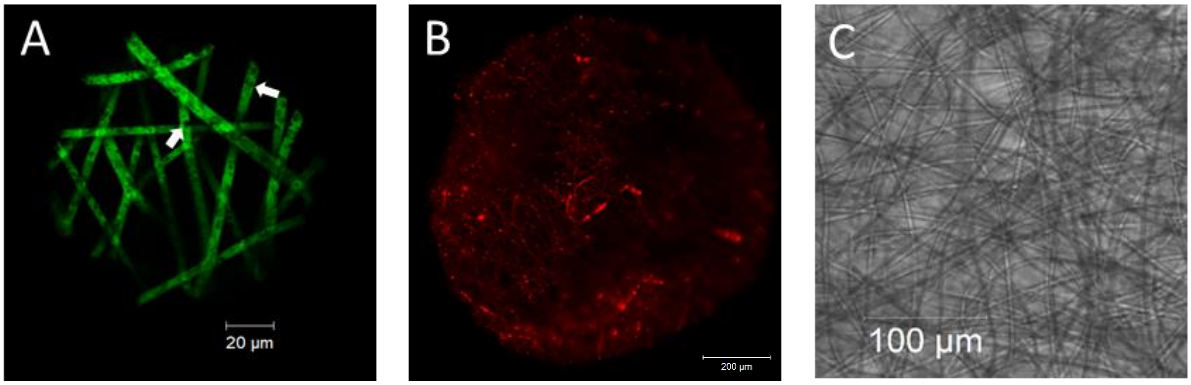

Figure 3.1. (A) Scaffold fibres stained with Rhodamine 6G, arrows highlight the small iron particles within the fibres. (B) Fluorescence image of the excited quantum dots within the scaffold material. (C) Zoomed imaged of the scaffold material. All imaged using a Zeiss Z.1 light-sheet microscope.

Initially the scaffold material was laser cut into 100 µm x 50 µm, with the idea that this size was pipettable and could be automated in this manner. The issue, however, was that it was difficult to count the number of scaffolds per well and due to their small size; could easily be accidentally aspirated, would stick to the meniscus of the media in the well or to the walls of the well itself, and were difficult to see by the naked eye. Therefore, work started using a larger scaffold of 1 mm x 50 µm. The scaffold material was supplied as sheet of A5 and the scaffolds were cut using a 1 mm biopsy punch. The 1mm scaffolds were much easier to visualise during culture and due to being heavier and larger, faced less issues of sticking inside of the well; whilst still being pipettable using a p200 tip with the end removed using a scalpel.

Although the scaffold cultures offer many advantages it was important to ensure that they also had the ability to recapitulate the *in-vivo* environment and had at least similar functionality compared with the currently used spheroid cultures. Spheroids were, therefore, selected to compare with the scaffold cultures. In this case, referring to a single multi-cellular spheroid and not those grown in hydrogels.

There are various spheroid culture methods; each with different advantages and limitations. Hanging drop and ultra-low attachment (ULA) plates were initially identified as the two techniques to test, with liquid overlay technique selected as a cost-effective equivalent to ULA plates (Shen et al., 2021). Both

methods, hanging drop and ULA plates, have a number of advantages in common; they are both available in 96 or 384 format, are relatively inexpensive and allow for co-cultures to be performed (Leite et al., 2016). The hanging drop method however, has the benefit that the spheroid size is controlled by the size of the droplet whereas in ULA plates there is no constraint on size (Messner et al., 2013). Hanging drop techniques are, however, much more labour intensive along with the potential of losing samples through mishandling; they also are more difficult to collect into wells once the spheroids are formed. It is for this reason that InSphero have developed a hanging drop plate (GravityPLUS™) that is paired with a plate-based collection system (GravityTRAP™) that allows for the easy collection of the spheroid once formed (Figure 3.2.)

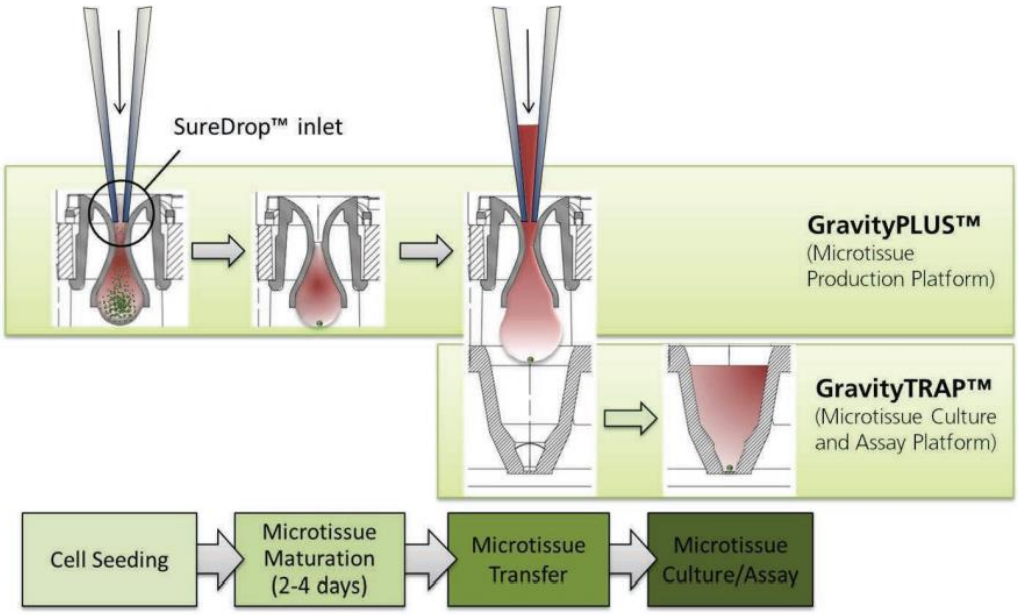

Figure 3.2. Spheroid formation using the GravityPLUS™ plate and subsequent collection to the non-adhesive wells of the GravityTRAP™ plate for further culture or analysis (InSphero, 2015). This system works by adding media to the top of the hanging drop causing the spheroid and droplet to fall into the well below.

Although they reduce the risk of loss or damage during spheroid formation, ULA plates also face issues regarding handling and media changes (Figure 3.3.) and as spheroids formed in hanging drops are typically moved into ULA plates for analysis, both techniques experience these issues.

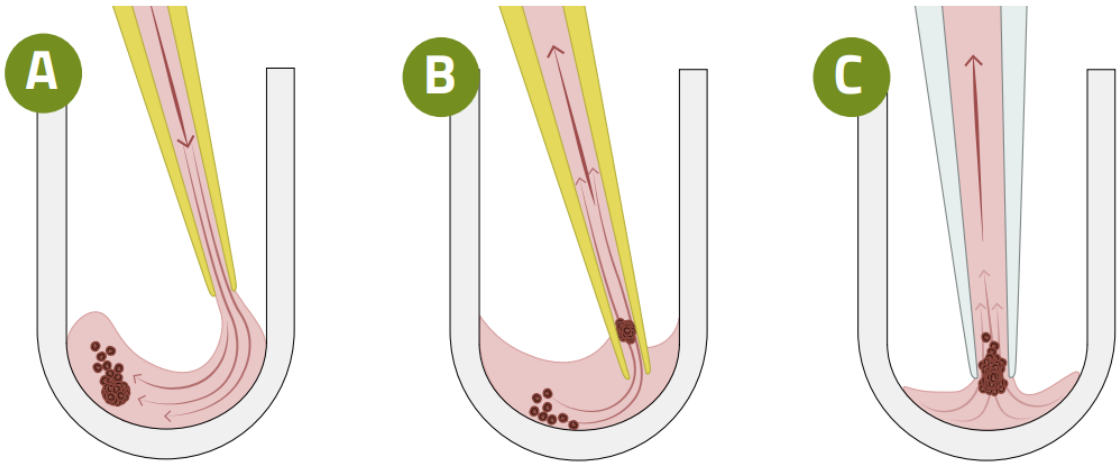

Figure 3.3. Main challenges faced during spheroid manipulation in ULA plates. (A) Destruction of spheroid caused my media flow. (B) Accidental aspiration. (C) Disintegration of spheroid during aspiration (Wardwell-Swanson et al., 2021).

The potential risk of loss or damage associated with spheroid cultures, regardless of culture method, makes them difficult to automate for high-throughput applications and typically requires careful manual handling. The Mimetix® scaffolds not only offer a more robust model due to their sturdier mechanical properties, but through their ability to be manipulated with magnets they can be held at the bottom of wells during aspiration or could even potentially be moved from well-to-well utilising robotics. These features of the scaffolds make them an exciting 3D culture for high-throughput applications.

As discussed previously, the major issue with spheroid cultures is that once over ~ 300 µm in size they start to form a hypoxic core and the diffusion of nutrients, gases and assay reagents to the cells in the centre is dramatically hindered. These scaffold cultures offer the potential to overcome this issue due to their high porosity and thin structure (50 µm). As the thickness of the scaffolds increase with the addition of cells, it was important that the correct seeding distribution of cells is achieved. The aim for scaffold seeding was to have a thin layer of cells on both sides, with minimal clumping, particularly at the edge, and avoid spheroid-like formations. As the cells grow and populate the scaffold over time, the overall thickness of the scaffold will increase, however, it does not exceed 400 µm (for scaffolds

used in this study) and will still maintain some porosity due to the fibrous structure, although it will be greatly reduced from 80%. Here I describe the method development for spheroid formation along with optimisation of scaffold seeding and the imaging of these cultures in 3D to allow for in-depth analysis and cell counting.

3.2. Scaffold-free cell culture

The scaffold-free cell culture methods tested include Ultralow attachment plates, Hanging drop plates and the Liquid overlay technique (Figure 3.4.). These methods were selected based on their practicality and availability. The liquid overlay technique was specifically chosen to test a cheap alternative to ultralow attachment plates.

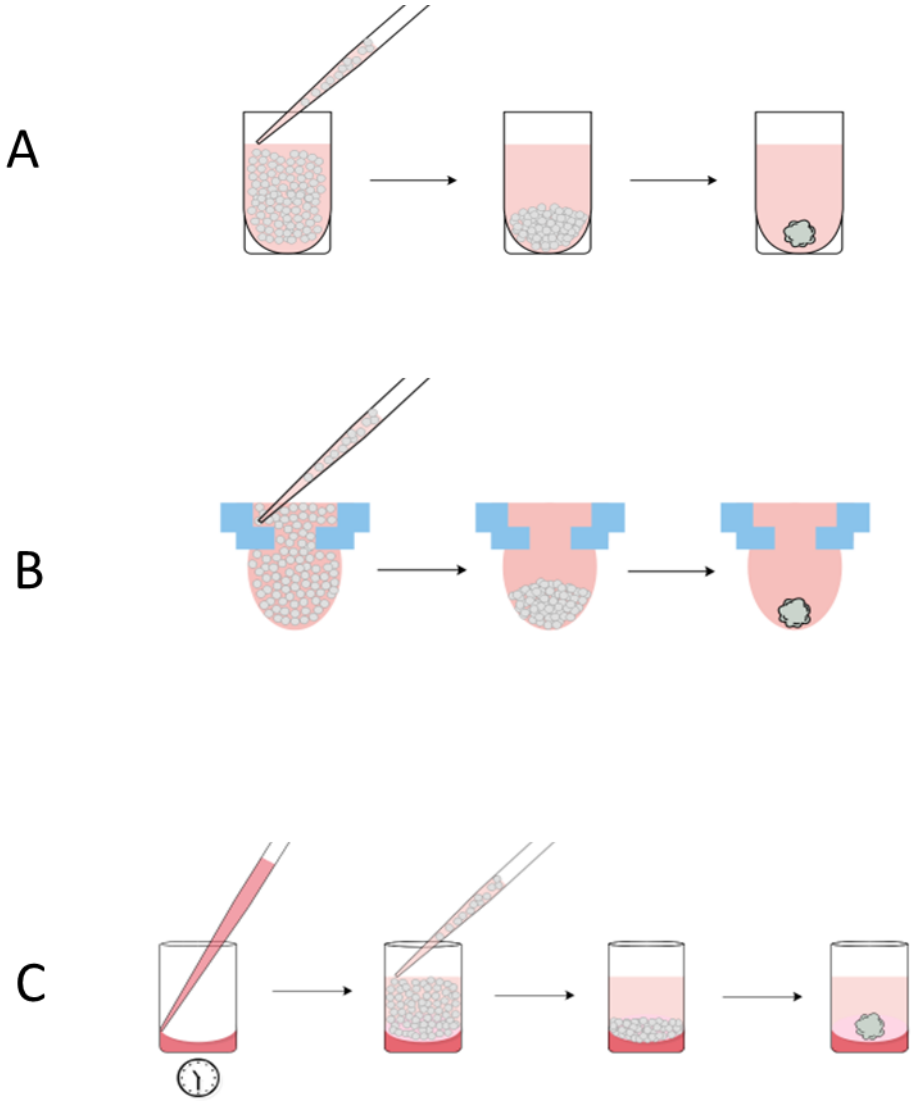

Figure 3.4. Spheroid formation using scaffold-free tissue culture techniques: Ultralow attachment plate (A), Hanging drop plate (B), Liquid overlay technique (C). All methods work through the accumulation of the cells at the bottom of the droplet or well before they accumulate into a spheroid.

For each of these scaffold-free methods, cell suspension is pipetted into the well where the cells cascade down the edge of its low attachment surface, aggregating in the centre to form a spheroid. In the case of the liquid overlay technique, 100 µL of 1.5% agarose in DMEM was pipetted into the wells of a standard 96 well tissue culture plate, which once cooled formed a low attachment surface.

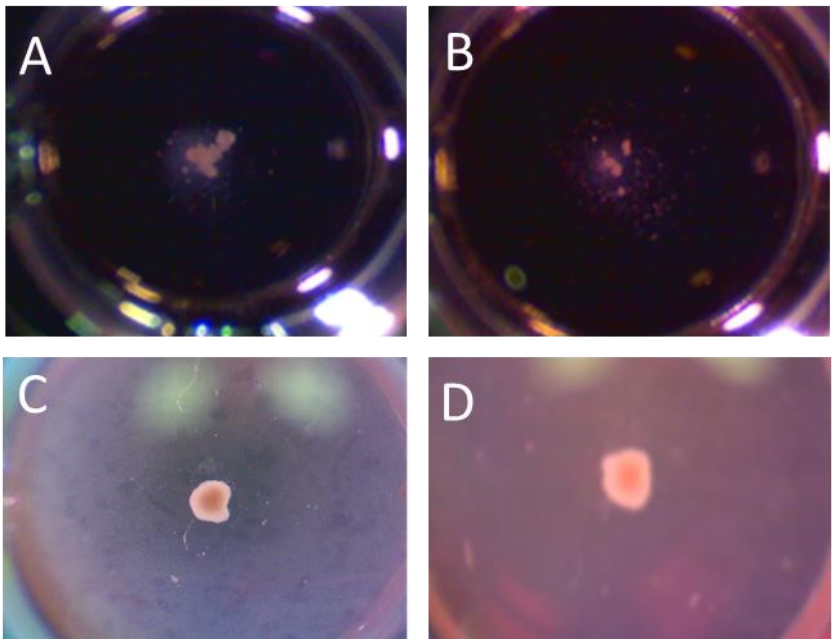

Figure 3.5. Typical cell growth pattern seen when attempting to form spheroids using the Liquid overlay technique (A, B). Ultralow attachment plates (C) and hanging drop (D), consistently formed a single spheroid per well. All spheroids were grown for 4 days with a seeding concentration of 500 cells per well.

Of the three scaffold-free cell culture methods, the liquid overlay technique was the only culture method that did not form a single spheroid per well, likely due to an inferior low attachment surface when compared to ULA plate coatings (Figure 3.5.). Both the ULA and hanging drop plates reliably produced single spheroids per well and gave high yields. Hanging drop was then selected of the two successful techniques for a few reasons. Firstly, the ULA plates are expensive and upon testing are not reusable for spheroid formation. The hanging drop plates (Perfecta3D® hanging drop plates), however, are re-usable for up to three times, after soaking in 70% ethanol for an hour, without the risk of infection. Secondly, it was important to try to keep the spheroids as small as possible to limit issues of diffusion, hanging drops hinder the grown of the spheroids, to a point, unlike the ULA plates which have a large area for them to grow in. The smallest seeding number of cells that reliably formed a spheroid was also optimised to reduce spheroid size, with culturing 500 cells per well for fours days, giving the smallest spheroids that were still manipulatable and stable.

Finally, the hanging drop method also allows all the spheroids to be collected simultaneously by placing the 96 well hanging drop plate over a 245 mm tissue culture dish and washing with media. This is similar in theory to the InSphero GravityPLUS™ and GravityTRAP™ systems from InSphero, however, results in all the spheroids in a single suspension where they can be collected for imaging or moved to plates for biochemical analysis. This is beneficial for imaging using the Zeiss Z.1 light-sheet microscope as multiple spheroids can be loaded in a single capillary. It is also allowed the cultures to be easily visualised, compared to within wells, when transferring them to plates for analysis. To avoid the losses associated with spheroid cultures, spheroids were moved to standard tissue culture 96 well plates ~3 hours before any biochemical analysis was performed. This allowed time for the cells at the bottom of the spheroids to bind to the plate, which aided in keeping them at the bottom of the well and reduced the risk of them being them being aspirated when changing solutions.

3.3. Scaffold cell culture optimisation

Initially work began using the 100 µm diameter scaffolds, however, after a couple of months of work with these smaller scaffolds various problems became evident. Whilst being 'pipettable' the micro-scaffolds were too small to handle efficiently, and it was difficult to quantify the number per well. They were also difficult to image and seed with cells. It was therefore decided that work would begin using a larger version of the Mimetix® scaffold. Scaffolds 1 mm in diameter were created using a biopsy punch from a A5 sheet of electrospun PLLA polymer. To culture these larger scaffolds, various culture methods were tested to achieve the desired distribution of cells. The aim for the scaffold was to culture an even layer of cells across the entire scaffold surface, avoiding spheroid like clumping. This was important as the aim was to perform a comparison specifically between cells cultured in a spheroid/tissue like model and cells cultured completely on the PLLA scaffold.

Three methods were decided on to test culturing cells on the 1 mm scaffolds: Lawn culture, Hanging drop and ULA plates (Figure 3.6.A-C).

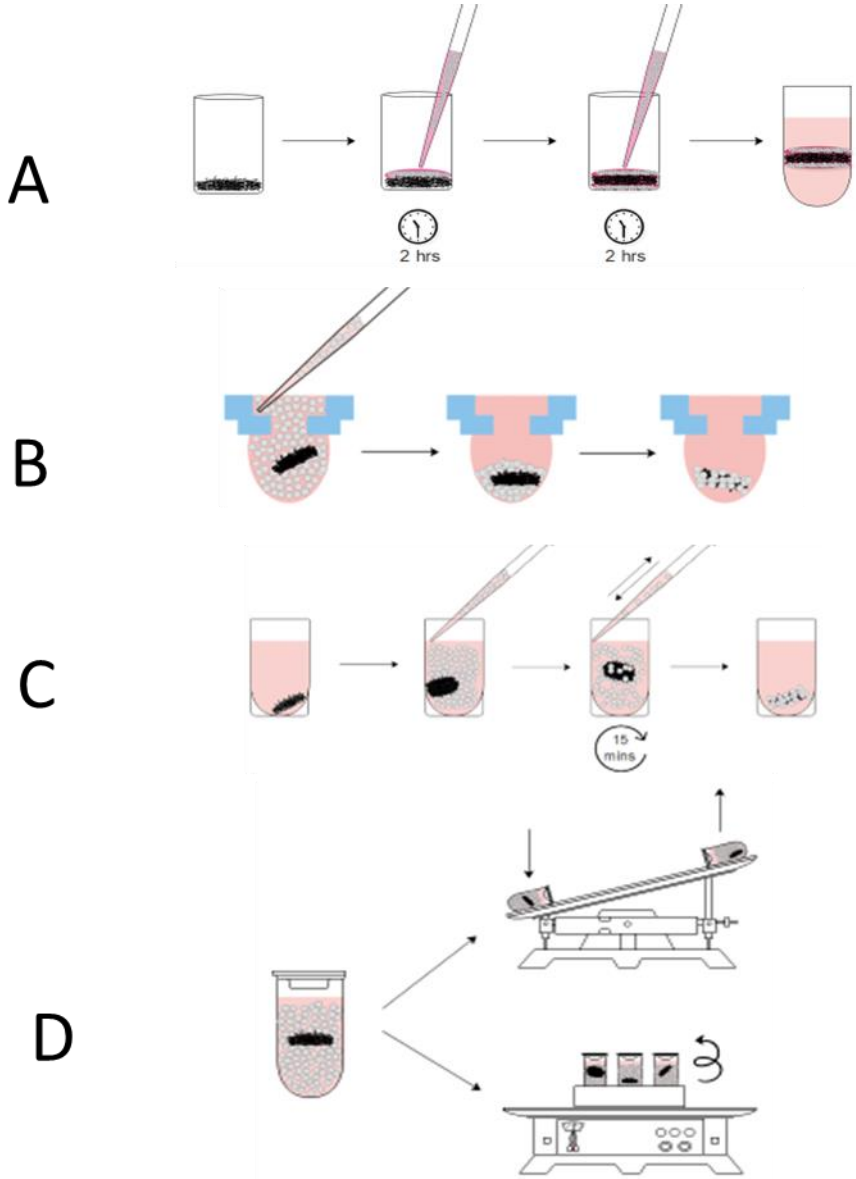

Figure 3.6. Techniques for culturing cells onto the Mimetix® scaffolds. Lawn culture technique (A), Hanging drop (B), ULA plate (C), Loose/suspension using available lab equipment (D).

The lawn scaffold technique (Figure 3.6.A), also referred to as the drop-on method, involved placing the scaffold at the bottom of a tissue culture well. Cell suspension was added to the top of the scaffold and left for 2 hours. The scaffold was then flipped 180° and again cell suspension added. After a further 2 hours the seeded scaffold was transferred to an ultralow attachment well or a hanging drop for the remainder of the culture.

For the hanging drop method (Figure 3.6.B) scaffolds were placed either in droplets of cell suspension formed on the lid of a Petri dish or in droplets made using a specialised 96 well hanging drop plate (Perfecta3D® hanging drop plates). Once formed droplets were left undisturbed for 4 days.

The third culture method utilised ultra-low attachment plates (Figure 3.6.C), the scaffold was placed into the well and cell suspension added. The scaffold was then re-suspended every 15 minutes by pipetting up and down inside the well over a 2-hour period.

Multiple cell seeding concentrations and other conditions such as droplet size or time in between resuspension were trialled for each method and the resulting scaffolds were imaged using the Zeiss Z.1 light-sheet microscope. The quantum dots within the scaffold fibres fluoresce in the red (600 nm) and the nuclei of the cells were stained using Hoechst 33342 allowing the distribution of the cells across the scaffolds to be easily studied.

3.4.1 Lawn culture technique

The lawn culture technique posed multiple experimental issues including keeping the cell suspension on top of the scaffold as well as difficulties manipulating the scaffold through 180°. It also produced a clumped and uneven distribution of cells across the scaffolds. The cells formed into spheroid-like masses on the scaffold, particularly around the edges, with most scaffolds having the majority of cells on only one side (Figure 3.7.).

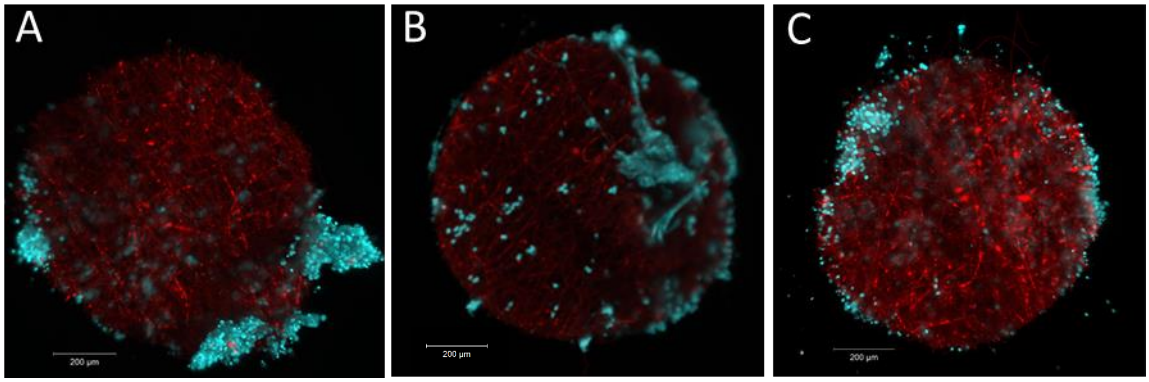

Figure 3.7. Representative images of scaffolds cultured using the Lawn culture technique. Various seeding concentrations of HepG2 cells (25,000 – 150,000 cells/ mL) and incubation times (30 mins – 180 mins) were used for these scaffolds. The quantum dots within the PLLA fibres of the scaffold emit in the red whilst the nuclear Hoechst dye emits in the blue. (Scale bar = 200 µm).

The main issue regarding the lawn culture technique was the ability to manipulate the smaller (1 mm) scaffolds using tweezers or a pipette to ensure that cells were seeded on both sides rather than one side twice. After a discussion with Dr Stefan Przyborski, Professor of Cell Technology, Durham University, at a conference regarding the culture of the scaffold cultures, holders utilised for Alvetex® scaffolds were supplied. These holders clamp the scaffold between two pieces of plastic and are then inserted into either a 6 or 12 well plate (Figure 3.8.A). This allowed the scaffolds to be seeded with cells, ensuring that all of the cells land on the surface, with seeding densities of 500,000 to 3,000,000 cells per side of scaffold tested. The scaffold was then be flipped through 180° and reinserted into the holder. The holders required a much larger piece of scaffold material making it easier to manipulate. The desired size (1 mm) was then cut using a biopsy punch from this larger piece of cell laden, scaffold material. This method worked well for initial cell seeding, achieving an even and well populated distribution as all the cells landed on the scaffold, however, an issue arose when cutting this larger piece into the desired diameter of 1mm. The biopsy punches utilise a plunger to remove the scaffold from inside of the punch and it appeared that this action was removing the attached cells from the scaffold material, even if the cells were given long periods (24/48 hours) to attach (Figure 3.8.B,C). There were also concerns regarding the health of the cells after cutting as the process is slow and

required the scaffolds to be removed from the incubator for long periods, even if cut in small batches, along with the cutting and plunging action itself causing physical damage.

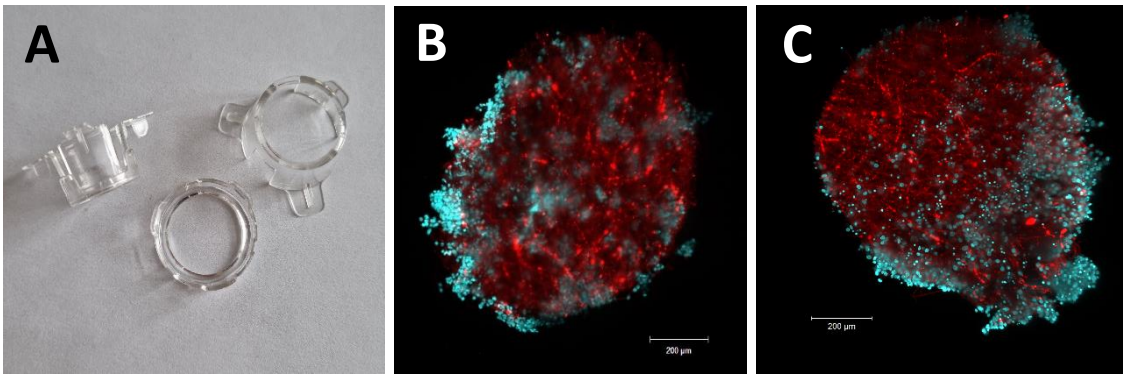

Figure 3.8. Alvetex® holders (A) and representative images of scaffolds cultured using them (B,C). After cutting the scaffolds, areas of the scaffold material became unpopulated by HepG2 cells even though they were even covered prior to cutting. Cell densities of 3 x 10^6 cells per well were used (B, C). The quantum dots within the PLLA fibres of the scaffold emit in the red whilst the nuclear Hoechst dye emits in the blue. (Scale bar = 200 µm).

3.4.2 Hanging drop technique

The hanging drop method was technically more difficult to set up compared to the ULA plates whilst having the potential for loss of cultures through mishandling. It did offer the potential of high-throughput production of the scaffolds, with the 96 well plate, but the distribution of the cells across the scaffold was poor. The cells collected around the edge of the scaffold likely due to the cascade of the cells within the droplets and without agitation clumped around the edge and remained there (Figure 3.9.). Even at higher cell concentrations the cells still aggregated around the edge of the scaffold with few cells coating the centre (Figure 3.9.C).

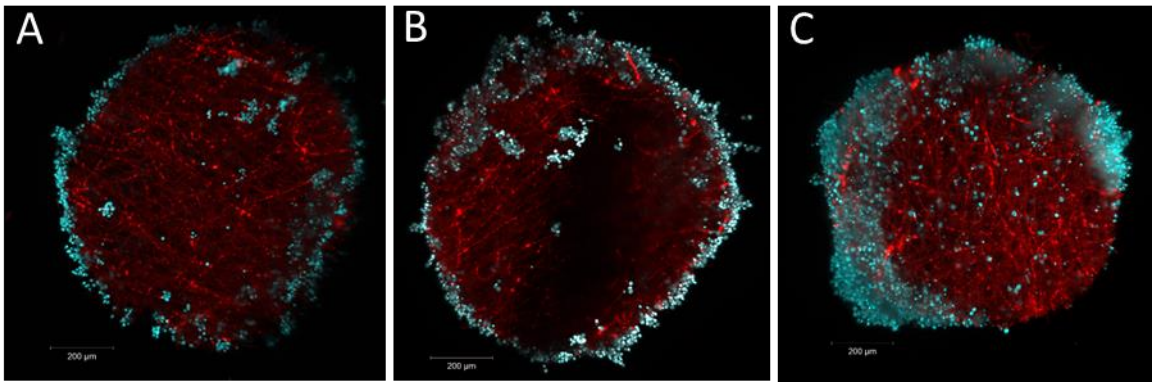

Figure 3.9. Representative images of scaffolds cultured using the Hanging drop technique. Various seeding concentrations of HepG2 cells (25,000 – 150,000 cells/ mL) and droplet sizes (30 – 50 µL) were used for these scaffolds. The quantum dots within the PLLA fibres of the scaffold emit in the red whilst the nuclear Hoechst dye emits in the blue. (Scale bar = 200 µm).

3.4.3 ULA plate technique

Using the ultra-low attachment plates to culture the cells onto the scaffold was the most practical and easy to perform protocol, although inconvenient due to the repeated need to re-suspend the scaffolds manually. Of the three methods tested the ULA plates represented the desired distribution of cells most whilst also being possible for high-throughput production in a 96 well plate (Figure 3.10.). Although there were still high quantities of cells around the edges of the scaffold, the number of cells on the centre of the scaffolds increased, as well as having similar coverage on both sides. This is likely due to the repeated re-suspension of the cells and the scaffold giving them more opportunity to bind to one another.

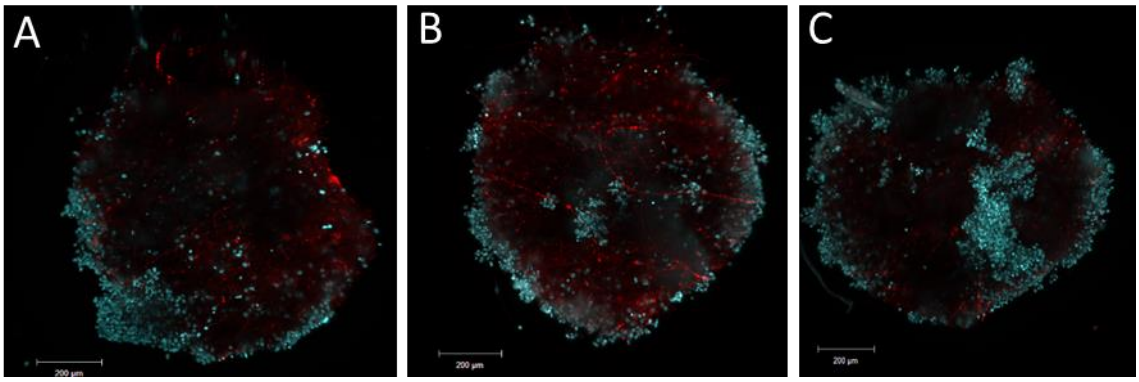

Figure 3.10. Representative images of scaffolds cultured using ultra-low attachment plates. Various seeding concentrations of HepG2 cells (25,000 – 150,000 cells/ mL) and amount of times re-suspended were used for these scaffolds. The quantum dots within the PLLA fibres of the scaffold emit in the red whilst the nuclear Hoechst dye emits in the blue. (Scale bar = 200 µm).

The ULA plate method was optimised regarding cell seeding concentration. However, the distribution remained the same as the examples shown in Figure 3.10. to attempt to further improve the binding of cells to the scaffolds many different parameters were tested (Table 3.1). The binding of cells to the surface of the scaffold (excluding the outer edge) was quantified to determine if any of the parameters improved scaffold population using FUJI.

Table 3.1. Parameters tested to improve cell-scaffold binding

Culture parameter	Conditions	Theory	Result
Scaffold type	• Unstained • Rhodamine 6G • Quantum dots	• To check that scaffold type was not effecting cell binding	• No difference was observed
Sterilisation technique	• RO water • Ethanol	• RO water was tested as a non-solvent sterilisation method • Ethanol is a standard sterilisation method	• No difference in binding was observed • Longer sterilisation with high ethanol concentrations impacted scaffold structure
Coatings	• Poly-L-Lysine • Fibronectin • Collagen-I	• Coatings have been shown to improve hepatocyte function (1,2,3,4) • ECM protein coatings also improve binding (1,4)	• No increase in cell binding was observed for any of the coatings even at different concentrations • Coatings reduce scaffold porosity
Dissociation technique	• Versene • Trypsin • Cell scraper	• Trypsin cuts adhesion proteins, it takes time for cells to replenish them for binding • Versene is a calcium chelator and avoids breaking these bonds	• Cells dissociated using just Versene showed increased binding by up to 13.8 % (n = 10) • Using Versene and a cell scraper resulted in large/spheroid like clumps
Pre-wetting the scaffold	• PBS • Serum-free media • Complete media • Dry (no pre-wetting)	• Pre-wetting with complete media is recommended by the scaffold manufacturer. • Length of time and different wetting agents were tested	• Dry scaffold showed poor binding • Different solutions showed no change
Resuspension events	• Number of total resuspension events • Frequency	• The number of collisions of cells and scaffolds appears to improve binding • Do cells need time to settle onto the scaffold?	• Higher numbers of total resuspensions improved scaffold population by up to 38.2 % coverage (n = 10) • Higher frequency improved scaffold population by up to 25.7 % coverage (n = 10) • Move opportunities for collisions improved cell distribution
Cell passage	• Passage number	• Earlier passages often have weaker binding in 2D cultures, particularly if recently thawed	• No difference was observed
Cell type	• HepG2 • U87 • Hela • HEK293T	• Important to determine if the binding issues were caused by cell type • HEK293T cells typically have weak binding	• No difference was observed for U87 and Hela cells • HEK293T cells showed reduced binding
Confluency	• Cell confluency in 2D	• Cells may have better binding efficiency if in a higher growth stage	• No difference was observed

(1) Dehili et al., 2006; (2) Wang et al., 2016; (3) Brown et al., 2018; (4) Das et al., 2020)

3.4.4 Continuous suspension technique

From testing the different parameters in Table 3.1, it became apparent that the use of Versene to dissociate cells along with the total number and frequency of resuspension events should be the focus to achieve the desired cell distribution. As a larger total number of resuspension events at a high frequency delivered the best scaffold coverage it was evident that culturing the scaffolds in continuous suspension would improve binding by greatly increasing the collision interactions between the scaffolds and the cells.

To achieve continuous suspension of the cells and scaffolds would be impossible manually and therefore, would require automation. Whilst simple in theory, the ability to perform tissue culture over a prolonged time period, whilst continually agitating the culture vessel was not something that the lab was equipped for. It was particularly challenging due to the need for a culture vessel that was sealed to help prevent infection as well as the spillage of the cell/scaffold suspension but, still allowed gas exchange to take place.

Two different pieces of equipment were found that were suitable for installation inside of a tissue culture incubator (Figure 3.6.D). The first was a rocker which moves the scaffold side to side within the cell suspension and the second, a heating block orbital shaker which rotates the culture vessel clockwise through 360 °.

Scaffolds were initially cultured in various vessels including 3.5 cm petri dishes, tissue culture flasks, sealed 1.5 mL Eppendorf's and 5 mL test tubes with varied volumes, cell concentrations and agitation speeds. The resulting scaffolds had a range of coverages; some with large masses of cells covering sections of the scaffold (Figure 3.11.A), others completely engulfed by cells (Figure 3.11.B) and finally, several scaffolds that had complete and even coverage however, still had large clumps of cells in some areas (Figure 3.11.C).

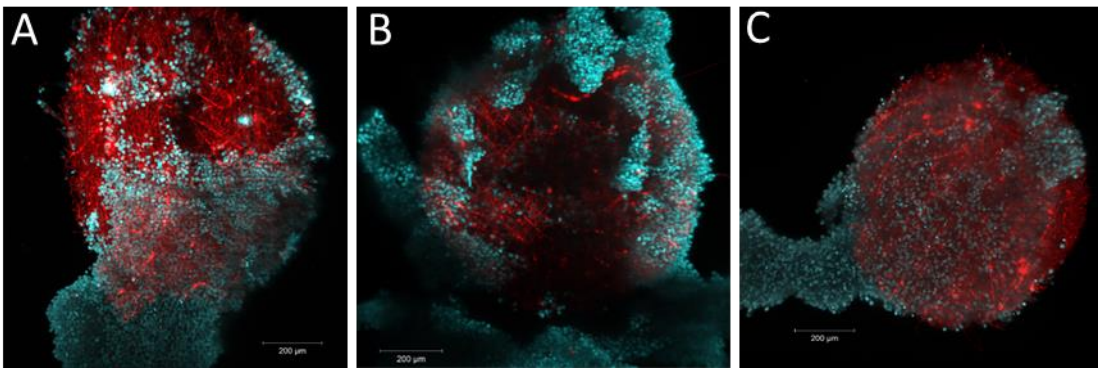

Figure 3.11. Representative images of scaffolds cultured using various suspension techniques. Various seeding concentrations of HepG2 cells (25,000 – 150,000 cells/ mL), culture vesicles and agitation methods were used for these scaffolds. The quantum dots within the PLLA fibres of the scaffold emit in the red whilst the nuclear Hoechst dye emits in the blue. (Scale bar = 200 µm).

Due to the successful coverage of some scaffolds using the suspension techniques it was evident that with optimisation this approach could achieve the desired cell seeding and would, therefore, be the method of focus for the culture of cells onto the PLLA scaffolds. The method also required minimal scaffold handling, particularly scaffold laden with cells, and was more efficient, automatable and less time consuming compared with the lawn culture technique.

The most appropriate vessel for the scaffold culture was the sealed tubes as they prevented leakage and infection whilst allowing easy optimisation of the media volume and tube size to keep the scaffold in continuous suspension.

For the orbital shaker, specialised CELLSTAR® 4.5 mL tubes with "tissue culture lids" were utilised (https://shop.gbo.com/en/england/products/bioscience/cell-culture-products/cellstar-cell-culture-tubes/120190.html). These lids have two positions, one of which is fully sealed and another that holds the lid slightly open to allow gas exchange. Although fine for the orbital shaker as they are positioned upright, these tubes were not appropriate for use on the rocker as they would leak.

The optimal conditions to maintain the scaffold in suspension using the heating block shaker were, 2 mL supplemented DMEM and shaking continuously at 750 rpm. The scaffolds were cultured at various

cell concentrations, with 175 cells / µL being found to be optimal for giving the scaffold an even coverage. Although the coating of the scaffolds was dramatically improved and very close to the desired distribution there was still a large amount of cell clumping around the edges (Figure 3.12.).

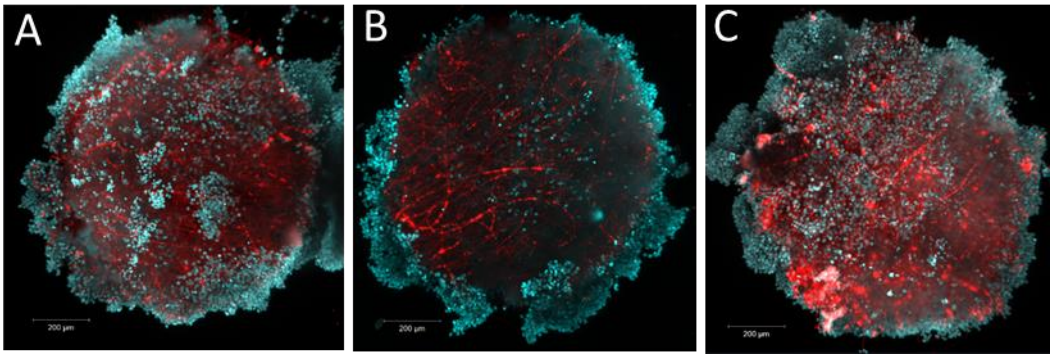

Figure 3.12. Representative images of scaffolds cultured using shaking suspension techniques. The scaffolds were cultured in 2 mL supplemented DMEM with 175 HepG2 cells / µL. The quantum dots within the PLLA fibres of the scaffold emit in the red whilst the nuclear Hoechst dye emits in the blue. (Scale bar = 200 µm).

To culture the scaffolds on the rocker 1.5 mL Eppendorf's were used, using the same cell concentration (175 cells / µL) as the shaker, and taping them down horizontally at the end of the rocking platform with a speed of 1 rocking cycle every 2 seconds. The tubes were filled with 1 mL of cell suspension, leaving a small pocket of air for gas exchange, the bubble of air within the tube also helped with agitation of the scaffold and ensured it did not remain stuck to the side.

To initially test the ability of the rocker to culture the scaffolds they were cultured in sealed Eppendorfs, opening daily for 20 minutes to allow gas exchange. The resultant scaffolds had an even and ubiquitous distribution of cells (Figure 3.13.) fitting the desired aim for the scaffold cultures. The problem however was that although the culture conditions are optimal for cell distribution, there was a lack of gas exchange. To solve this, different approaches were tested to modify the Eppendorfs to allow gas exchange including culturing at different angles, sealing them with breathable film and designing new 3D printable lids. These approaches, however, were not promising and either lead to leakage or infection of the culture.

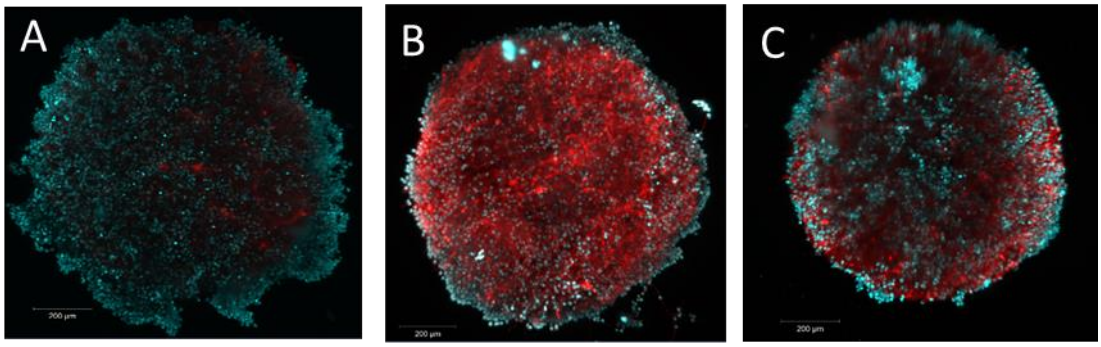

Figure 3.13. Representative images of cells cultured on scaffolds using rocking suspension technique in sealed Eppendorfs. The scaffolds were cultured in 1 mL supplemented DMEM with 175 HepG2 cells / µL. The quantum dots within the PLLA fibres of the scaffold emit in the red whilst the nuclear Hoechst dye emits in the blue.

Building on the idea of using a breathable film, lids were created using Polydimethylsiloxane (PDMS) that allowed gas exchange. PDMS is a hydrophobic, silicon based organic polymer that has an oxygen diffusion coefficient similar to that of water, making it the ideal material for biological applications (Cox & Dunn, 1986; Cussler, 2009). Firstly, the inner area of a tube was removed by melting a hole using a soldering iron and then tidied up using a scalpel (Figure 3.14.A). This inner area of plastic was then replaced with a thin layer of PDMS by placing the lids top down in a thin layer of liquid PDMS and pushing down firmly (Figure 3.14.B). Once the PDMS had cured the lids were removed and any excess cut off using a scalpel. After testing, 1.5 mL cryovials were found to be more effective as their lids are more robust and held up better to the removal of the centre piece compared with Eppendorf, pop lids. It is evident from figure 3.14.C that in the 1.5 mL sealed tube (middle) the phenol-red within the media has changed to a more yellow shade due to a decrease in pH, caused by the presence of the cells, whereas the tube with the modified PDMS lid (Right) has remained unchanged in colour, similar to that of the tube used for the orbital shaker (Left). The tubes were cultured in the same conditions with the same number of cells, however, the CO_2 was not able to buffer the media in the sealed tube resulting in the colour change, indicating that the PDMS lid is allowing gas exchange.

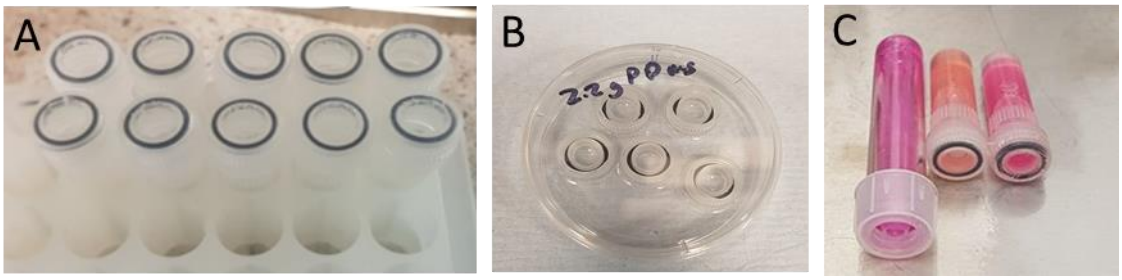

Figure 3.14. Modification of 1.5 mL cryovials for tissue culture. (A) Tubes with the inner area removed, (B) Lids curing in PDMS to form a breathable lid, (C) 5 mL tube used for culturing the scaffolds on the shaker (left), 1.5 mL tube without modification (middle), 1.5 mL tube with modified PDMS lid (right).

Using the modified tubes and the same conditions as the 1.5 mL Eppendorfs, the same ubiquitous distribution across the scaffolds was achieved (Figure 3.15.). This method allowed the culture of cells on the scaffolds with the desired distribution using a method that less labour intensive (once the tubes are made) and automated.

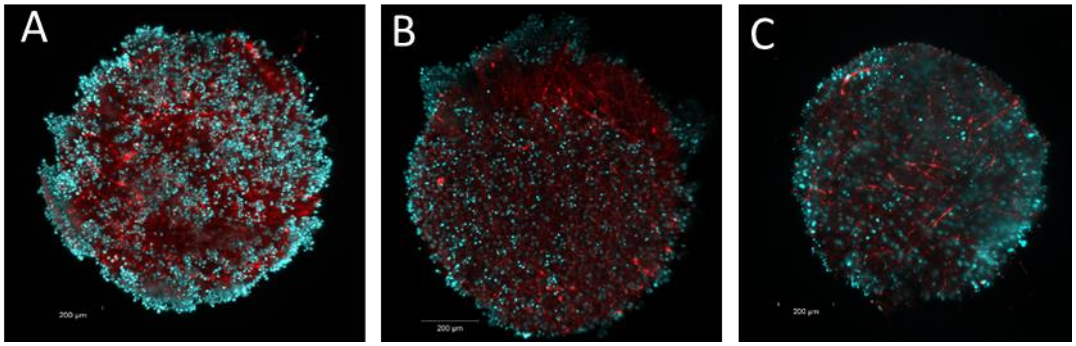

Figure 3.15. Representative images of scaffolds created using rocking suspension technique with modified PDMS tubes. The scaffolds were cultured in 1.4 mL supplemented DMEM with 175 HepG2 cells / µL. The quantum dots within the PLLA fibres of the scaffold emit in the red whilst the nuclear Hoechst dye emits in the blue.

This method of culturing the scaffolds in cryovials with PDMS lids is effective and achieves the even distribution of the cells desired. The issue, however, is that only one scaffold can be cultured per tube or they aggregate and are difficult to separate. This makes utilising this method for high-throughput applications a major bottle neck as each scaffold, once seeded with cells, must be washed to remove

any excess, unbound cells and transferred to a 96 or 384 ULA plate for use. This process would take hours for large numbers of scaffolds and although suitable for the application of comparing scaffolds with spheroids, if the goal is to apply these scaffolds to high-throughput screening it is unfeasible. We therefore started to look for alternative culture vessels and apparatus to increase scaffold yield.

Bioreactors were the obvious direction and in 2021, CELVIVO released the ClinoStar®, a climate-controlled system that holds up to 6 ClinoReactors® (Figure 3.16.). These small bioreactors rotate through 360°, at a speed determined by the user, and are designed to produce high volumes of spheroids and organoids. They consist of two chambers; a main cell culture chamber and a humidification chamber which are separated by a gas permeable membrane. This membrane allows gaseous exchange, whilst the humidification chamber reduces evaporation and maintains the culture volume. Upon receiving the ClinoStar® system for a trial period, its ability to culture 1 mm scaffolds at a high volume was tested. 100 scaffolds per bioreactor were tested, as this number would give enough scaffolds to fill a 96 well plate without too much crowding in the culture chamber.

To culture spheroids or organoids in these reactors they can either be pre-formed using another method and inserted into the chamber or formed from a single cell suspension within the chamber. For this to occur, the manufacturers insist that the chamber must be free from bubbles so that the spheroids or organoids are not disturbed by colliding with them. When this method was tested with the scaffolds, they would aggregate in the centre of the chamber within a few hours, no matter the rotation speed or number of dispersal functions (the system allows the user to set the bioreactor to quickly change direction three times to disperse the 3D cultures before returning to normal rotation). Bubbles were deliberately introduced into the cell culture chamber and found that their presence prevented clumping by colliding with scaffolds and breaking them free from one another. The rotation speed and number or dispersal functions was optimised, with 35 rpm and a dispersal every minute found to hold the scaffolds in suspension. It is important to check the Scaffolds periodically as once laden with cells the rotation speed must be increased to maintain them in suspension.

Figure 3.16. Left - ClinoStar® system from CELVIVO. This system is a climate-controlled bioreactor designed for the formation of spheroids and organoids. Right - ClinoReactor® for use in the ClinoStar® system. (A) Top plug for the addition and removal of media, (B) Vents for gaseous exchange, (C) Chamber for humidification, (D) Pretri dish style lid to allow for easy collection, (E) Culture chamber, (F) Port for access to culture chamber, (G) Port for the hydration chamber, (H) Feet to allow the chamber to stand.

Once cultured in a ClinoReactor® for two days the scaffolds become laden with cells in the desired distribution (Figure 3.17). Utilising the magnetic properties of the scaffold material, by placing a strong magnet underneath the cell culture chamber, it is possible to easily remove all the unbound cells using a 5 mL strippette, via the port, without risk of loss (Figure 3.16.F). The scaffolds can then be resuspended in media and cultured for longer in the ClinoStar® system or removed from the culture chamber and distributed into a 96 well ULA plate. It also allows the possibility of co-cultures, firstly by seeding one cell type before washing and adding a second or third suspension, in a density dependent manner by controlling the number of cells in the culture chamber along with the length of time in culture.

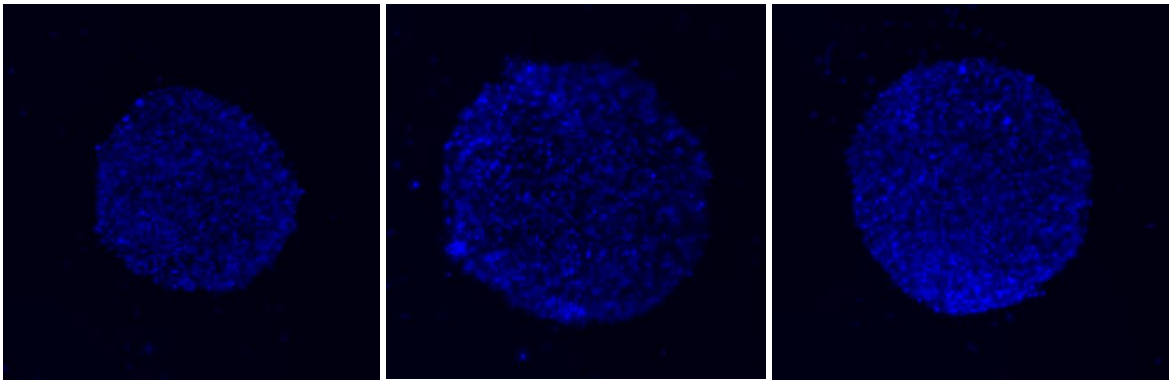

Figure 3.17. Representative images of scaffolds created using the ClinoStar® system . The scaffolds were cultured in supplemented DMEM with 175 HepG2 cells / µL. Cells were stained with Hoechst and imaged using the EVOS cell imaging system.

The spheroid culture optimisation process was a far simpler task when compared to the optimisation of covering the scaffold material with cells in the desired distribution. This was due to spheroid culture being well documented in the literature along with the unique geometry of the scaffold material, resulting in trial-and-error approach to be taken. Conventional polymer scaffold population techniques including the 'drop-on' method and seeding cells in a well did not translate to the smaller sized scaffold used in this work, with repeated collisions between the cell and scaffold proving to be the best approach to achieve a ubiquitous cell coverage across the scaffold surface. Beginning with modified cryo-vials, this continued suspension approach was optimised until the desired cell population was attained, although this method was tedious and not scalable for high-throughput applications. Utilising the same principles of continued suspension of the scaffolds in cell suspension, in a container that allowed gas-exchange, the ClinoStar® system was tested as an alternative technique that allowed the production of higher volumes of scaffolds.

This system allows access to all the scaffolds at once with simple media changes and collection, whilst enabling high volumes to be cultured, efficiently and in a non-time-consuming manner. This permits the scaffolds to be produced for high-throughput applications and the industrial partner has since

purchased the ClinoStar® system to enable them to begin utilising the scaffold cultures in their bioassays and screening trials.

3.4. 3D culture growth

The two models were cultured for 4 weeks to allow for comparison; day 1 here refers to cultures that have been in culture for 4 days as the spheroids form and scaffolds are seeded with cells. Hepatic function has been shown to change over time, so it is important to study the cultures at different time points (Bokhari et al., 2007a; Kammerer, 2021; Lauschke et al., 2016).

Spheroids and scaffolds were imaged using a EVOS Cell Imaging System at the same laser intensity (Figure 3.18.). In the spheroid culture it is possible to see the increased density of cells in the centre as they grow and compact. By day 28 the spheroids begin to branch out and grow evenly, likely due to only the outer layer of cells being healthy enough to proliferate. HepG2 spheroids at day 7 have an average shortest diameter of 323 µm (n = 15) meaning that by this point they will likely begin to form hypoxic cores and by day 14 have an average shortest diameter of 553 µm (n = 15). At day 28 spheroids had an average shortest diameter of 768 µm (n = 15) with some having diameters similar in size to that of the scaffold (~1000 µm); likely resulting in large hypoxic and necrotic areas within the culture. These predicted hypoxic and necrotic areas within the spheroids will result in unhealthy cultures and will impact biochemical results, particularly for hepatotoxicity testing. This highlights the issue of spheroid cultures, regarding continual growth, unless using a cell line that exhibit strong contact-inhibition like C3A cells which are a subclone of HepG2 cells (Gaskell et al., 2016).

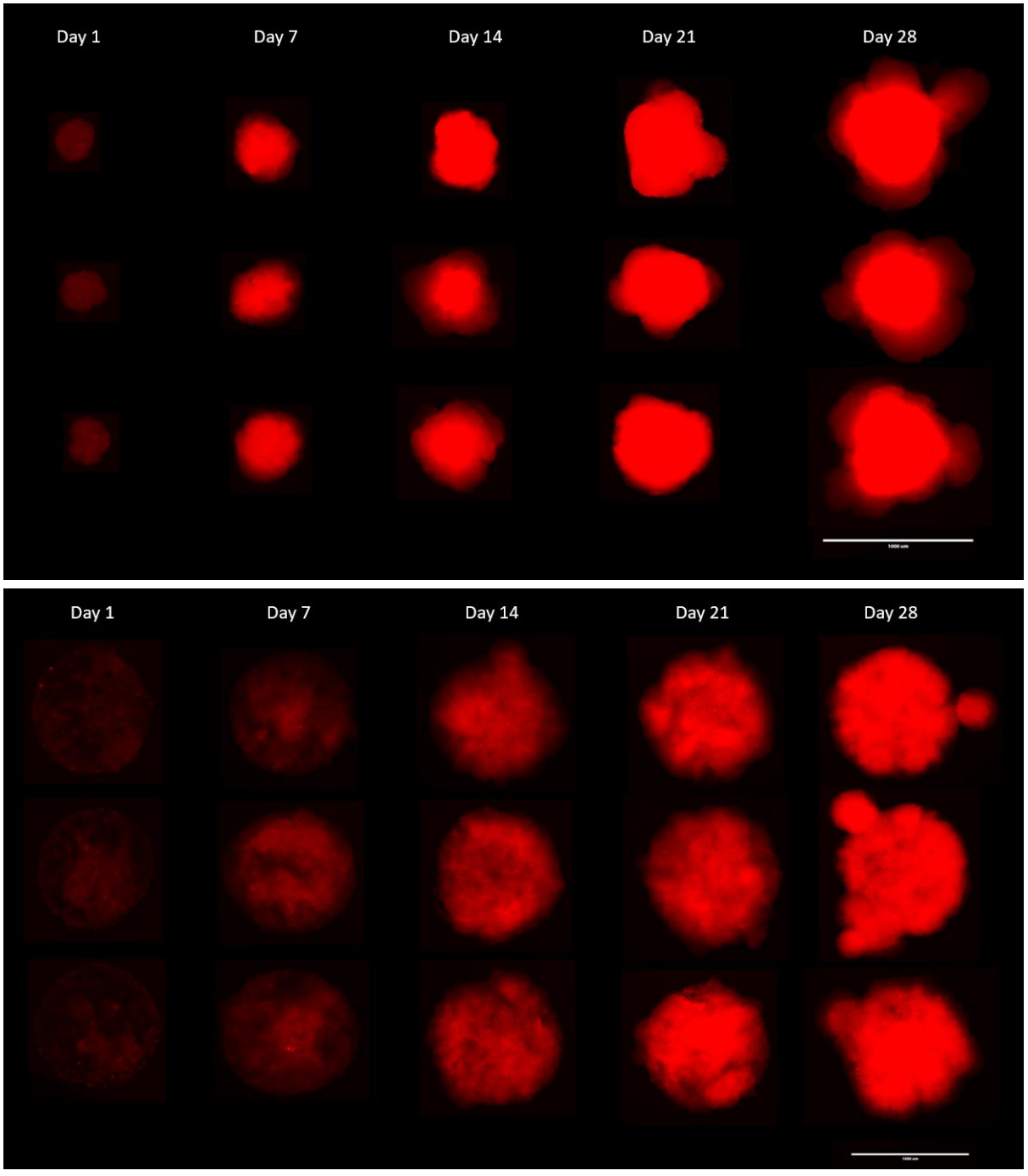

Figure 3.18. (Top) Spheroid and (Bottom) Scaffold growth over time. Both cultures remain compact at 21 days, however, begin to form additional growths by day 28. By day 28 the spheroids are larger than the scaffolds and will likely have large hypoxic cores. All cultures were imaged at the same laser intensity using a EVOS cell imaging system. HepG2 cells which have been stably transformed to express RFP-H2B in their nuclei were used (Scale bars = 1000 µm).

Cells on the scaffold grow over time and begin to populate the outer surface of the scaffold. Like the spheroids, by day 28 they also begin to form small spheroid-like growths. Scaffolds at day 21 had an average widest diameter of 287 µm (n=15) (Figure 3.19). Although this is close to the range to avoid the formation of a hypoxic core, the scaffold cultures do not fully populate the centre of the scaffold and mostly grow in a thick layer surrounding the scaffold instead. This means that on the most part, it is not expected that the scaffold cultures will not possess hypoxic areas and, therefore, are more reliable for applications in hepatotoxicity screening.

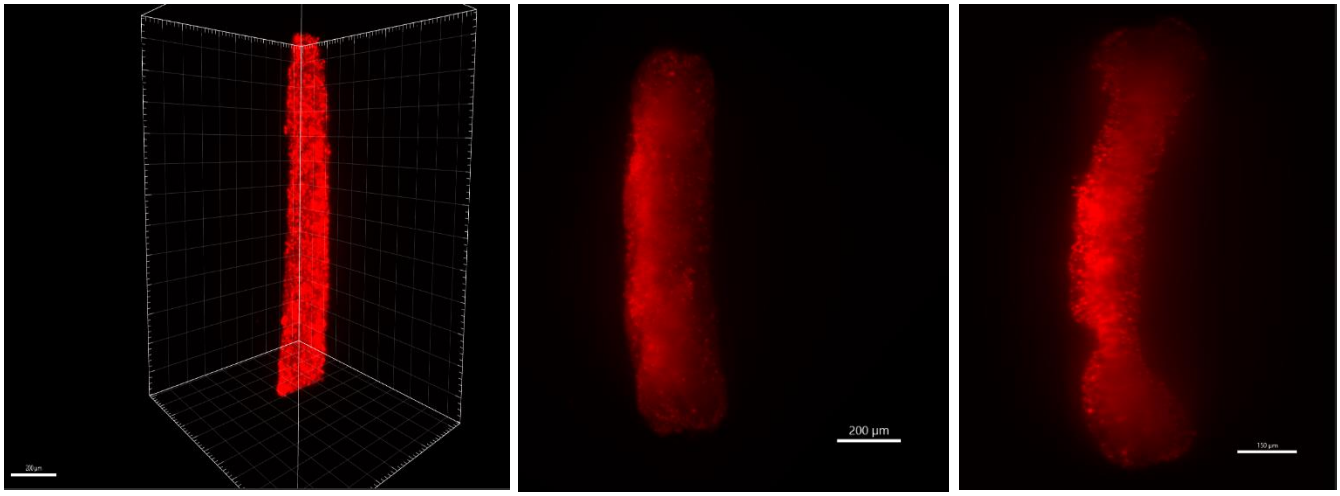

Figure 3.19. 3D reconstruction of side angle of a representative at day 21 scaffold populated with HepG2-RFP (Scale bar = 200 µm) (A). Z-Stack images of side angle of representative scaffolds at day 21 scaffold populated with HepG2-RFP (B,C). Scale bar = 200 µm for A, 150 µm for C. Demonstrating that the scaffold cultures at this time point are not thicker than 300 µm.

3.5. Optimisation of light-sheet imaging of 3D cell cultures

One of the main difficulties when studying 3D cell cultures are the limitations that arise when trying to image the tissues produced. However, using the optical sectioning and live imaging capabilities of light-sheet microscopy it is possible to visualise the cells deep within the obtained 3D structures as well as offering the potential to produce 3D images using multi-view reconstruction (Figure 3.20.).

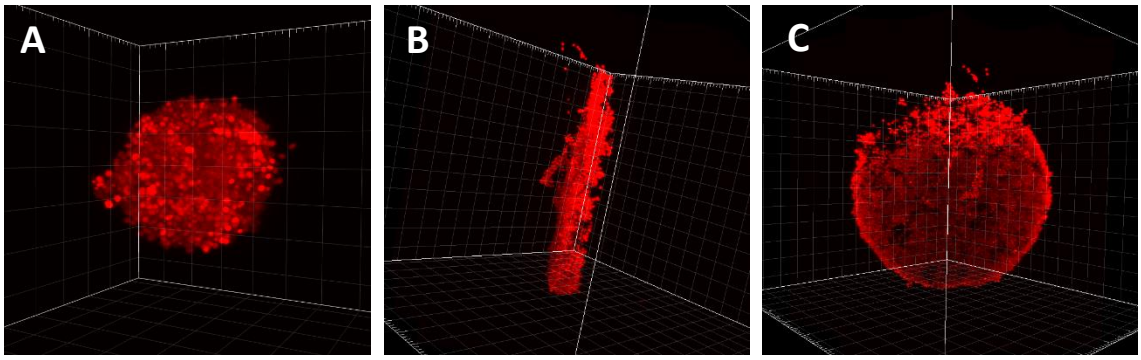

Figure 3.20. Multi-angle light-sheet microscopy images of a spheroid (A) and a scaffold (B, C) that have been imaged at 8 angles, reconstructed using the FIJI and visualised using IMARIS.

For 2D cultures there are multiple well-practiced techniques for cell counting that enable normalisation across wells and conditions. However, this is not the case for cells cultured in 3D. For microscopic analysis the easiest and most logical way to quantify cell numbers within the models is nuclei counting. There are issues with this approach when it comes to imaging 3D systems due to reduced dye penetration and light scattering. These imaging complications are reduced in the scaffold cultures due to their thin, disk like shape. For spheroids cultures, however, their dense and compact nature makes cell counting problematic, particularly at the core. It is apparent from Figure 3.21.A that nuclei are not visible at the centre of the spheroids using Hoechst 33342 nuclear dye. This appears to be due to dye penetration as when stained with a smaller mitochondrial dye (TMRM), for the same amount of time, the dye is clearly visible at the centre of the spheroid. HepG2 cells were, therefore, stably transformed using Lentivirus to express RFP-H2B in their nuclei (Figure 3.21.C). This allowed nuclei counting deep within the cultures and meant that the only limiting factor was light penetration, this penetration issue could be overcome, in part, by imaging the samples from multiple angles, increasing the signal deeper within.

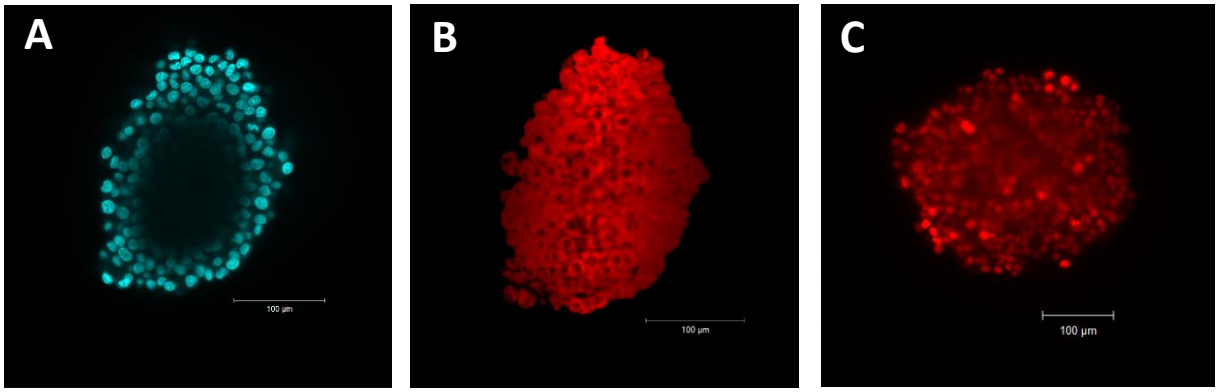

Figure 3.21. Spheroid stained with Hoechst (A) and TMRM (B). The larger Hoechst dye is excluded to the periphery of the spheroid whereas the smaller TMRM dye can penetrate to the core. (C) A single z-stack of HepG2 cells which have been stably transformed to express RFP-H2B in their nuclei allows visualisation of all the cells in the culture. (Scale bar = 100 µm).

IMARIS is a powerful 3D visualisation software that allows the counting of 'dots' and the measuring of 'surfaces' that can be fitted onto the fluorescent signal visualised within the 3D cell culture. Using IMARIS it is, therefore, possible to fit 'dots' to the signal from every nuclei which correlates to the number of cells within each 3D culture, assuming every cell only contains a single nuclei. This measurement of cell number can then be used for normalisation purposes.

To enable accurate cell counting using IMARIS, the 3D models must firstly be imaged using multiple angles and reconstructed into a 3D image using the multi-view reconstruction plug-in in FIJI (Preibisch et al., 2010, 2014). The reconstruction process works by locating the same points, in this case nuclei, in the corresponding angles and using them to numerically fit the images together (Figure 3.22.).

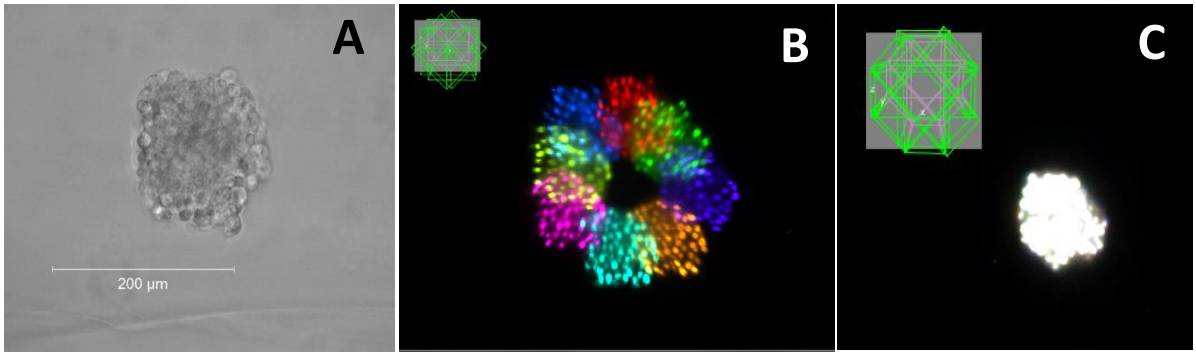

Figure 3.22. Example of a 3D reconstruction, utilising 8 angles, of a small spheroid culture (A). The 8 angles before reconstruction are shown in different colours (B) and the same spheroid after reconstruction (C). Imaged using Zeiss Z.1 light-sheet microscope (scale bar = 200 µm).

The reconstruction method and the number of imaging angles required to produce reliable and accurate 3D reconstructions, without being too time consuming and computationally demanding, was laborious to optimise. This was due to a lack of literature and understanding around the plug-in meaning the optimisation process relied mainly on trial and error. This was a major pitfall with the image analysis due to difficulties during the reconstruction, resulting in a low success rate, with a waste of both time and samples. As there was only one computer powerful enough to perform these reconstructions, it was also a concern of user time and availability that hindered this process. Over time, an effective protocol was established using a combination of two reconstruction methods, Centre of mass (translation variant) and Redundant geometric local descriptor match (translation variant). Utilising these two methods allowed for reliable reconstruction of the images into 3D, as the Centre of mass function brought the images from each angle closer together, making it easier for the Redundant geometric local descriptor match function to fit the angles.

The optimisation of the number of angles required for reconstruction was a trade-off between accuracy and time. Comparing the same samples imaged at 16 angles, and then reconstructed utilising different combinations of these angles, found that 8 angles was sufficient to accurately reconstruct the 3D samples without being too time consuming. 16 angles, 22.5° apart, was the highest feasible number of angles used to image the 3D culture; this was then compared to a reduced number of angles regarding both time and reliability (Table 3.2.). As imaging using 8 angles produced similar cell

counts to that of 16 angles, with a significantly reduced burden on time, data storage and computational power, 8 angles was selected as the most appropriate for 3D reconstruction.

Table 3.2. Optimisation of multi-view reconstruction

Culture	Number of imaging angles	Cell count for one example 3D culture	Average standard deviation compared with 16 angles (n = 10)	Average reconstruction time (hrs)
Spheroid	2	6643	1444.43	1
	4	8125	520.27	2
	8	8662	11.63	6
	16	8675	-	9
Scaffold	2	-	-	-
	4	13490	1818.86	5
	8	15312	57.44	12
	16	15363	-	21

3.6. Discussion

Culturing spheroids is a well reported technique, with many different methods available from simple hanging drops, using petri dishes, to advanced systems like the InSphero GravityPLUS™ and GravityTRAP™ plates (Shen et al., 2021). Unfortunately cell seeding for 3D scaffold cultures is not as well documented and typically relies on the 'drop-on' method mentioned previously (Danti et al., 2013; German & Madihally, 2019; Rajendran et al., 2017; Ruoß et al., 2018).

What was initially thought of as a simple task, culturing cells onto the scaffold, turned out to be extremely difficult. The initial test of smaller (100 µm) scaffolds resulted in poor cell binding and difficulties regarding controlling the number of scaffolds per well. Therefore, work began using a larger scaffold which was 1 mm x 50 µm and had comparable cell numbers to that of spheroid cultures.

The aim for this larger scaffold was to seed an even layer of cells that encompassed the scaffold, without forming spheroid-like clumps. The focus of the scaffold was to produce a 3D culture that avoided the diffusion limitations of spheroids, allowing gases, nutrients, and reagents access to all the cells within the culture. To achieve this desired cell distribution required the scaffolds and cells to be cultured in continuous suspension through automation. Other parameters to improve cell binding including coating the scaffold with ECM protein or Poly-L-Lysine were tested but were unsuccessful. The incorporation of cell binding domains is something that could improve cell uptake further, however, was beyond the scope of this work (Carletti et al., 2011). Further to this the distribution of the cells within the scaffold material was something that was also something of interest and could have been studied using light-sheet microscopy or using H&E staining of a section of the cell populated scaffold but was not undertaken due to time restraints (Montesanto et al., 2019).

The tubes created using PDMS worked well, allowing gaseous exchange, and enabling the cells to bind to the scaffold in an even distribution. The issue, however, was that the desired application for the scaffold cultures was to be used in a high-throughput manner which these tubes didn't facilitate. For the purpose of comparing spheroids and scaffolds this was adequate as only a small batch was required but not for the development of the scaffolds for screening purposes.

Building on the theory and success of the PDMS tubes, the CELVIVO bioreactor was tested. This system works on the same principles of the tubes, keeping the scaffolds and cells in continuous suspension and allowing multiple collision events, whilst enabling gaseous exchange. After a short test period the CELVIVO system was shown to reliably produce 100 scaffolds per ClinoReactor® with the assistance of dispersion events and the inclusion of air bubbles. This system has since been purchased by the industrial partner to allow them to mass produce the scaffolds based on the work described here. To further improve the throughput of the 3D scaffold culture they have also contracted Scitech Precision in Cambridge to laser cut the scaffolds into 200, 300, 400 and 1 mm x 50

µm discs and remove the need for using biopsy punches, which at this point is the bottle neck of scaffold culture. These smaller scaffolds will be tested in their current liquid handling robot. Aurelia Bioscience are also in talks with companies about the feasibility of developing an automated system which utilised magnets to manipulate the scaffolds. Although this is an emerging partnership, it demonstrates the potential of these scaffolds for high-throughtput applications, in an automated manner.

Chapter 4 - Addressing the challenges of biochemical analysis faced by 3D cell cultures

This chapter is a technical paper that is currently being written by myself and our collaborators Dr Eirini Velliou and Priyanka Gupta, to highlight the issues faced by 3D cultures and demonstrate the effectiveness of different cell number proxies.

When writing a review together Dr Eirini Velliou and I had many conversations regarding the complexities and difficulties of extracting accurate and reliable data from 3D cultures. We discussed the prospect of writing a technical paper together to highlight some of the issue that researchers in the field should be aware of and what data we would want to include. The resulting paper is found below. All the writing and figure making was done by myself, as were all of the experiments other than the work in figure 4.2 which was performed and created at UCL by Dr Eirini Velliou and Priyanka Gupta. The paper has been adapted to fit the style of the rest of the thesis.

Addressing the challenges of biochemical analysis faced by 3D cells cultures

Jonathan Temple[1], Eirini Velliou[2], Priyanka Gupta[2], Raphaël Lévy[1,3].

1 Bioscience building, University of Liverpool, Liverpool.
2 Centre for 3D Models of Health and Disease, University College London, London.
3 Laboratoire for Vascular Translational Science, Université Sorbonne Paris Nord, Bobigny.

4.1 Introduction

The field of 3D cell culture has seen a dramatic uptake in last four decades as researchers aim to recapitulate the *in-vivo* environment (Jensen & Teng, 2020; Vantage Market Research, 2021), with

the variety of different 3D culture systems available continuously expanding and each having aspects that aim to improve the function and physiological relevance of the cells. Conventional 2D culture is still the gold standard in most laboratories due to its simplicity and ease. This raises the question of when is 3D culture relevant and when is 2D sufficient? If the purpose of the culture is to over express proteins for purification, then 2D is clearly the obvious choice, it is technically simple and cost effective, there are no issues with the diffusion of reagents and the cells are easier to harvest and lyse. Instead, one of the main motivations for the development of 3D cultures is to complement or replace current research models to better represent the *in-vivo* environment for studies including disease phenotypes or drug toxicity screening.

The known advantages of 3D cultures are unfortunately hindered by the very thing that makes them more akin to *in-vivo*, their geometry. Due to more extensive cell-to-cell contacts and cells often being multiple layers thick the diffusion of nutrients, waste, reagents and gases in and out is dramatically reduced. As oxygen is only able to diffuse through ~200 µm of tissue, the diffusion of larger molecules such as nutrients and biochemical reagents is further impeded (Asthana & Kisaalita, 2012; Griffith & Swartz, 2006). 3D cultures will experience this to different degrees depending on their physiology; with larger, more compact cultures like spheroids likely to exhibit hypoxic cores once over a particular size unless their size is restricted through contact inhibition. Scaffold based cultures aim to overcome these issues by being more porous but may over time still experience diffusional limitations due to cell growth and the entrapment of nutrients and waste.

This issue is overcome *in-vivo* through vascularisation but this is not so easily achieved in the lab with most approaches involving the use of advanced technologies, such as 3D bioprinting, and the incorporation of grafts and vascular cells (Bellani et al., 2021; Paulsen & Miller, 2015; Pitaktong et al., 2020). The issues with these types of cultures, however, are that even with the vascular architecture and cell types, they require flow to be incorporated to mimic blood flow and its ability

to mass transfer nutrients and gases; making these expensive and complex models even more intricate and not suitable for high-throughput/content screening.

The geometry of 3D cultures not only influences the functionality and health of the cells incorporated but also the ability of researchers to get useable and meaningful measurements from them. Assay reagents and drugs face issues of diffusion making it difficult for researchers to be confident of whether they are indeed analysing all the cells in the sample or only those that are accessible. The same is also true for when performing microscopic analysis of the models as not all cells will take up the stains or antibodies required for labelling. Light penetration is also highly affected by the geometry of the cultures and will highly depend on the method of illumination and the overall transparency.

Furthermore, most biochemical and microscopic readouts must be normalised to the number of cells to be statistically relevant and ensure that any difference is down to the functionality of the cells. In 2D cultures, this is easily achieved and the accuracy of the cell count is high, in 3D cultures this is not the case, as conventional cell counting techniques do not transfer well due to difficulties visualising the cells or retrieving them into a single cell suspension. There are various approaches to overcome this issue. Some researchers will use the number of cells seeded but this doesn't account for pipetting errors or the heterogeneous nature of 3D cultures, assumes that there is no variation in cell growth across conditions and that all the cells are taken up into the culture (Tasnim et al., 2016; Wu et al., 2019). Others use a control well or spheroid diameter. however, these techniques are likely to be inaccurate for the same reasons as using seeding density (Baze et al., 2018; Foster et al., 2019; Ogihara et al., 2017; Shin et al., 2018). The most common practice in the field is that researchers will use a proxy measurement, such as total protein or the level of house-keeping genes, to estimate the number of cells that are present in the culture. These methods are not without their complications either, again due to issues of diffusion and penetration, and most are endpoint, in that they require the lysis of the cells meaning further analysis cannot be performed.

Here we explore these limitations of 3D cultures and demonstrate the accuracy of some proxy measures by comparing their readouts to the exact number of cells counted using light-sheet microscopy. We use HepG2s that have been transduced to express RFP in their nucleus, cultured in spheroids and electrospun scaffolds. Using stably transduced HepG2s that also express luciferase we show that it is possible to achieve accurate cell number proxy measurements that are non-destructive allowing continued analysis of the same sample.

4.2 Results

4.2.1. Demonstrating the problem

The impact of tissue thickness, and therefore spheroid diameter and compaction was demonstrated by firstly showing the difference in dye penetration between two different size dyes, Hoechst 33342 (MW – 615.9861) and TMRM (MW - 436.93), in HepG2 spheroids cultured using hanging drop plates (Figure 4.1. A-C). The smaller/more compact of the two (TMRM) penetrates much further than that of the larger (Hoechst) demonstrating that molecular size and potentially chemistry has an impact on the diffusion into tissue. The compaction of these spheroids can also be seen using a widefield image (Figure 4.1D), compaction here referring to the decreased volume of a fixed mass and not the process by which cells form gap junctions enabling the exchange of ions and small molecules during embryogenesis.

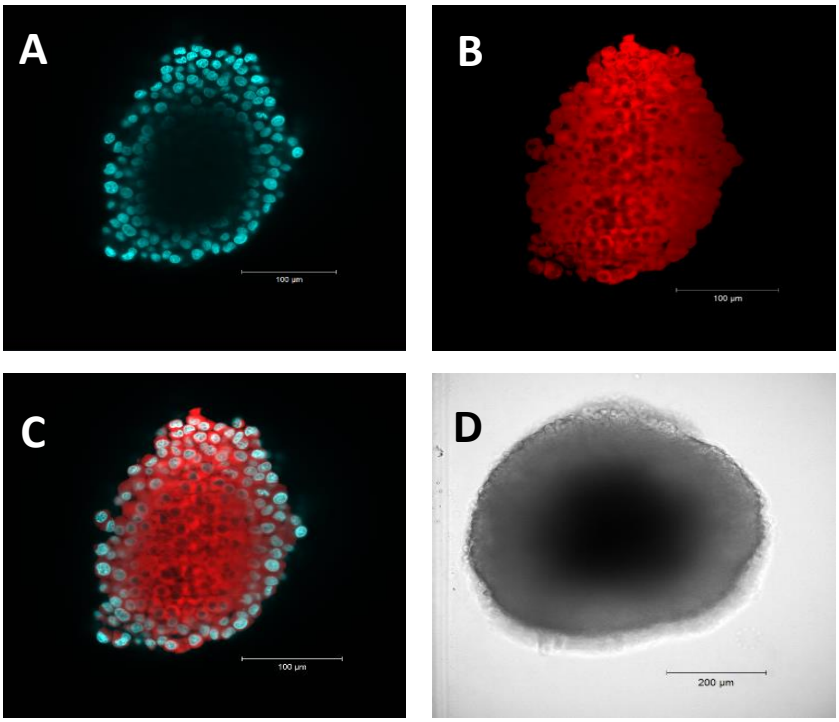

Figure 4.1 Spheroid treated with TMRM and Hoechst stain for 30 minutes (A-C). The spheroid was incubated with the two stains for the same amount of time, however, the Hoechst dye is contained to the periphery of the spheroid, unlike the TMRM dye which was able to penetrate to all of the cells, even those at the centre. Evidence of compaction in a larger spheroid can be seen using widefield imaging. The darker inner area indicates the compaction of the cells, reducing the amount of light that can pass through (D). **(Images A and B have been reused here due to their incorporation into the draft technical paper)**

To demonstrate the effect of compaction on diffusion, Human Mammary Epithelial Cell (HMEC) spheroids were prepared with precise control over construct sizes and compactness through variations in collagen concentrations. Nuclear staining with DAPI was carried out to visualise the relation between compactness and diffusion limitation (Figure 4.2.). Diffusion limitation studies with DAPI suggested that the compactness (density) of the aggregates had greater effect rather than aggregate sizes.

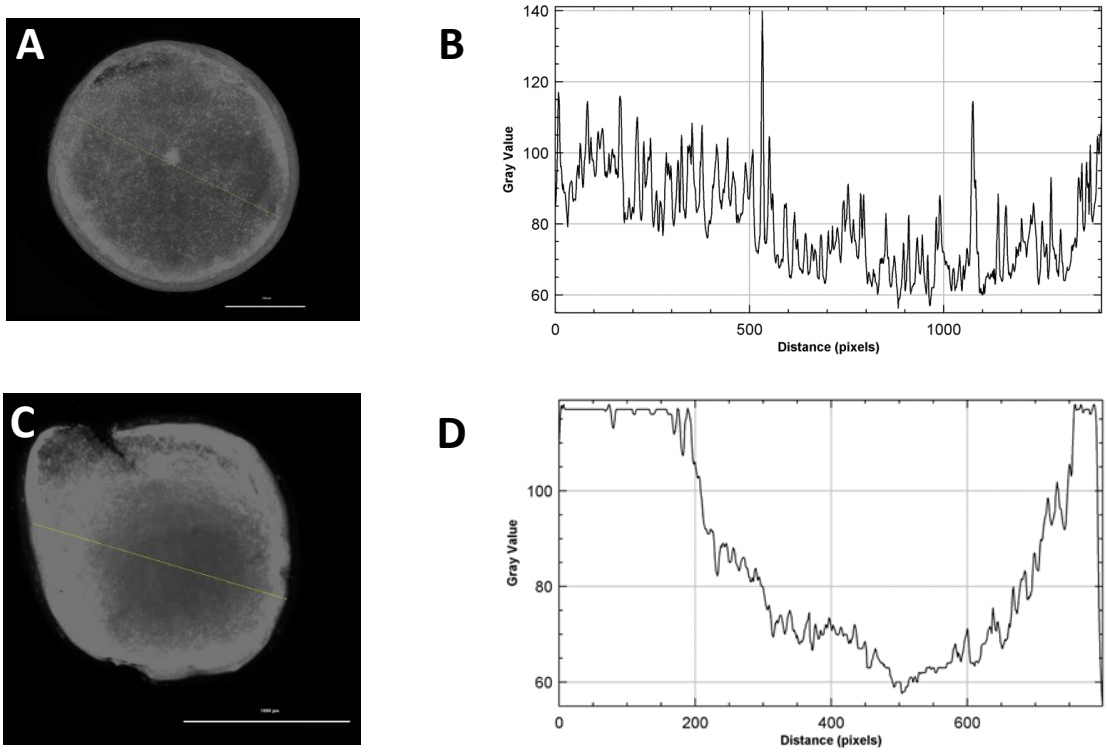

Figure 4.2. HMEC cells cultured into spheroids, prepared using the same number of cells but with varying concentrations of collagen incorporated. (A, B) DAPI diffusion in loose HMEC constructs has a more even distribution across the spheroid compared with DAPI diffusion in compact HMEC constructs (C,D), where the dye is concentrated at the periphery of the spheroid (scale bar = 1000 µm). This indicates that the compactness of the spheroid culture has a larger impact on diffusion compared to spheroid diameter. **This work was performed by our collaborators and is included here as part of the technical paper (Dr. Eirini Velliou and Priyanka Gupta, UCL).**

4.2.2 Methodology for measuring exact cell number and spheroid diameter/area

To circumvent the issues of diffusion of reagents and light penetration, only HepG2 spheroids under ~400 µm were used for all measurements of cell number using light-sheet microscopy as penetration limitations would influence both the ability to count the cell number accurately but also lead to inaccurate measurements of the cell number proxies. The spheroids and scaffolds were imaged from 8 different angles, 45° degrees apart and fused into a single 3D image to ensure that all the cells had been counted (Figure 4.3.A, E). A single z-stack image of a representative spheroid demonstrates

that all cells were visible in the samples used (Figure 4.3.B). After measuring 30 nuclei across 10 different samples the average nucleus size was calculated as 7.21 µm. Therefore, spots of 7 µm were fitted to the nuclei using IMARIS to measure exact cell count; here we assume that each cell will contain only one nuclei (Figure 4.3.C, F). The IMARIS surface function was then applied to measure the volume and area of the spheroid (Figure 4.3.D) and the diameter was measured in IMARIS.

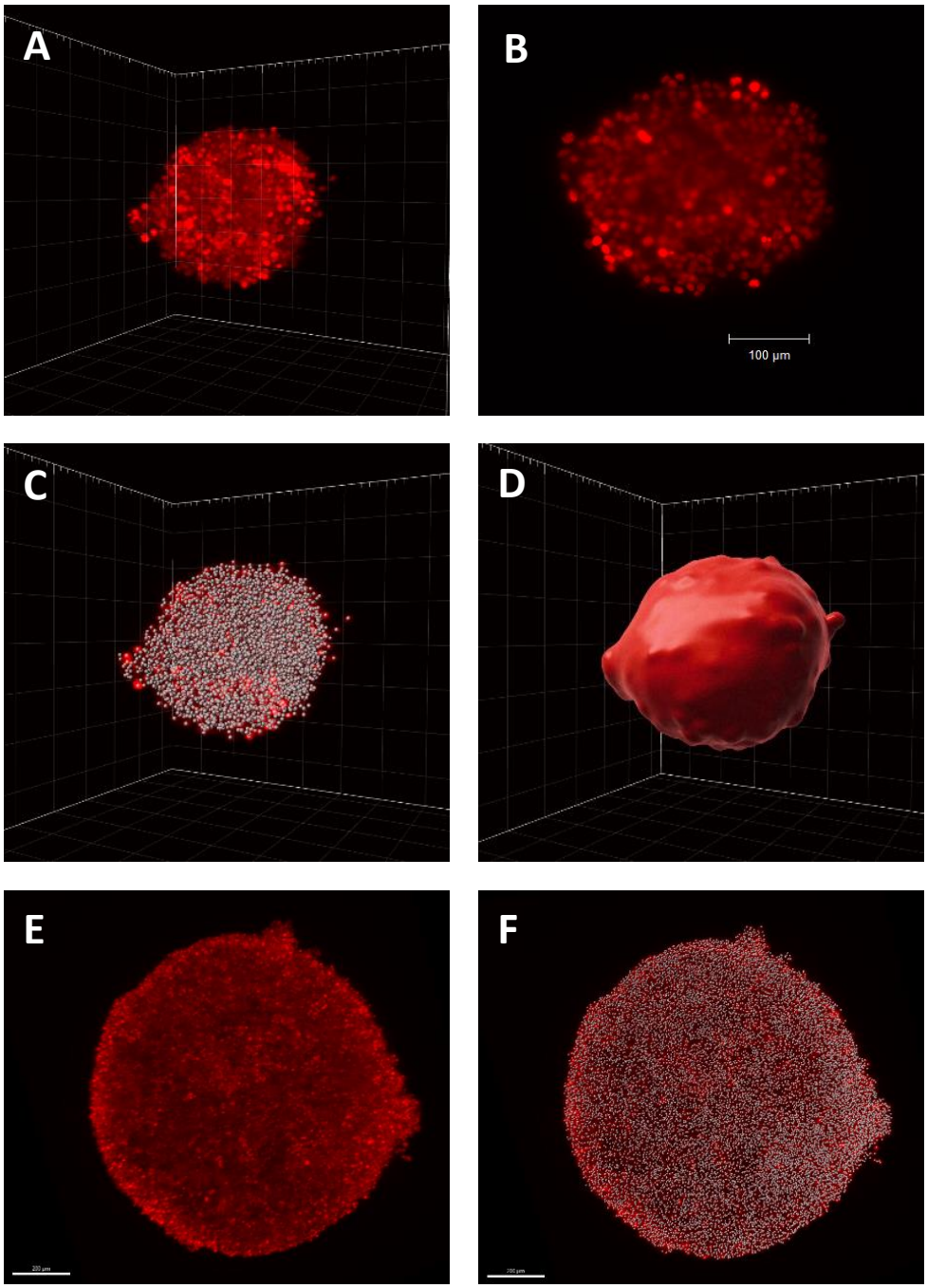

Figure 4.3. Measuring cell number by light-sheet microscopy. 3D reconstructed images of a representative spheroid (A-D) and a scaffold culture (E-F) in IMARIS. A single z-stack through the same spheroid demonstrates that all the cells are visible within the culture enabling accurate cell counting to be performed (B). Spheroid dot analysis indicates how the number of nuclei are counted in IMARIS (C) and volume analysis indicates how the volume of the spheroids was measured (D). Scaffold culture dot analysis (F).

4.2.3. Measuring Luminescence

Luminescence readings were taken for both HepG2s cultured in 2D and in the 3D spheroids/ scaffolds in 96 well plates on three different instruments. The first, a HIDEX plate reader, which measures the luminescence produced by the cells across a defined area in the well, worked well for cells in 2D at a range of seeding densities. This is due to the cells in 2D cover the entirety of the bottom of the well and have an even distribution. As the HIDEX measures the luminescence from the cells, it records a stable reading across the whole sampling area. With the much smaller 3D samples, however, the luminescence reading were highly varied even after testing several different measurement area sizes; likely due to the 3D cultures only occupying a small section of the sampling area (Figure 4.4.). As the luminescence should peak and then plateau before tailing off until the luciferin is exhausted, we did not continue to use this instrument, however, highlights the importance of understanding how different plate readers records values and checking they are fit for the intended purpose.

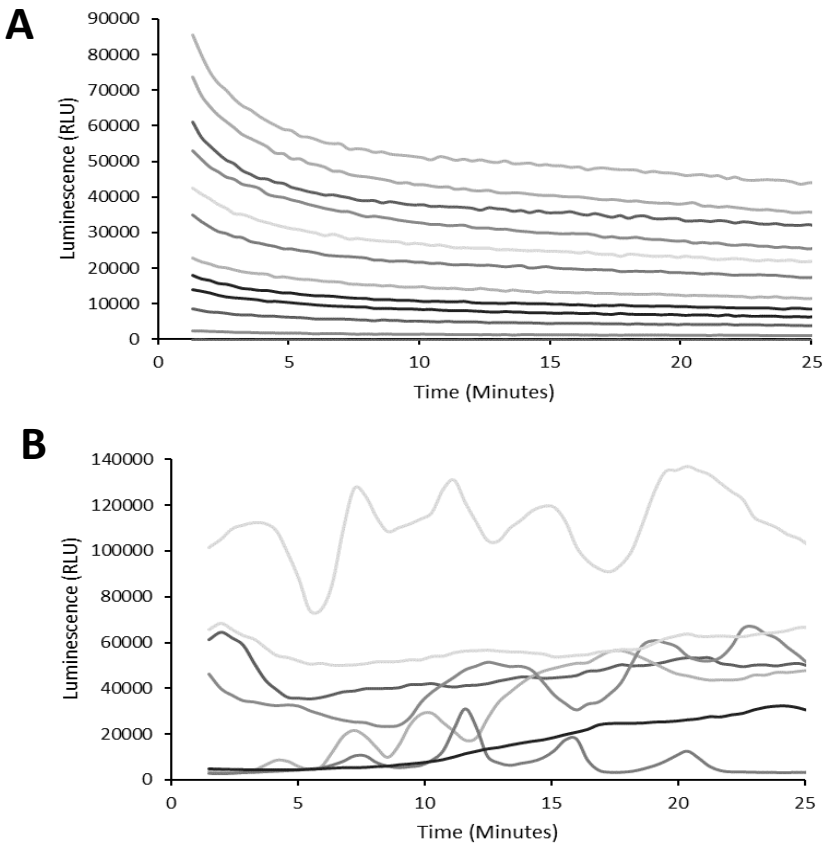

Figure 4.4. Luminescence values recorded for stably transduced HepG2 cells at different concentrations (1000 – 20,000 cells) in 2D (A) and 3D spheroids (B) on a HIDEX plate reader.

The next plate reader tested was a FLUOstar OMEGA, this instrument samples from individual points within the well and then gives an average. This plate reader again worked well for cells in 2D due to there even distribution across the whole well (Figure 4.5.A), however, initial testing produced similar, highly variable, results to the HIDEX system for the 3D models (Figure 4.5.B). Upon increasing the number of points sampled to the maximum (16), it was possible to achieve steady luminescence readings like that of the cells in 2D (Figure 4.5.C). It is thought that this increasing of the sampling points improves the stability of the luminescence reading for the 3D samples as it increases the chance that at least one of the points records the values for the 3D culture at each timepoint.

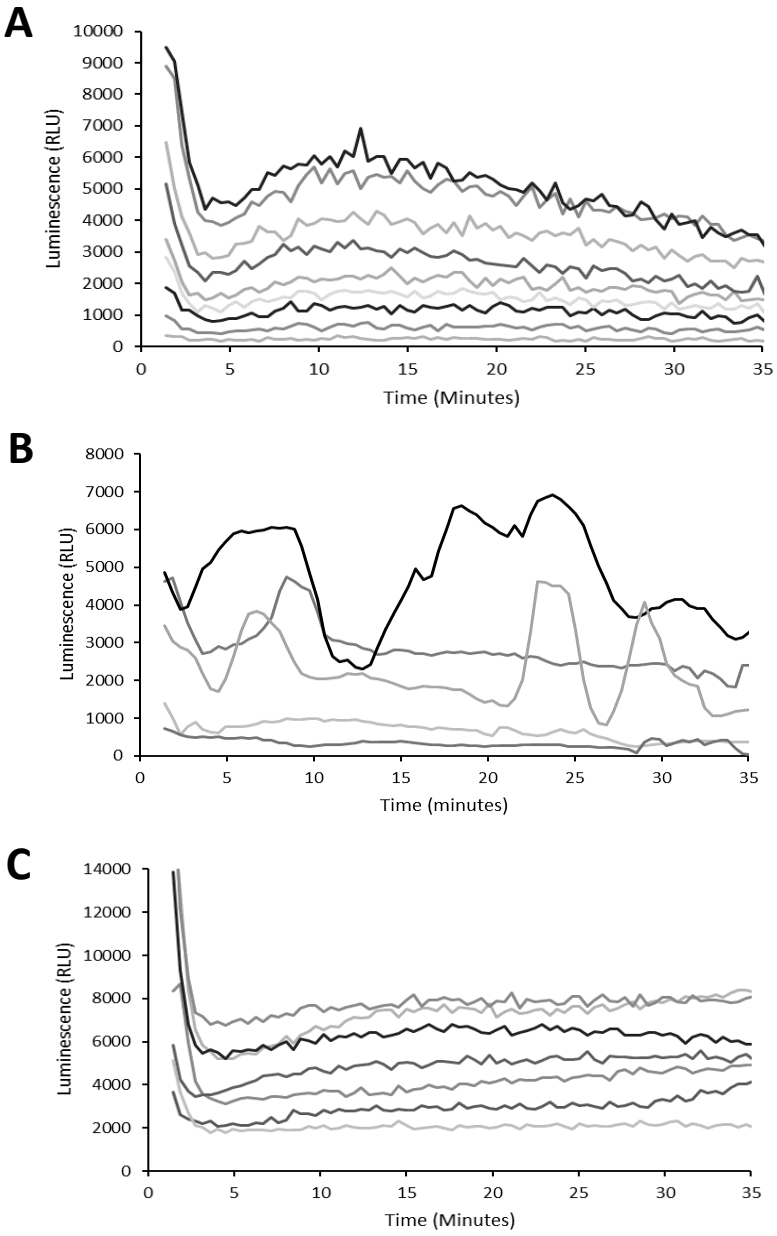

Figure 4.5. Luminescence values recorded for stably transduced HepG2 cells at different cell concentrations (1000 – 20,000 cells) in 2D (A) and 3D samples (B, C) using the FLUOstar OMEGA plate reader.

To make sure that the luminescence plots measured using the plate readers were accurate, a high-sensitivity luminescence imager was tested (IVIS Spectrum *In-Vivo* Imaging System). The IVIS imager allows all the Luminescence from the samples to be measured ensuring no loss of signal takes place resulting in inaccurate results (Figure 4.6.).

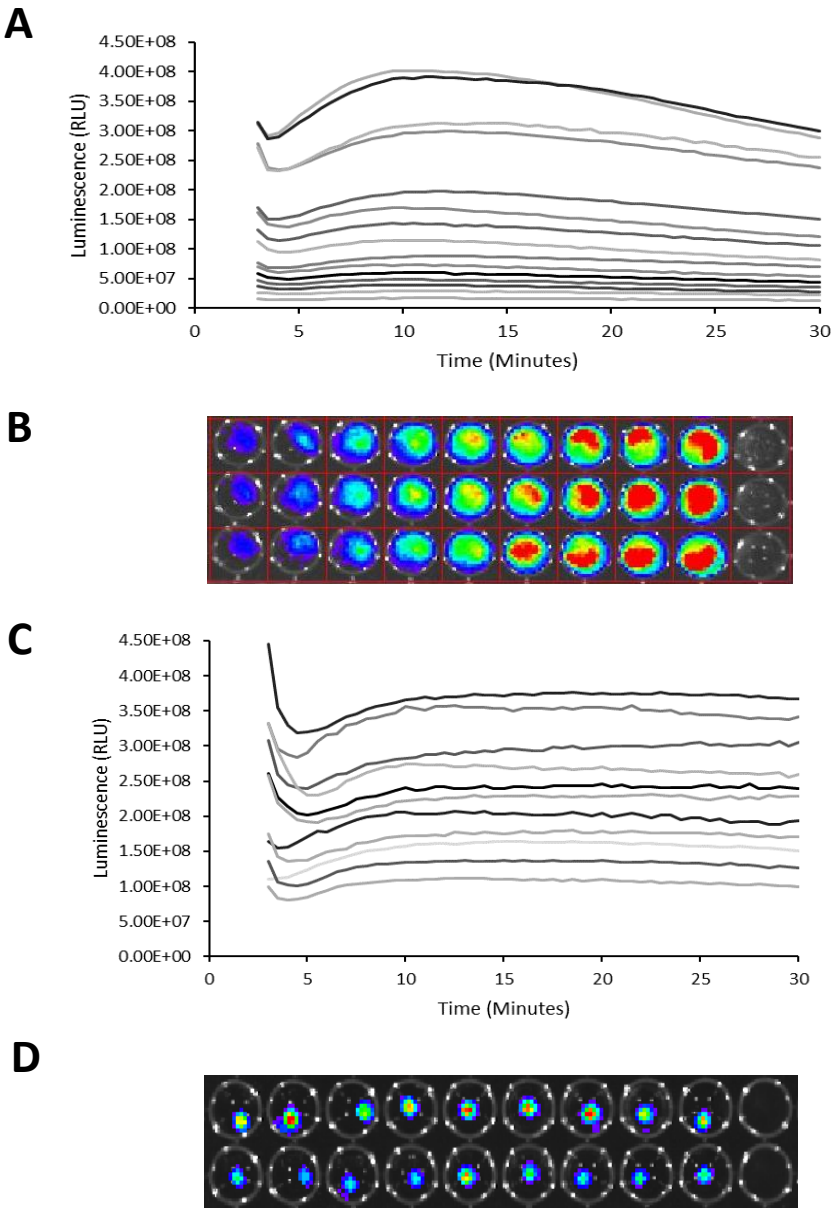

Figure 4.6. Luminescence values and luminescence images recorded for stably transduced HepG2 cells at different cell concentrations (1000 – 20,000 cells) in 2D (A, B) and 3D cultures (C, D) using a IVIS imager.

The luminescence readings from the IVIS produced similar shaped plots to that of the FLUOstar OMEGA plate reader for both the 2D and 3D cells. The IVIS did create smoother curves, likely due to its higher sensitivity and accuracy as no signal can be lost.

4.2.4 Assessing different cell number proxies

The ability to count the exact number of cells in the 3D samples using light-sheet microscopy made it possible to compare this number to different cell number proxies routinely used by others including spheroid diameter and volume, protein concentration, viability, inherent luciferase expression (luminescence) and levels of housekeeping gene expression measured by JESS analysis.

Ideally, the method of normalisation should be non-destructive to allow for further analysis of the cultures. For spheroids, researchers implement diameter readings as a rough proxy for the number of cells present (Baze et al., 2018; Foster et al., 2019). This, however, is an inaccurate measure, particularly due to spheroids rarely being completely spherical. The effect of compaction is evident as the cell number increases with spheroids with a diameter of 300 µm containing anywhere from 1000 to 4000 cells (Figure 4.7.).

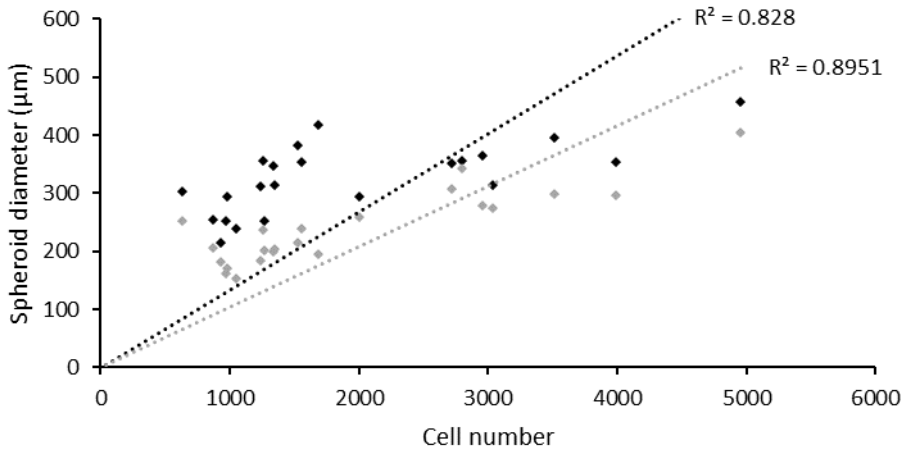

Figure 4.7. Measured spheroid diameter plotted against number of cells counted using IMARIS, imaged using light-sheet microscopy. Largest diameter (black) and smallest diameter (grey) (n = 22).

Measured volume, therefore, is a much more accurate proxy for the number of cells in the spheroid, however, this requires the culture to be imaged and reconstructed into a 3D image which is time consuming and an endpoint and destructive measurement so is rarely utilised in the field and is not applicable for other culture types like scaffolds or hydrogels (Figure 4.8.).

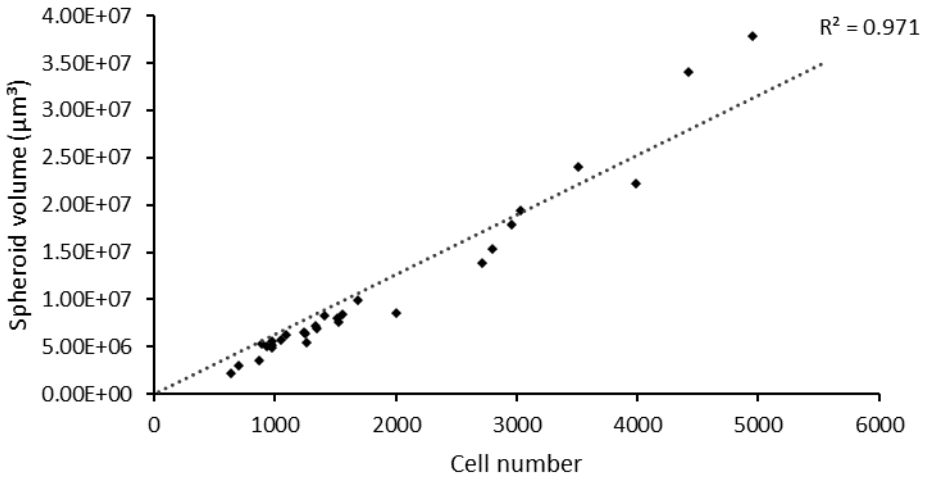

Figure 4.8. Spheroid volume measured using IMARIS plotted against cell number counted using light-sheet microscopy.

Total protein or total DNA are commonly used for normalisation across different time points or conditions. They do, however, require all the cells to be collected and lysed to ensure accuracy; this also means that they are also an endpoint measure and do not allow the culture to be continued forward. Scaffolds and spheroids were first imaged using a light-sheet microscope and then collected before sonication in PBS. Samples were pooled in twos or threes to ensure that the protein concentration was high enough for detection before they were subjected to a Bradford assay (Figure 4.9.). Bradford was used here as it has a low detection limit and is not as susceptible to chemical interference as other protein assays; this was important as the cultures are still mounted in a small volume of 1.5% agarose from the imaging step. The protein concentration has a positive correlation to the number of cells in the culture, however, there are several outliers with spheroids containing 3000 – 6000 cells all containing ~ 0.08 mg/mL of protein. This indicates that total protein is not an accurate proxy for cell number for small culture sizes.

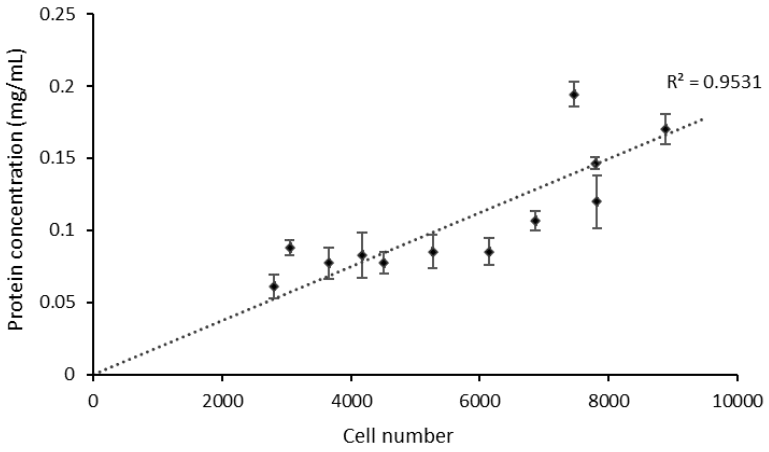

Figure 4.9. Protein concentration measured using Bradford assay plotted against cell number counted using light-sheet microscopy.

The number of viable cells in a culture is often used as a proxy to allow normalisation. This was performed in the same way as protein concentration with the measurement taken after imaging. It is evident that viability does have a positive correlation to the number of cells counted however, there are still several outliers that would lead to inaccurate normalisation (Figure 4.10.).

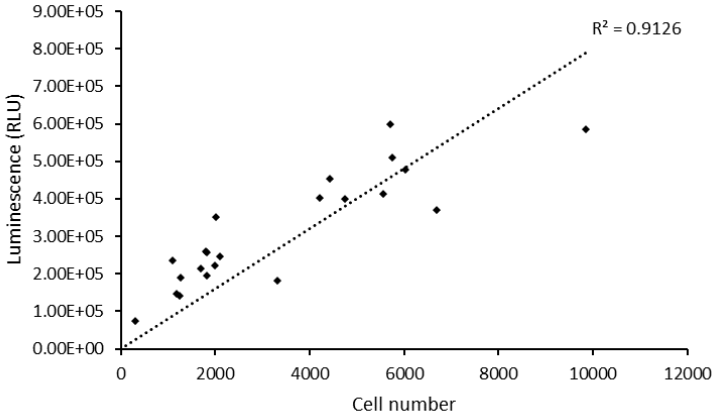

Figure 4.10. Viability measured using cell titre glo 3D in 3D samples plotted against cell number counted using light-sheet microscopy

The most desirable proxy for cell number is one that is both accurate and non-destructive allowing continued analysis of the culture. As most of these cultures, particularly the scaffold cultures, are

highly variable it is important to get as much information as possible from each individual sample. Inherent luminescence meets both these criteria both in 2D (Figure 4.11.) and in 3D cultures (Figure 4.12.).

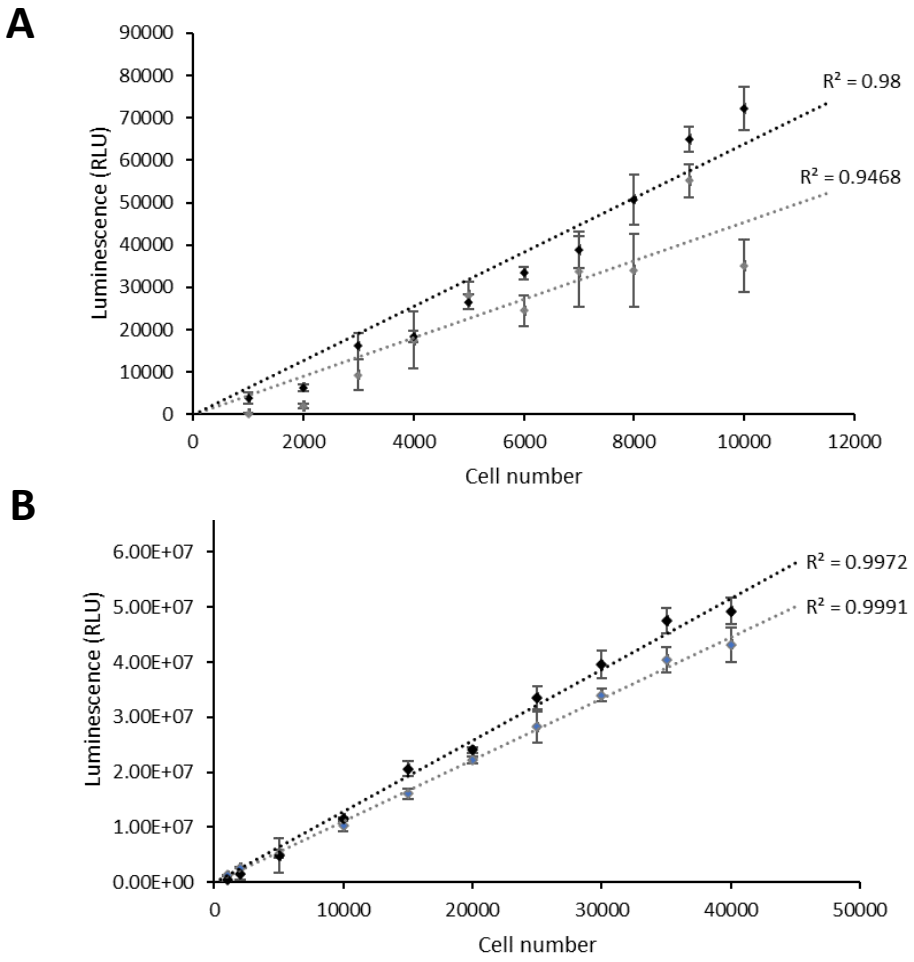

Figure 4.11. Luminescence plotted against seeded cell number in 2D for both the FLUOstar omega (black) and the HIDEX plate readers (grey) (A). This highlights that the sampling method in the FLUOstar omega is superior even when an even distribution of 2D cells is used. Luminescence in 2D cells plotted against seeded cell number for 24 hrs (black) and 2 hours (grey) using the IVIS imager(B). Here cells were left for either 2 or 24 hrs to attach to the well before luciferin was added and luminescence recorded. The luminescence values recorded for the cells that were left for only 2 hours were almost perfectly correlated to seeded cell number, highlighting the accuracy of the IVIS imager. The cells left for 24 hrs still had a strong correlation between luminescence emitted and cell number seeded but not as strong as the cells left for 2 hrs, likely due to slight changes in cell number over the 24 hrs.

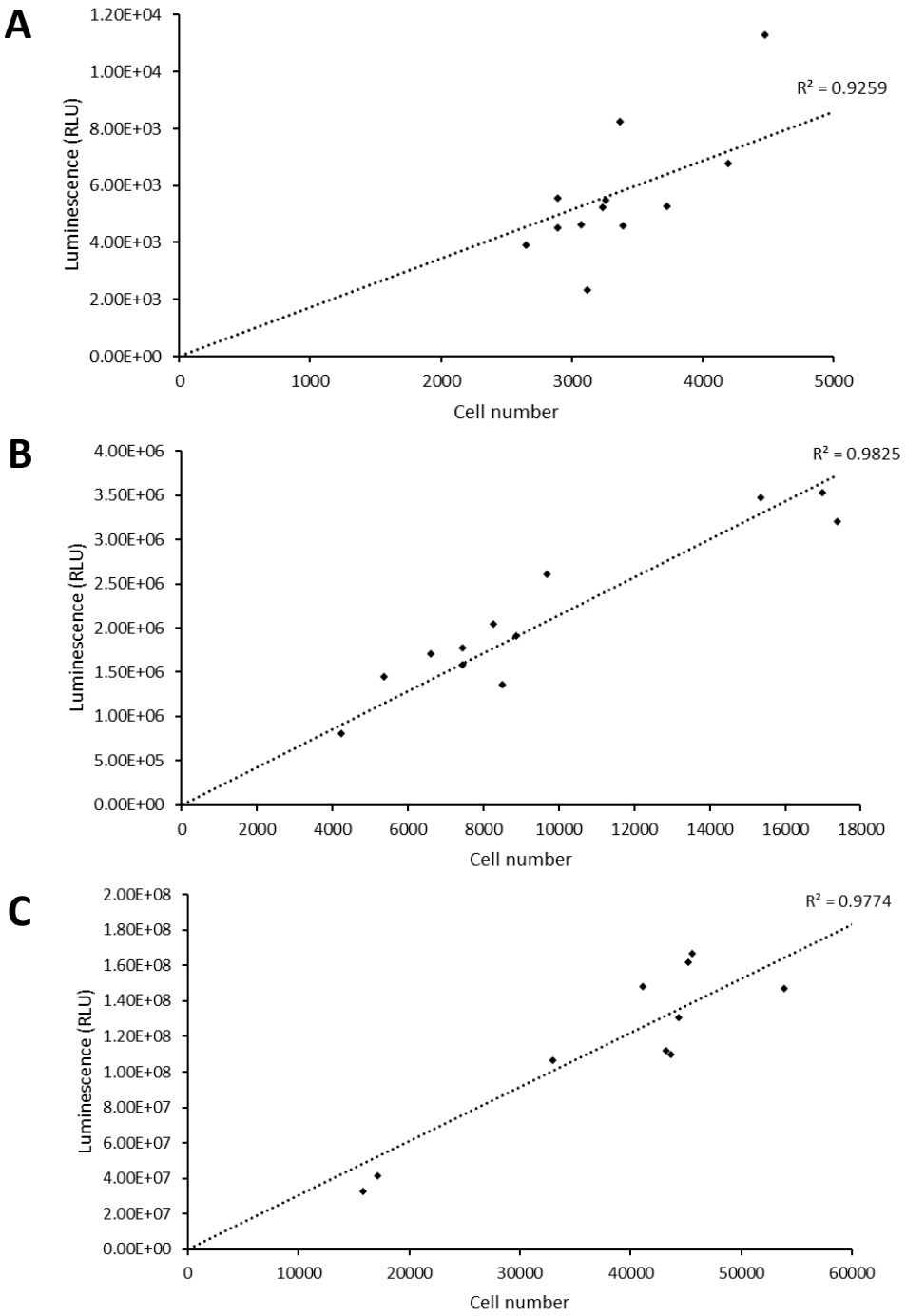

Figure 4.12. Luminescence plotted against seeded cell number in 3D for the FLUOstar omega plate reader (A). Luminescence in 3D cells plotted against cell number for smaller/younger samples (B) and older/larger samples (C) using the IVIS imager. It was important to test that the IVIS imager was still accurate for the older/larger samples (21 days in culture) to ensure that the luminescence measurements from the cells would still be an accurate method of normalisation across samples even at later time points.

House-keeping genes are a powerful tool and have been used for normalisation across samples and conditions, particularly for assays like western blotting or PCR. It was possible to detect bands through standard western blotting for samples as small as one spheroid at 7 days (Figure 4.13.).

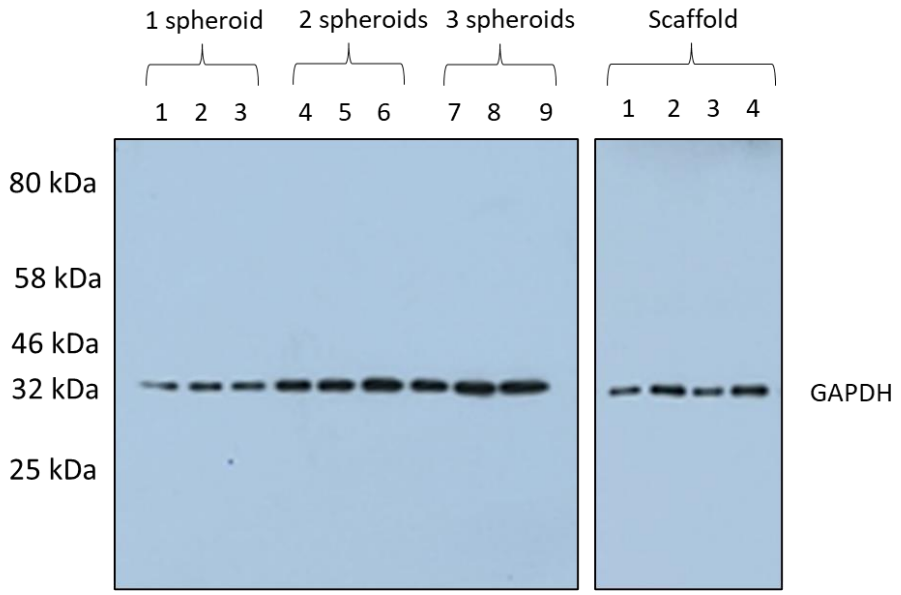

Figure 4.13. Western blot of GAPDH for HepG2 spheroids and scaffolds at 7 days of culture. The scaffold cultures were all seeded using the modified cryovials whilst in suspension with 175 cells / µL, however, the variation between the number of cells bound to the scaffold varies even under the exact same culture conditions.

To test the reliability of housekeeping genes, 3D samples were ran on a highly sensitive JESS system which allowed the small volume of each sample to be ran in triplicate after recording their inherent luminescence on the IVIS imager (Figure 4.14.A). The JESS system works through automated capillary electrophoresis where the sample is separated by molecular weight before fluorescence antibodies are utilised to record the abundance of each target protein. Due to the use of a thin capillary and a sensitive fluorescence reading, the abundance of even lowly expression proteins can be detected in small sample volumes. CYP2B6 expression (selected for its known expression in HepG2 cells) decreased when comparing day 14 and day 21 spheroids whether normalised using GAPDH expression or inherent luminescence, however, when comparing day 14 and day 21 scaffolds

normalisation using GAPD showed a decrease compared to an increase when normalised using inherent luminescence (Figure 4.14.B) (Maruyama et al., 2007). This means depending on the method of normalisation, the result could be completely different. The signal from GAPDH was then plotted against inherent luminescence signals measured before lysis of the samples to test the accuracy of the house keeping gene (Figure 4.14.C). The spread of points indicates that for this particular assay GAPDH expression is not a good proxy for cell number.

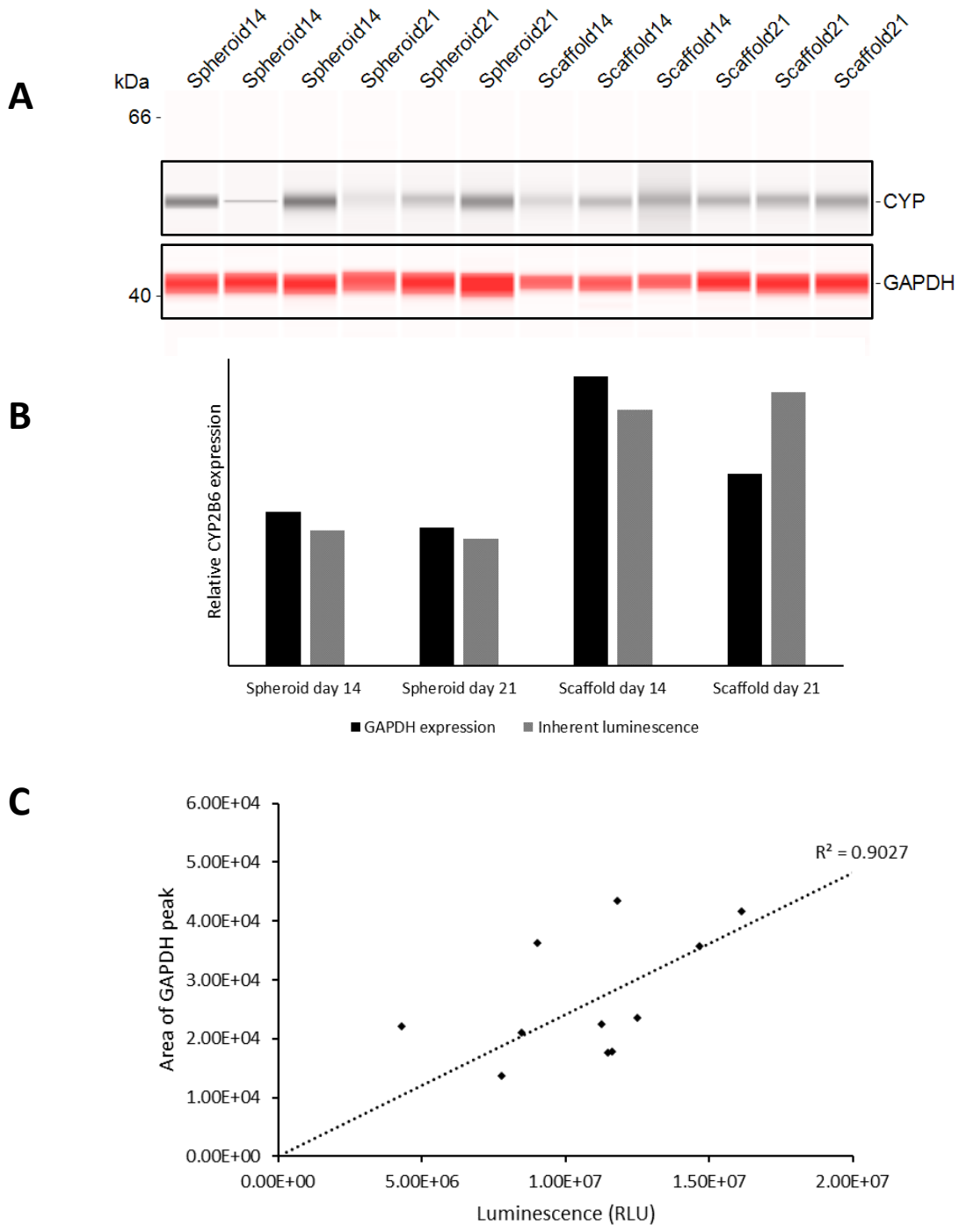

Figure 4.14. JESS analysis of two different spheroid and scaffold time points, blotting for CYP2B6 and GAPDH (A). The levels of CYP2B6 normalised to either GAPDH or luminescence, demonstrating that the levels of CYP2B6 can change depending on the method of cell number normalisation (B). Each value in (B) is an average of three repeats for the same sample. Luminescence plotted against GAPDH expression to demonstrate the correlation between known cell number and GAPDH expression as a proxy for cell number (C).

4.3. Discussion

We believe that accurate characterisation of 3D culture models is one of the main hindrances that the field currently faces and is one reasons 3D cultures have not had rapid uptake into certain areas like pharmaceutical testing. Many assays that are standardised for 2D culture do not translate well into 3D due to issues with diffusion and taking accurate readings. As most 3D cultures are highly variable and heterogeneous, along with issues regarding cell uptake and varied growth it is important to know exactly how many cells are in the culture so that variations of signal in biochemical assays can be interpreted correctly.

The aim of this study was to explore the accuracy of cell number proxies that are routinely used. We have demonstrated the issues of diffusion of reagents into spheroids and how this will have a direct effect on the accuracy of any readings, particularly for quantitative imaging, unless they are either permeabilised or broken apart and lysed; the later being undesirable as this results in the loss of information specific to the 3D culture. We have also demonstrated that compaction appears to have a greater impact on the diffusion of reagents compared with overall size meaning that cultures with higher diffusion potential such as the electrospun scaffolds are less likely to face the same level of hindrances as denser cultures like spheroids or hydrogels.

Using different technologies, we have also demonstrated that plate readers, whilst sufficient for both 2D and 3D cultures that are ubiquitous across the well, are inaccurate for 3D cultures that only occupy a smaller region in the well. The HIDEX system works by reading across a defined area across each well which in theory should make for better detection of the luminescence from the spheroids and scaffolds compared to the FLUOstar OMEGA which records in a defined number of locations in a circular pattern; however, the HIDEX system gave unstable readings and was therefore not used for the remainder of the study. The FLUOstar OMEGA had a positive correlation between luminescence and cell number but there were a few outliers that would have resulted in inaccurate results had this method been used for normalisation across samples. The IVIS imager, however, is an effective and

accurate method for recording the luminescence from these smaller samples due to its ability to record all of the luminescence across the plate using a camera based system. It measured a strong correlation between cells both in 2D and in 3D even at high cell concentrations (>30000) making it a powerful tool for when studying 3D samples over long culture times. We understand that this is relatively niche equipment and is mainly used for the tracking of luminescence in *in-vivo* models but it demonstrates well that inaccurate readings are not necessarily down to the complex 3D cultures but can be down to the equipment used to measure readouts. The plate reader systems are still adequate for cultures that fill the well or when the sample is firstly lysed and homogenised like in the case of measuring viability using Promega's CellTitre Glo ® 3D.

To be able to test the accuracy of different cell number proxies, HepG2 cells were stably transduced to express RFP in their nuclei. This allowed the exact number of cells in each 3D sample to be accurately counted without penetration issues faced by stains such as Hoechst 33342. RFP was selected as red light has better penetration in tissue due to its longer wavelength reducing the risk that measurements would be inaccurate due to the inability to count all the cells (Ash et al., 2017; Zhao & Fairchild, 1998). Further to this all samples were imaged from 8 different angles and reconstructed into a single 3D image before analysis to increase accuracy.

Spheroid diameter is often used as a quick and non-invasive method for normalisation across samples and conditions, however, depending on the cell type or the culture method spheroids are not always spherical (Baze et al., 2018; Foster et al., 2019; Ogihara et al., 2017). Here the diameter of spheroids was measured using IMARIS for both the longest and shortest diameter of the spheroids and plotted against the number of cells counted using imaging. Both measurements have a positive correlation, with the shortest measurement being the most accurate, but once spheroids have over 3000 cells, it appears compaction begins to influence the overall diameter with the results beginning to plateau resulting in inaccurate results if used for normalisation. Interestingly the diameters predicted from the volume measurements calculated using $V = 4/3\pi r^3$ were of similar accuracy as

that of the actual measurements and the two had a strong correlation (Supplementary figure 1). This measurement, however, assumes that the spheroids are perfectly round which is not the case for most. As diameter measurements don't account for uneven growth there is a large degree of inaccuracy with using this measurement for normalisation. This is further supported by the spheroid volume and area (Supplementary figure 2) accurately predicting cell number, indicating that it is more the non-spherical nature of these spheroids, or errors when measuring the diameter, that is leading to the inaccuracy and less the effects of compaction at this size.

Protein concentration and cell viability were also measured to determine their accuracy when compared with cell number. Both demonstrated a positive correlation with protein concentration having a better correlation and allowing replicates, further increasing its reliability. However, there are several outlies for both measurements which could lead to inaccurate results. Creating a calibration curve, like the graphs demonstrated here could improve reliability but is time consuming and requires specialised equipment. These approaches are also both destructive and although it may be possible to use a sample that was seeded at the same time and concentration as a measure for the number of cells present in alike samples, the high degree of variability between the cultures, particularly the scaffolds, means that it is unlikely to be an accurate approach. We acknowledge that the viability measurement will only take into account the viable cells whereas the cell count may still factor in dead cells; this should, however, be negligible at this stage and size, particularly for the scaffold cultures and even the spheroids as they are without a hypoxic or necrotic core. Once these cultures had been in culture for longer then viability could be more useful, as it is normalising by only the metabolically active cells. This, however, is also true for the luminescence measurements as it requires the expression of luciferase by the cell and these measurements gave a high degree of accuracy even at much larger cell numbers.

Using HepG2s transduced to express both RFP and Luciferase we were able to plot inherent luminescence with counted cell number for cells both in 2D and the 3D samples. Cells in 2D showed

positive correlation with seeded cell number for all the instruments tested. The HIDEX instrument was inaccurate for 3D cultures, however, the FLUOstar OMEGA showed a very high degree of accuracy with the same samples demonstrating that the choice of instrumentation is important for accurate readings. As both are plate readers it is likely down to the way that they sample in the well rather than the equipment itself that causes the differences. As expected the IVIS imager was extremely accurate for samples in 2D with cells that had been seeded for only 2 hours having an almost perfect correlation. Luminescence translated well into 3D cultures with a high correlation to cell number, particularly for the IVIS imager which was accurate even at later time points with more cells. The FLUOstar OMEGA plate reader was not as accurate, although did still perform well. Most importantly for our purposes inherent luminescence was the most accurate of the cell number proxies tested; allowing us to normalise across conditions and samples in a non-destructive manner, enabling multiple measurements such as toxicity testing to be performed on the same sample.

The final proxy for cell number tested was housekeeping genes, which are widely used for different assays. Interestingly although the same volume and concentration of sample was loaded for each replicate the detected levels were not always consistent, particularly in the case of the 21 day spheroid. This demonstrates that although house keeping genes are an internal control, they can still be affected by factors including pipetting errors and technical issues. When the peak areas of GAPDH were compared with the luminescence readings taken for the same samples before lysis there was positive correlation between the two. The data however, is dispersed out with some heavy outliers which would lead to inaccurate normalisation and therefore unreliable results.

We have highlighted some of the issues faced when trying to achieve accurate measurements for 3D cultures, including issues with diffusion and compaction in spheroids whilst using stably transduced cells to demonstrate the accuracy of different proxies for cell number. For future experiments inherent luminescence will be used to control across different samples and conditions as it is the most accurate of the cell number proxies tested, is quick and easy to measure and most importantly

is non-destructive allowing further analysis of the same sample. This will allow normalisation of further readouts from the same culture and ensure that any recorded differences are down to the biology of the cell rather than the number of cells present.

Chapter 5 – Experimental comparison of cells in 2D, 3D spheroid and 3D scaffold cultures

5.1. Introduction

Spheroid cultures are the go-to 3D culture for high-throughput applications for many reasons; they are cheap and easy to culture and have been shown to greatly improve hepatocyte function, morphology and phenotype, whilst, also allowing co-cultures (Gaskell et al., 2016; Kyffin et al., 2019; Messner et al., 2013). The problem with these cultures, however, is that for the purpose of compound screening they can be unreliable or overly sensitive due to already possessing unhealthy cells. This is due to diffusional limitations, which effect the migration or nutrients and gases in, but also the diffusion of waste out. The movement of test compound is also affected in the same manner, which could lead to unreliable results and false negatives for toxicity. The industrial partner, Aurelia Bioscience, therefore, sought out a 3D cell culture that overcomes these issues and found Mimetix® electro-spun scaffolds engineered by the Electrospinning Company® as a viable option. These scaffolds offer better mechanical stability, porosity and have a reduced thickness further circumventing the issue of diffusion. They are of particular interest due to their magnetic and robust properties enabling robotic automation. Spheroids are currently the most popular 3D cell culture for high-throughput applications but are flawed, scaffold cultures were therefore compared to spheroids to determine if their high porosity improved viability or function.

After optimising the culture protocol for the scaffolds and demonstrating an accurate and non-destructive method for normalisation it was possible to perform this comparison. The main areas of focus were cell health, hepatic function, and the ability of the scaffolds to be used in screening assays. For toxicity screening it is important that the number of unhealthy or dying cells is kept to a minimum as to not influence the results of compound treatment. Three different viability assays, used within the field of 3D culture, were tested to compare cell health: MTT, lactate dehydrogenase

(LDH) and CellTitre-Glow® 3D, which utilise different principles to assess cell viability. Although these assays are well established and validated in 2D cell culture, the same is not true in 3D so it was important to test whether their results were consistent.

The MTT assay relies on the diffusion of a tetrazolium compound (3-(4,5-dimethylthiazol-2-yl)-2,5-diphenyltetrazolium bromide) into viable cells where it is converted to formazan in the mitochondria, which is purple in colour. The quantity of formazan is then measured using a plate reader at 590 nm and is directly proportional to the number of viable cells in the culture (Riss et al., 2016). The LDH assay works in the opposite manner to that of the MTT assay by measuring the release of cytoplasmic lactate dehydrogenase upon cellular damage (Kaja et al., 2017). Both of these assays have the potential to be affected by lack of diffusion of MTT into or LDH out of the 3D culture. Even with longer incubation times it is unlikely that all the MTT with be able to reach all the cells, particularly in the spheroid, whilst entrapment of LDH within the culture is to be expected. It is for these reasons that companies are beginning to develop 3D cell culture specific assays like CellTitre-Glow® 3D from Promega. This assay kit works on the same premise of the original CellTitre-Glow® assay where the amount of ATP present within the cells is measured using the luciferase reaction. This new 3D version, however, has improved penetration in 3D Microtissue and has better lytic capacity to enable all the cells within the culture to be analysed (Promega, 2022). To further asses the overall health of these cultures we have also utilised Promega's Caspase-Glo® 3/7 3D assay kit to measure the level of apoptotic cells present in the culture.

Along with cell health, the hepatic function of the three different geometries was studied using well-known liver markers including albumin production, lipid synthesis and cytochrome p450 (CYP) expression. We also tested the 3D cultures for their ability to be used in screening assays by utilising the inherent expression of luciferase by the stably transduced HepG2 cells.

3D cultures can be highly variable in size and cell number. Although more reliable, spheroids can have differences in growth depending on factors like their position in a plate or pipetting errors

during initial seeding. Scaffold cultures are typically more varied in cell population due to the diffusion of cells into different regions and their ability to bind the scaffold material. Therefore, the aim was to obtain as much information from each individual culture as possible. As most of the biochemical assays discussed above require the lysis of the cells, it was invaluable to have a non-destructive proxy for cell number. A measurement of inherent luminescence was taken before each assay and used to normalise across conditions, time points and culture geometry. The results for each assay were compared with HepG2 cells growth for 4 days in 2D (Day 1 for 3D cultures) as this was when the cells in 2D were at 70 % confluency to avoid any impact of over-confluency on cell health and function.

5.2. Results

To allow for normalisation, luminescence readings were taken before any other biochemical analysis. The cultures were then washed and moved to a standard tissue culture plate, to aid in avoiding damage and loss. Due to having lower cell quantities compared to typical 2D cell concentrations, 3D cultures were pooled into two or three cultures per well for analysis depending on their time point to ensure the level of any assay signal was at a detectable level (Figure 5.1.)

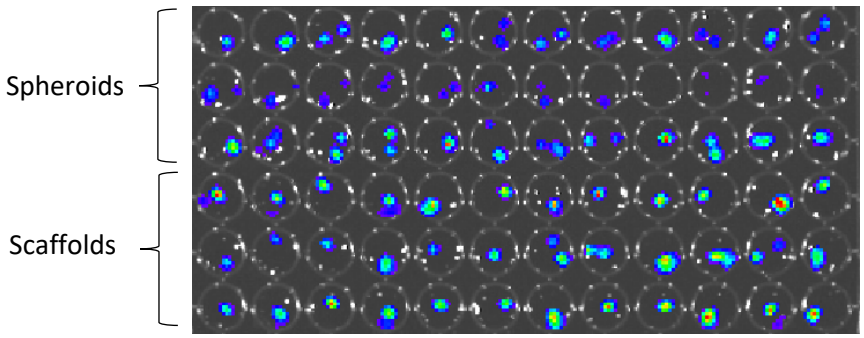

Figure 5.1. Luminescence image of stably transduced HepG2 cells cultured in spheroids and scaffolds recorded using an IVIS imager. Cultures were pooled to ensure that readouts were measurable.

5.2.1 Evaluation of cell health

To assess the viability of HepG2 cells cultured in the different geometries, three different viability assays were used to ensure that the 3D nature of the cultures did not affect the results. Firstly, MTT was tested due to its popularity across various fields (Figure 5.2.) (Adcock, 2015; Samimi et al., 2021).

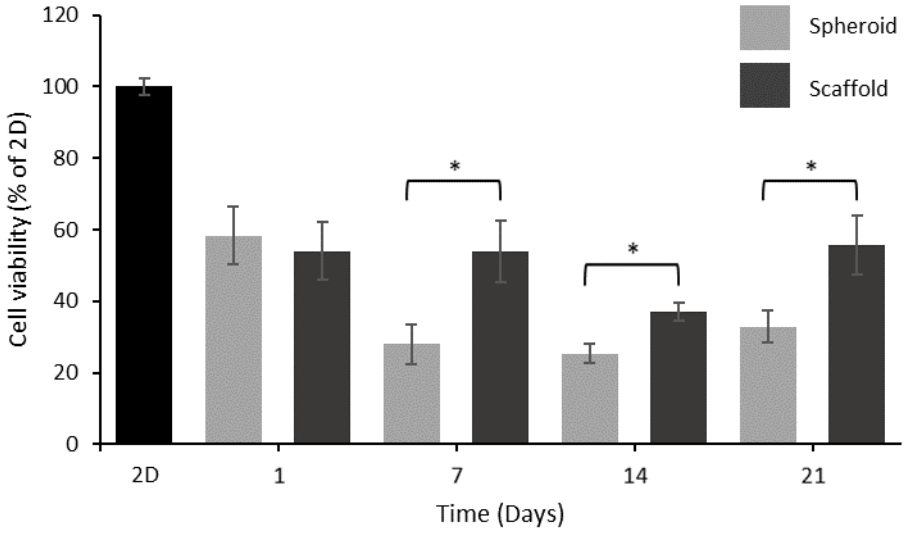

Figure 5.2. HepG2 cells cultured in 3D spheroids and scaffolds were grown to different time points, up to 21 days, and their viability was tested using the MTT assay. Absorbance values were normalised to cell number using inherent luminescence and plotted as a percentage of cells grown in 2D for 4 days. Results are expressed as mean ± SD. *$p < 0.05$ ($n = 3$). Here all results are significantly different to that of cells in 2D (*$p < 0.05$).

The viability of cells cultured in the two 3D models was significantly lower than that of cells grown in 2D. At day one (4 days in culture) there was no significant difference in the viability between cells in the spheroid or the scaffold, however, the viability of the cells was significantly higher in the scaffolds at all other time points. The viability of the cells on the scaffolds also did not decrease over time from day 1 compared to that of the spheroids which had dropped significantly by day 7.

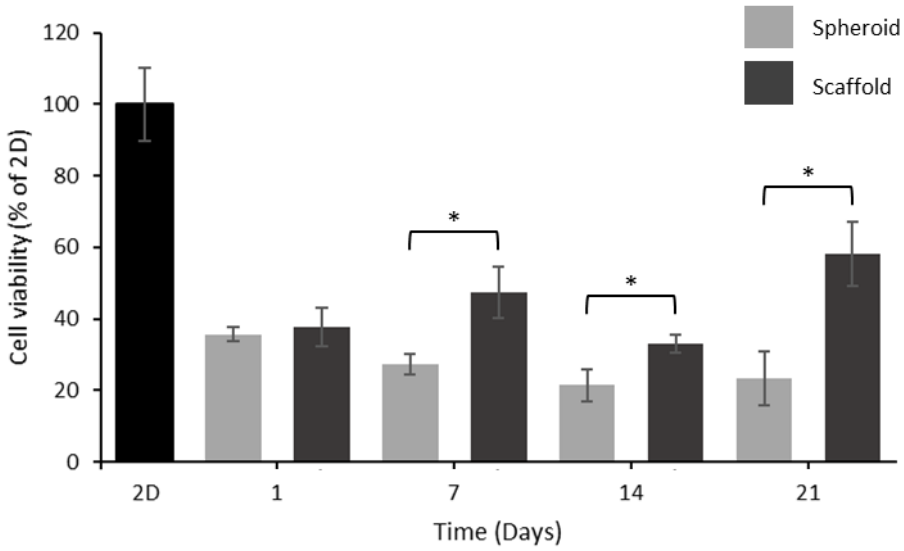

Figure 5.3. HepG2 cells cultured in 3D spheroids and scaffolds were grown to different time points, up to 21 days, and their viability was tested using CellTitre-Glow® 3D. Assay luminescence values were normalised to cell number using inherent luminescence and plotted as a percentage of the viability of cells grown in 2D for 4 days. Results are expressed as mean ± SD. *$p < 0.05$ ($n = 3$). Here all results are significantly different to that of cells in 2D (*$p < 0.05$).

To validate the MTT assay, CellTitre-Glow® 3D was also used to test the viability of the cells in the three geometries (Figure 5.3.). The results follow the same trend as that of the MTT assay with cells in 2D having significantly higher viability compared to that of the 3D cultures. The scaffolds again had higher levels of viability compared to spheroids after day 1 and did not see a reduction in cell health over time.

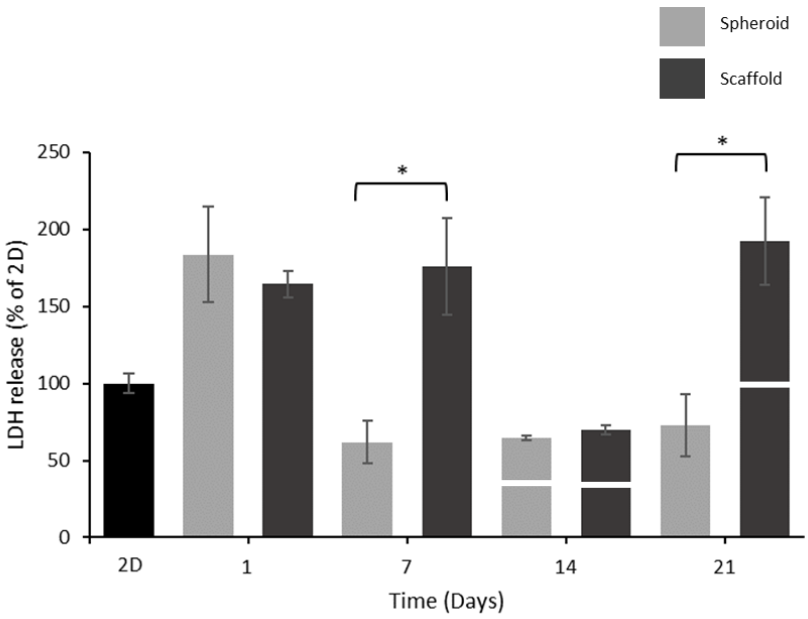

Figure 5.4. HepG2 cells cultured in 3D spheroids and scaffolds were grown to different time points, up to 21 days, and their viability was tested using the LDH assay. Absorbance values were normalised to cell number using inherent luminescence and plotted as a percentage of the viability of cells grown in 2D for 4 days. Results are expressed as mean ± SD. *$p < 0.05$ ($n = 3$). Results significantly different to that of cells in 2D are marked with a white line (*$p < 0.05$).

The final cell health assay tested was the LDH assay which works on the release of LDH into the culture media upon cell damage (Figure 5.4.). The levels of LDH release were significantly high in both the day one spheroid and scaffold culture compared to 2D, with the levels being significantly higher for all scaffold time points except those at day 14. The spheroid cultures had lower LDH release compared to 2D for days 7, 14 and 21 with their levels significantly lower than that of the scaffolds for both day 7 and 21.

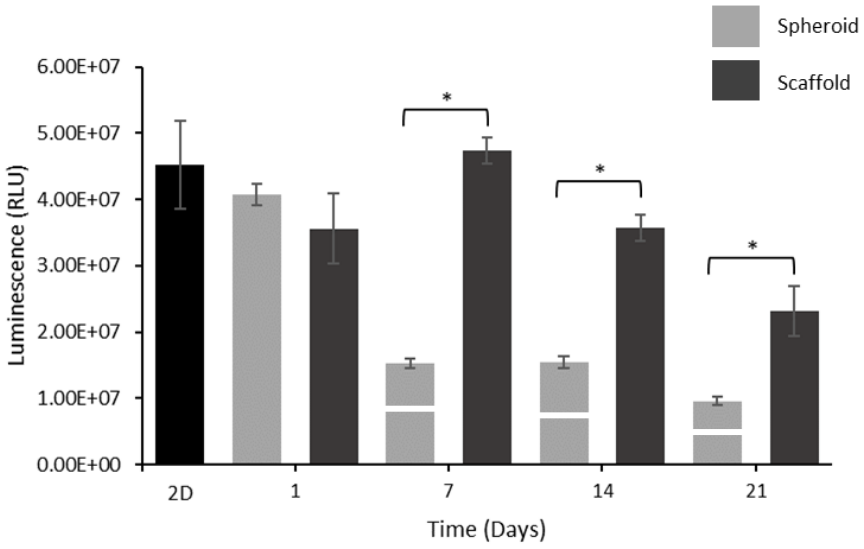

Figure 5.5. HepG2 cells cultured in 3D spheroids and scaffolds were grown to different time points, up to 21 days, and their level of apoptosis was measured using Caspase-Glo® 3/7 3D. Assay luminescence values were normalised to cell number using inherent luminescence. Results are expressed as mean ± SD. *$p < 0.05$ ($n = 4$). Results significantly different to that of cells in 2D are marked with a white line (*$p < 0.05$).

To finally assess the health of the different cultures the levels of apoptotic events was measured using Promega's Caspase-Glo® 3/7 3D assay (Figure 5.5.). This assay contains a caspase 3/7 substrate that when cleaved generates a luminescent signal proportional the level a caspase activity caused by apoptosis. Cells in 2D had the same level of apoptotic events as those in day 1 spheroids and scaffolds, however, day 7, 14 and 21 spheroid cultures had significantly lower levels of apoptosis occurring compared to cells in 2D and 3D scaffolds of the same time point. The level of caspase activity in the scaffold cultures remained high up to day 21 and was not significantly different to that of the cells in 2D at any time point.

5.2.2 Assessment of hepatic function

HepG2 cells grown in the three geometries were next evaluated on their functionality using various techniques. Firstly, lipid metabolism was measured using Cholesterol/Cholesterol Ester-Glo™ to measure total cholesterol production (Figure 5.6.).

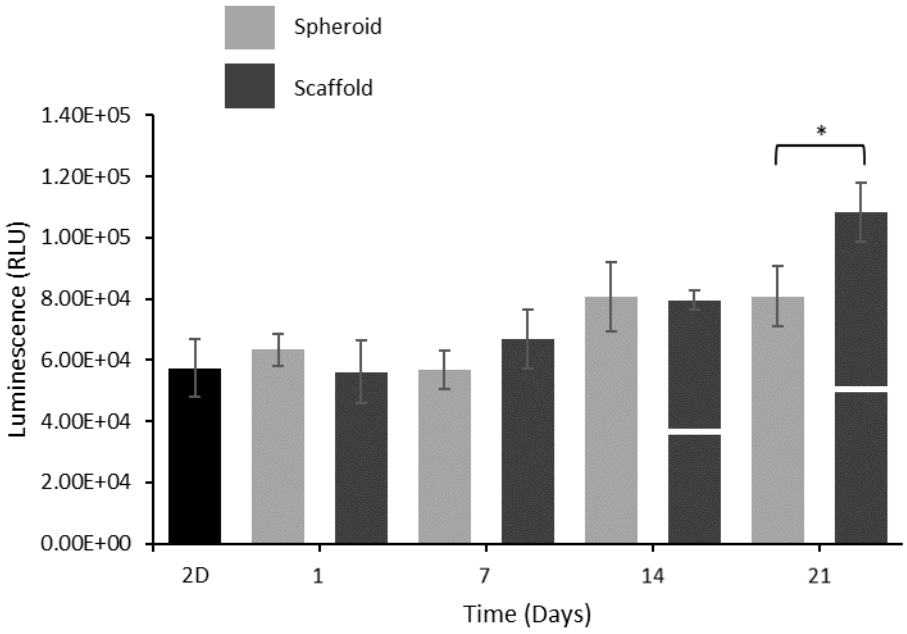

Figure 5.6. HepG2 cells cultured in 3D spheroids and scaffolds were grown to different time points, up to 21 days, and their level cholesterol production was measured using Promega's Cholesterol/Cholesterol Ester-Glo™. Assay luminescence values were normalised to cell number using inherent luminescence. Results are expressed as mean ± SD. *$p < 0.05$ ($n = 3$). Results significantly different to that of cells in 2D are marked with a white line (*$p < 0.05$).

For spheroid cultures there was no increase in total cholesterol production at any time point compared to levels in 2D. For scaffold cultures, however, day 14 and 21 scaffold cultures showed significantly higher levels compared to that of 2D cells. This demonstrates improved function of the scaffold culture over time, with the levels of total cholesterol being significantly higher than that of the spheroids at day 21.

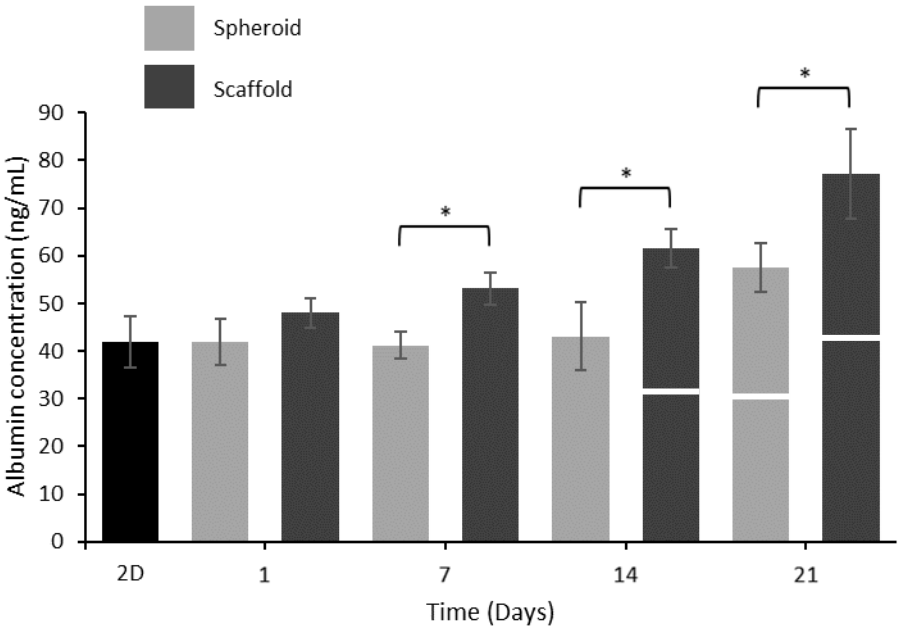

Figure 5.7. HepG2 cells cultured in 3D spheroids and scaffolds were grown to different time points, up to 21 days, and their level albumin production was measured by ELISA. Absorbance values were normalised to cell number using inherent luminescence. Results are expressed as mean ± SD. *$p < 0.05$ (n = 3). Results significantly different to that of cells in 2D are marked with a white line (*$p < 0.05$).

To further assess the metabolic function of the cells, albumin levels were also measured by ELISA. By day 7, the levels of albumin within the cultures was significantly higher in the scaffolds compared to the spheroids, whilst also being significantly higher at all proceeding time points. Albumin production increased over time for both cultures compared to cells in 2D with levels being significantly higher at day 14 and 21 for scaffolds and day 21 for spheroids demonstrating the importance of prolonged cultures for improving hepatic function.

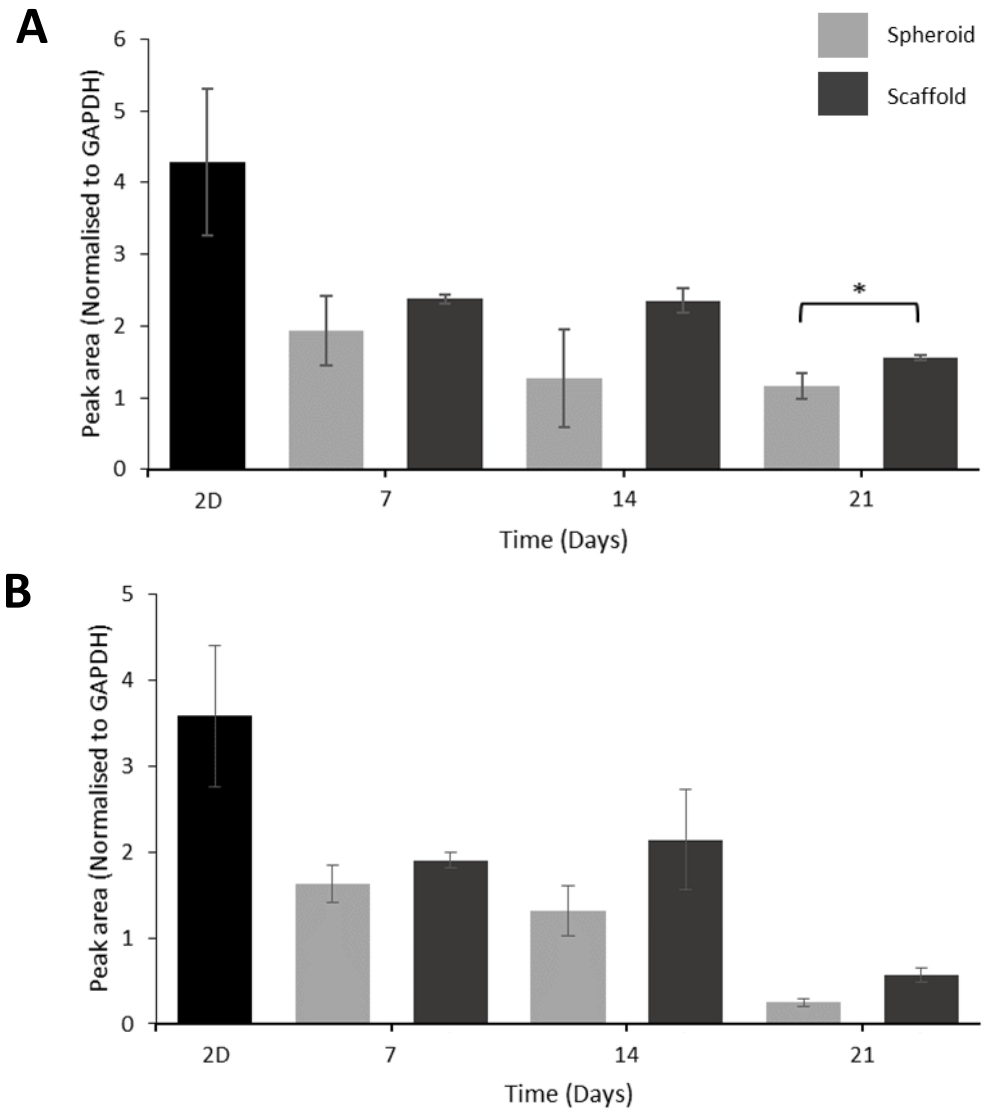

Figure 5.8. HepG2 cells cultured in 3D spheroids and scaffolds were grown to different time points, up to 21 days and their expression of CYP2B6 (A) and CYP2D6 (B) was measured using JESS analysis. The area of the peaks was recorded and normalised using GAPDH expression. Results are expressed as mean ± SD. *$p < 0.05$ ($n = 3$). Here all results are significantly different to that of cells in 2D (*$p < 0.05$).

Finally, the expression of two key drug metabolising enzymes that are known to be expressed highly in HepG2 cells, CYP2B6 and CYP2D6, was measured using JESS analysis (Figure 5.8.)(Maruyama et al., 2007). Expression was significantly higher in 2D cells compared with all 3D cultures. Levels of both enzymes decreased in the scaffold cultures from day 14 to day 21 with spheroid cultures also showing a decrease in the expression of CYP2D6 between day 14 and day 21. Comparing the two 3D cultures, only levels of CYP2B6 at day 21 was found to be significantly different.

5.2.3 Hepatotoxicity testing

To test the ability of the models in screening assays for compounds or drugs was tested by measuring inherent luminescence over time and normalising to the control (Figure 5.9.). Sorafenib was used as the test compound at 10 µM, due to its use as a treatment for advanced liver cancer, and was compared to a vehicle control and positive control (Staurosporine). The models were cultured for 8 days (12 days including 4 days of formation for spheroids and scaffolds) with drugs administered on day 7 and 11.

Figure 5.9. Toxicity screening of Sorafenib

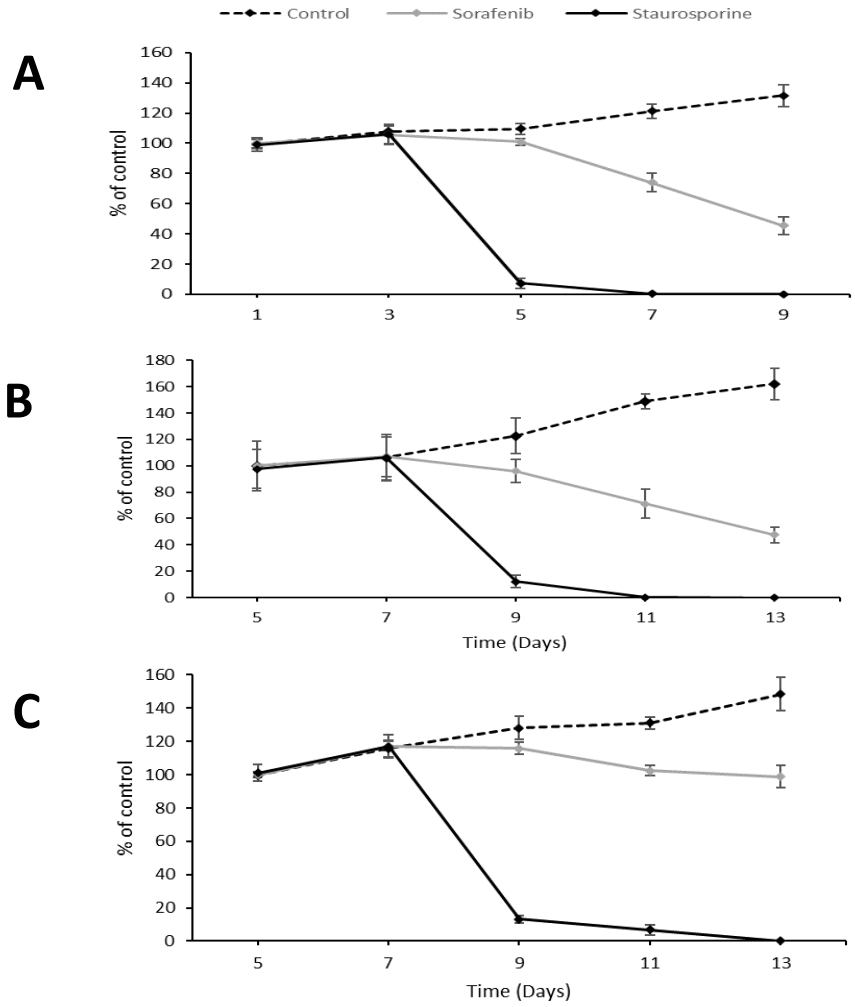

Figure 5.9. HepG2 cells were cultured in 2D (A), 3D spheroids (B) and 3D scaffolds (C) for 8 days (12 for spheroid and scaffolds) before drugs were administered on day 3 (7) and 5 (11). 10 µM Sorafenib and 2 µM Staurosporine were added without removal. Inherent luminescence was measured every two days and normalised to the vehicle control. Results are expressed as mean ± SD (n = 3). 2D cells and spheroids show similar response to test drug, however, scaffolds maintain higher cell concentration percentages compared to the control indicating their effectiveness for repeat dose experiments.

After drug administration at day 7 all cultures had a sharp decline in cell number by day 9 for the positive control, with minimal viable cells remaining and by day 11 with only the scaffold cultures having remaining signal, likely due their more *in-vivo* like state improving cell viability, functionality and their ability to tolerate drug treatments (Samimi et al., 2021). For the tested drug, Sorafenib the response was similar between cells in 2D and the 3D spheroid with over 50 % loss of viable cells compared to the control by day 13. The scaffolds, however, only experienced a 30 % loss in viable cells by day 13 likely due to their improved overall viability.

5.2.4. Other assays

Various other assays were tested with the two 3D cultures, however, yielded no results. Due to the confusing results for CYP expression, Promega's P450-Glo assays were tested but showed no signal for the 3D cultures even when a large number of samples were pooled together. Multiple attempts were taken to quantify the protein levels of ATP51A to measure mitochondrial abundance, and HIF1α as a measure of the level of hypoxia. However, no signal was recorded even when using the JESS system. It is suspected that this is due to either low levels of expression in the cultures, poor antibodies or due to the rapid degradation of HIFα upon exposure to oxygen during collection and analysis (Strowitzki et al., 2019).

To try and further study the abundance of mitochondria, lipid production and hypoxia, spheroids and scaffolds were imaged using the light-sheet microscope. For mitochondrial abundance MitoTracker™ and CellLight™ Mitochondria were tested along with BODIPY for lipid production and HypoxiTRAK to identify hypoxic regions. Unfortunately, whilst these dyes produced nice looking images it was not possible to quantify their levels due to low penetration of the cultures, particularly the spheroid (Figure 5.10)

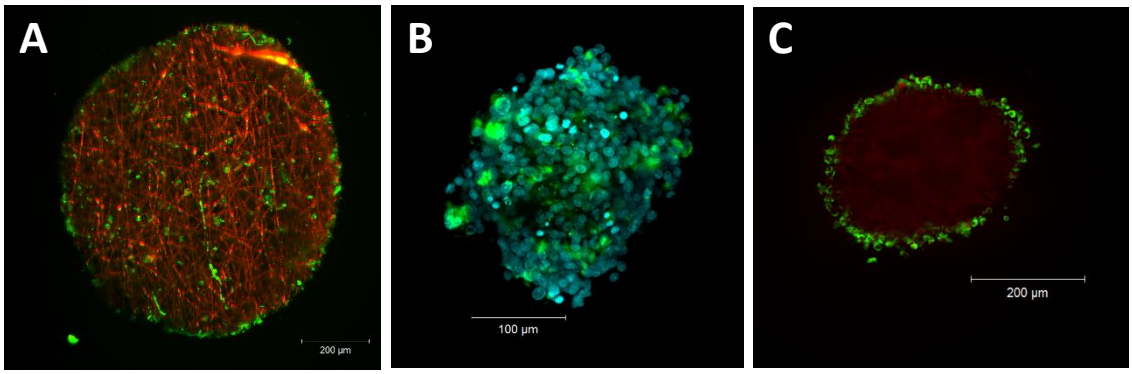

Figure 5.10. Maximum intensity projections of a scaffold containing quantum dots (Red) populated by cells stained with MitoTraker™ (green) (A) and a spheroid stained with Hoechst (blue) and BODIPY (green) (B). Z-stack of a spheroid which was treated with CellLight™ Mitochondria over night (C). Even with an overnight incubation the CellLight™ Mitochondria stain was still unable to penetrate past the outer layer of cells. All imaged using the Z.1 light-sheet microscope.

5.4. Discussion

The primary focus for this work was to determine if the advantages of the scaffold cultures effect viability and functionality of HepG2 cells compared with spheroid cultures. Spheroids are currently the most used 3D culture for high-throughput analysis as they are simple and have been shown to improve functionality when compared to cells in 2D (Gaskell et al., 2016; Kyffin et al., 2019; Ramaiahgari et al., 2014). The problem, however, is whilst primary hepatocytes can be a useful model when cultured in spheroids, the same is not true for most cancer cell lines. This is due to primary cells not proliferating in culture and unless using a cancer cell line like C3A cells, which have strong contact inhibition, the cells will continue to proliferate and their viability will drop after only a few days in culture (Bell et al., 2016; Edmondson et al., 2014).

As primary cells can be difficult to obtain, are expensive or come from diseased tissue, most researchers turn to cheaper and more accessible cancer cell lines, with the most prominent liver cancer cell line being HepG2 cells. To try to limit the issues associated with spheroid cultures and allow the use of cancer cell lines, a variety of scaffold-based 3D cultures have been developed. These

cultures can limit spheroid size, like in the case of hydrogels, or improve the diffusion of nutrients and gases into the cells, like in the case polymer scaffolds.

Here the cancer cell line, HepG2, has been cultured in 2D, 3D spheroids and on a 3D electrospun scaffold and assessed for cell health and function. With an overall porosity of 80% these scaffolds offer the potential for a healthier 3D culture over a longer period.

The ability to compare these two 3D models was possible using a stably transformed HepG2 cell line that expressed luciferase. This inherent luminescence is an accurate proxy for cell number allowing normalisation between the different cultures and ensuring that any differences are down to cell health or functionality and not the number of cells (Figure 4.12.).

Cell viability and health in 3D cultures are important for all research purposes but particularly when performing compound and drug screenings to allow accurate results to be measured, that are not affected by the health of the culture. Comparisons of viability across different 3D cultures is rarely performed, likely due to difficulties with normalisation or that viability is used as a proxy for cell number to allow normalisation (Luckert et al., 2017; Sarkar et al., 2017). Here cell health is compared between cells in 2D, spheroids and scaffold culture using MTT assay, CellTitre-Glow® 3D, LDH assay and Caspase-Glo® 3/7 3D.

The results from the MTT, LDH and CellTitre-Glow® 3D assays show a reduction in the viability of both 3D cultures when compared to that of cells in 2D at the same time point of four days in culture (Day 1 for spheroids and scaffolds). This was unsurprising as firstly, the cells in 2D have not been subjected to the same culture conditions as those in 3D whilst they were manipulated and growing into the 3D models and had been able to settle into 2D within hours of seeding and remained there undisturbed until analysis. Secondly, the cells in 2D have a higher abundance of gases and nutrients without any diffusional limitations. If the cells in 2D had been allowed to become over 100% confluent in the culture vessel and cultured for prolonged periods it is expected that over time their viability would also decrease.

The MTT assay and CellTitre-Glow® 3D assays demonstrated that after day 1 the viability of both the spheroids and scaffolds remained constant throughout the culture. The exception here was the scaffolds at day 14 which had significantly lower viability than those at day 21. Upon analysing the results of these scaffolds it was found that the inherent luminescence values at day 14 were considerably higher than that of the scaffolds at day 21. This indicates that the number of cells on the scaffolds at day 14 was much higher than that of the scaffolds at day 21. This is likely the result of increased scaffold population during the first 4 days of culture. Interestingly this aligns with the reduced viability of the spheroid cultures, as these day 14 scaffolds were highly populated and experiencing reduced availability of nutrients and gases, their viability decreased. Importantly the results demonstrated that the viability of the scaffolds was significantly higher than that of the spheroids of the same age at time points 7, 14 and 21, even with an increased population at day 14. These results indicate that the scaffold allows a more viable cell population, due to increased access to nutrients and gases, than that of the spheroid which is maintainable for prolonged periods (21 days). It is expected that the scaffold cultures could be maintained for longer without loss of viability, however, this was not tested due to the focus of this work being to compare the 3D scaffold cultures with 3D spheroids, which at 21 days had significant reductions in viability.

The LDH assay showed a decrease in viability for day 1 spheroids and scaffolds compared with those in 2D and demonstrated a stable viability for scaffold cultures up to day 21 with the exception of the day 14 supporting the results of the MTT and CellTitre-Glow® 3D assays. Interestingly the LDH assay results indicate an increased viability for spheroids cultures after day 1 and for day 14 scaffolds. This assay works on the release of LDH into the culture media upon cell damage, a process that relies on the diffusion of LDH out of the culture. As this assay is not designed for 3D cultures, it was suspected that due to the increased size of these spheroid cultures and scaffolds at day 14 the diffusion of the LDH into the media was hindered leading to unreliable results. This is due to the smaller spheroids at day 1 having similar levels of LDH to that of day 1 scaffolds and that other than these larger cultures, the results are in line with those of the MTT and CellTitre-Glow® 3D assays. Recent work regarding

the use of LDH in 3D xenospheres demonstrates the effect of LDH release as cultures increase in size (Cox et al., 2021). They, however, show that the reason for no increase in LDH levels is down to saturation of the signal, they discuss how this could be solved by diluting the sample but unfortunately it was not tested. They show that by day 7 for larger cultures the signal reached saturation, however, they plot their results against seeding concentration and do not normalise for cell number. This could also be the case for Figure 5.4., the larger cultures have reached the saturation point of the assay, however, these results have been normalised to highest cell number using inherent luminescence which would lead to a lower signal when normalised. After looking at the luminescence values for spheroids at day 7, 14 and 21 along with day 14 scaffolds, they are considerably higher than that of the other cultures indicating that this contrasting result may be down to the method of analysis rather than the initially assumed problem of diffusion.

To finally assess the health of the different cultures the level of apoptosis present was measured using Caspase-Glo® 3/7 3D. Initially there was no difference between the level of any of the cultures at 4 days of culture (day 1 for 3D cultures), however, by day 7 there was a significant difference between the levels of caspase activity between the two 3D cultures with the level of apoptosis in the spheroids having reduced dramatically. As spheroid experience zonation due to the diffusion of oxygen and nutrients to the cells, over time, only the outer area of the spheroids are viable, followed by an inner area of hypoxic cells and finally a necrotic core (Gaskell et al., 2016). As HepG2 spheroids at day 7 were measured to have a shortest diameter of 323 µm as discussed in section 3.4, these results indicate that by day 7 most of the cells in the spheroid have moved from active cell death, apoptosis, and are now undergoing necrosis caused by the limited oxygen levels. This also explains why the level of apoptosis remained consistent across the spheroids for the two remaining time points as only cells that are viable can undertake apoptosis, not those damaged through environmental factors (Fink & Cookson, 2005). Therefore, only those on the outer edge, that are not experiencing hypoxic conditions, are able to die through apoptosis resulting in lower levels of apoptosis in the culture compared with a normal, healthy culture like that of cells in 2D.

This is further supported by the levels of apoptosis in the scaffold cultures, which have higher porosity and levels of oxygenation, remaining non-significantly different to that of the cells in 2D even at time point 21. There does, however, appear to be a slight reduction in the levels of caspase activity over time indicating that some cells in the scaffold cultures are also beginning to become necrotic. The results from the Caspase-Glo® 3/7 3D indicate that although the levels of caspase activity occurring in the spheroid cultures is reduced, this is due to only the out layers of cells being able to undergo apoptosis. This is supported by worked performed by Modulevsky et al., (2014) which shows that cells less than 100 µm into a scaffold culture begin to become apoptotic and necrotic. Therefore, of the viable cell population, a smaller number of cells undergoing apoptosis compared to that of the scaffold cultures where necrosis is limited. This could be further tested by looking at caspase specific markers such as Cytochrome C release, cleaved PARP and active caspases in the two 3D cell cultures. As the scaffold cultures retain similar levels of caspase activity compared to 2D cells this is an indication of a healthier cell population.

Albumin production and lipid metabolism are two important functions of the liver which are often tested when assessing the functionality of hepatic 3D cultures (Bacon et al., 2006; Das et al., 2020; Kuntz & Kuntz, 2008; Sarkar et al., 2017; Takahashi et al., 2015). The improved lipid metabolism of the scaffolds, along with the improved albumin production of both cultures demonstrates the importance of maintaining these cultures for long periods. Conversely the expression of two key drug metabolising enzymes was significantly lower than that of cells grown in 2D, whilst reducing in the 3D cultures over time. This goes against what has been published in many studies and, whilst the enzymes were not induced and HepG2 cells are known to have low levels of CYP expression, indicates that further analysis is required potentially using qPCR or proteomic analysis (Bell et al., 2016; Berger et al., 2016; Gerets et al., 2012; Godoy et al., 2013; Štampar et al., 2020).

Finally to assess the ability to utilise the scaffold culture for compound testing in long term, repeat dose experiments the cultures were treated with Sorafenib which is a multityrosine kinase inhibitor

with antiproliferative and proapoptotic properties in liver cells (Feng et al., 2021; Fernando et al., 2012; Ou et al., 2010). Whilst spheroid cultures showed similar decreases in the number of viable cells to that of 2D cells, sorafenib had less of an effect on the scaffold cultures. This is possibly due to the improved overall viability and functionality of the cells within these cultures when compared to spheroids, but also due to the improved *in-vivo* like characteristics where factors like polarity, hypoxia, dormancy and anti-apoptotic behaviour come into play. The purpose of this experiment, however, was to demonstrate the ability of the scaffolds for long periods of time for the purpose of compound and drug screenings and not to determine drug toxicity.

It has been demonstrated that these electrospun scaffold cultures offer long culture periods for drug toxicity screening, with improved porosity that allows the diffusion of nutrients and gases into the cells whilst potentially avoiding the formation of hypoxic cores. This would limit the level of necrotic cells, impacting the predicted hepatotoxicity of drugs, whilst allowing these compounds to reach a larger number of cells within the culture and not be hindered by diffusion. They also offer a culture that has better overall viability and functionality when compared to spheroid cultures, particularly if using the cancer cell line HepG2 that will continue to proliferate throughout the length of the culture.

Chapter 6 – Final Discussion

6.1. Introduction

Industrial context: Aurelia Bioscience specialise in bioassay development, pharmacological profiling and compound screening and utilise spheroid cultures for their 3D work. They, however, have faced issues regarding reliability and the labour intensity of these cultures, with attempts to increase the throughput using automation leading to loss or damage of the spheroids. Therefore, they contracted the Electrospinning company® to produce, 50 µm thick, electrospun scaffold material that had several potential advantages over spheroid cultures due to its high porosity, customisability, mechanical stability and its potential for automation in high-throughput studies. The focus was on utilising these scaffolds for screening assays in the early stages of the drug discovery pipeline in a high-throughput manner and over prolonged periods.

Scientific objective. The aim of this project was to establish these scaffold cultures and compare them to cells in 2D and the currently used spheroid cultures, thus investigating how the organisation and environment of cells affect their studying their ability viability and functionality. HepG2 cells were selected as this liver cancer cell line is readily available and cheap, so reduced costs while the culture technique was established, with the goal to move to more physiologically relevant cell lines and primary cells once the scaffold culture was established.

6.2. Spheroid and scaffold culture

Aim 1 - To establish robust and efficient protocols for the culture of 3D spheroids and scaffolds for use in high-throughput screening assays

6.2.1. Spheroid culture

There are a wide variety of techniques to generate spheroids cultures including ULA surfaces, hanging drops, rotating flasks, hydrogels, microfluidics and external force (Shen et al., 2021). Of these only ULA surfaces and hanging drops were feasible for establishing spheroid cultures in the University lab as the others require specialised equipment and hydrogels do not create a single spheroid per well. Both techniques reliably produced single spheroids per 'well' that were uniform in size and shape whilst being simple to set up and not too labour intensive. Hanging drops were selected as the technique used in Liverpool as they allowed the collection of all the spheroids simultaneously, into a single suspension. This was advantageous for imaging using the Zeiss Z.1 light-sheet, as multiple spheroids could be loaded at once, and additionally were easier to visualise and collect in a culture dish in comparison to a ULA plate when transferring the spheroids to a cell culture plate for biochemical analysis.

6.2.2. Scaffold culture

The most time-consuming and laborious task of this project was the establishment of the cell culture protocol for the scaffolds. The goal was to have a thin and even distribution on both sides of the scaffold to allow the cells to grow and populate the scaffold over time and to avoid spheroid like clumps that would become hypoxic/necrotic over the length of the culture.

The size of the scaffolds (1000 µm x 50 µm) was selected as they would fit inside 384 plate wells for high-throughput applications, whilst still being pipettable and visible to the naked eye. However, once inside of a well they could be difficult to see and could not be handled manually using tweezers. Although improved from the original 100 µm x 50 µm scaffolds there were also still losses

during culture, particularly in the beginning. Other commercial scaffold cultures like Alvetex®, SpongeCol®, 3D Biotek and even Mimetix® are designed for insertion into plates with 6 to 96 wells meaning they are no smaller than 5 mm and can be easily manipulated using tweezers or come already inserted in the well. These other plate based scaffold cultures are simple to culture and rely on the 'drop-on' method, where cell suspension is added to the top of the scaffold allowing cells to diffuse and migrate into the scaffold architecture (Brown et al., 2018; German & Madihally, 2019; Ruoß et al., 2018). Although not always the case, this method can lead to lower cell attachment, penetration and a heterogeneous cell distribution as cells remain on the top of the scaffold and do not migrate within (Asthana et al., 2018; Murphy et al., 2010). This method was tested for the electrospun scaffolds but showed poor cell uptake.

After testing three different techniques, it was clear that keeping the scaffolds in continuous suspension with cells would give the desired cell seeding distribution. Two pieces of equipment were tested, and results indicated that the rocking technique was the best suited. After manufacturing cryovials with a PDMS lid, the desired cell distribution was achieved. This method was utilised for most of the project, however, produced low yields and a better solution was required for high-throughput applications. The CELVIVO ClinoStar®, which works on the same premise of the PDMS tubes, showed similar scaffold population, whilst allowing gaseous exchange and enabling 100 scaffolds to be cultured in a single ClinoReactor®. The ClinoStar® system has since been purchased and the industrial partner has contracted Scitech Precision to laser cut the scaffolds as this was another bottle neck in the high yield production of the scaffold culture.

The first aim of establishing spheroid and scaffold culture was therefore achieved. Spheroids can be easily cultured in 96 or 384 hanging drop or ULA plates and up to 600 scaffolds can be cultured simultaneously with the desired starting cell distribution.

6.3. Accounting for cell number within the cultures

Aim 2 – Assess the current methods of normalisation in the field to allow accurate comparisons between cultures, conditions, and time points

The comparison between cells in different culture geometries is not often performed, likely due to the difficulties of accurately normalising between the cell models. 3D models are often compared to the same cells cultured in 2D (Bell et al., 2018; Gaskell et al., 2016; German & Madihally, 2019; Kim et al., 2018; Ruoß et al., 2019), however, comparisons between different 3D cultures are not as common and typically involve cultures that are alike in structure (Luckert et al., 2017).

Due to the very different geometries between spheroids and scaffolds it was important that the level of viable cells within each culture was accounted for to enable an accurate comparison, preferably in a non-destructive manner.

There are a variety of different normalisation techniques implemented within the field of 3D culture, depending on the type of biochemical analysis being performed. As it is not possible to count the number of cells through conventional measures like in 2D cultures, researchers employ proxy measures to normalise across cultures, conditions, and time points. For spheroid cultures some studies utilise spheroid diameter or area (Baze et al., 2018; Foster et al., 2019; Ogihara et al., 2017) to control across conditions but this is not applicable when comparing two very different geometries. Other cell number proxies include total protein or DNA (Chitrangi et al., 2017; Vu et al., 2016), viability (Luckert et al., 2017; Sarkar et al., 2017) and housekeeping genes (Shah et al., 2018; Štampar et al., 2020). To test the ability of these proxies for cell number the total number of cells were counted in both spheroids and scaffold cultures using light-sheet microscopy and compared to the values of each readout. As spheroid diameter was not applicable to the scaffold cultures and viability was one of the readouts of interest, both these proxies were unusable for this study. The level of housekeeping genes is also only useable for when studying the expression of different genes or proteins. This left total protein as the only viable option for normalising across the two 3D

cultures, however, this measure was found to be inaccurate and destructive. To avoid the use of total protein, HepG2 cells that had already transduced to express RFP in their nuclei were further transduced to express luciferase. The luminescence values from this culture were also measured against total cell number and were found to be an accurate cell number proxy, even at high cell numbers.

Using this stable cell line, it was possible to easily and accurately account for the number of cells in all three geometries using a high-sensitivity luminescent imager in a non-destructive manner allowing further analysis of the same culture.

6.4. Comparing the cell culture models

Aim 3 – Compare the models regarding health, function, and application in high-throughput screening studies with a focus on long culture times

After establishing the 3D cultures and being able to accurately normalise between the two, they were compared for both health and functionality.

As the intended use for these cultures is in compound screening over prolonged time periods, it was important that the cells within the 3D culture are healthy. To assess this several different assays were performed, ensuring that the results were not influenced by the geometries of the culture. The results of the MTT and CellTitre-Glow® 3D assays indicated that cells in the scaffold culture had increased viability to those in the spheroid at days 7, 14 and 21, although not as high as cells in 2D. The results from the LDH assay were inconclusive due to the assay becoming saturated by the larger cultures. Caspase-Glo® 3/7 3D was used to measure the levels of apoptosis in the cultures with the levels of caspase activity remaining consistent between 2D and the scaffold cultures up to day 21. The levels of apoptosis in the spheroids at days 7, 14 and 21 were significantly reduced indicating a shift from programmed cell death to necrosis, due to the limited supply of nutrients and gases.

These results demonstrate that the improved porosity of the scaffold culture results in a healthier 3D cell model compared to that of spheroids.

The liver has many functions *in-vivo* including bile formation, lipid metabolism, albumin and urea production, and drug metabolism resulting in a number of functional assays to choose from (Bacon et al., 2006; Kuntz & Kuntz, 2008). Albumin and Cholesterol production were selected as they require the lysis of the sample and will not be possibly influenced by diffusion limitations like in the case of urea assays. Albumin production increased in both cultures over time, however, the levels were significantly higher in the scaffolds than that of the spheroids at day 7, 14 and 21. The scaffolds levels were also significantly higher than that of the 2D cells at day 14 and 21. Total cholesterol levels in the spheroids remained consistent with that of the cells in 2D up to day 21. Scaffold cultures, however, demonstrated improved cholesterol production compared with 2D at days 14 and 21 and their levels were also significantly higher than that of spheroids at day 21. The results of the albumin and total cholesterol assays demonstrated improved hepatic functionality of the cells in the scaffold culture over those in the spheroids and 2D. They also demonstrate the importance of maintaining these 3D cultures over long periods to enable the cells to return to a more *in-vivo* like state.

One major application of *in-vitro* liver cells is in toxicity testing so the expression levels of two key drug metabolising enzymes (CYP2B6/2D6) was tested. The results, however, showed a significantly reduced level in both 3D cultures compared to cells in 2D. This is contradictory to what is well accepted within the field and indicates that further repeats are required (Berger et al., 2016; Gerets et al., 2012; Gu et al., 2018; Štampar et al., 2020). The three geometries were also tested for their ability in drug screenings for prolonged periods with treatment of Sorafenib, a potent multityrosine kinase inhibitor, with the scaffold culture demonstrating a reduced decline in cell number compared to cells in 2D and spheroids. This is important as it shows the potential of scaffolds for longer

compound screenings and repeat dosing making the scaffolds more pharmacologically relevant (Bircsak et al., 2021).

6.5. Future work

Aim 4 – Improve the models in their ability to recapitulate the *in-vivo* environment

At the beginning of the project the amount of time it would take to both establish the scaffold culture method and find an accurate proxy for cell number was underestimated and consequently there was not time to attempt to improve on the current model.

As HepG2 cells have low CYP expression and poorly represent *in-vivo* hepatocytes, the goal was to move to more physiological cell lines such as HepaRG or primary cells (Seo et al., 2019; Stanley & Wolf, 2022). In future work these liver cells would be tested utilising the scaffold culture, particularly HepaRG as they have a stable phenotype and have improved CYP expression (Lőrincz et al., 2021; Wu et al., 2016). Although primary cells are the gold standard and it would be interesting to study them using the scaffold culture, the method used for seeding the scaffolds requires a large number of cells to be in suspension. Due to difficulties expanding primary cells *in-vitro* and the associated cost and availability, more physiological cell lines like HepaRG are a better choice.

Whilst the scaffolds have been shown to improve the function of HepG2 cells compared with spheroid cultures, further improvements could be tested. The structure of the scaffold and the culture technique make it ideal for co-cultures, where the scaffold is populated with one cell type, such as fibroblasts, before layering hepatocytes on top. Different combinations of co-cultures could be tested including HUVECS and fibroblasts, which have been shown to improve hepatic function in other 3D cultures (Böttcher et al., 2022; German & Madihally, 2019; Yaqing Wang et al., 2018; Ware et al., 2021).

Although the coating of the scaffold with ECM proteins was tested for its ability to improve cell binding, work by Brown et al., (2018) demonstrates improved hepatic function of primary

hepatocytes when cultured on electrospun scaffolds that were treated with collagen and fibronectin. The coating of the scaffold with these ECM proteins could be tested alone or in combination with co-cultures to better recapitulate the *in-vivo* environment.

Finally, the potential to automate the scaffold cultures for high-throughput screening was one of the main draws to the scaffold material. The scaffold offers improved mechanical stability to that of spheroids and is customisable with different fluorophores, quantum dots and magnetic particles. The industrial partner has contracted the production of smaller 200, 300 and 400 µm x 50 µm scaffolds along with the 1 mm x 50 µm from Scitech Precision which they are going to test in their current automated liquid handling robot for applications in high-throughput screenings.

6.6 Final remarks

The aim for this project was to establish a scaffold culture that is very different in size to that of other 3D scaffold cultures. This allows them to be automated easily through robotics for high-throughput applications, whilst the thin structure of the scaffolds is mechanically stable and avoids the issues of limited diffusion into the cells. After establishing a cell culture protocol that enables high yields of scaffolds and being able to accurately normalise to cell number across the conditions the scaffolds were compared to 2D and 3D spheroid cultures. The scaffolds demonstrated improved health and hepatic function compared with the spheroid cultures whilst also allowing long culture periods. Although viability is higher in 2D cells, they cannot be cultured for long periods without passage. The scaffolds represent a more *in-vivo* like phenotype and can be cultured for up to 21 days which is important for drug and compound screening. This makes the scaffolds more pharmacologically relevant and allows for repeat dose experiments to be performed. Building on the work done in this project the industrial partner is aiming to establish protocols for the use of the scaffolds in high-throughput screening assays and eventually offer these 3D cultures out to clients.

7. Supplementary data

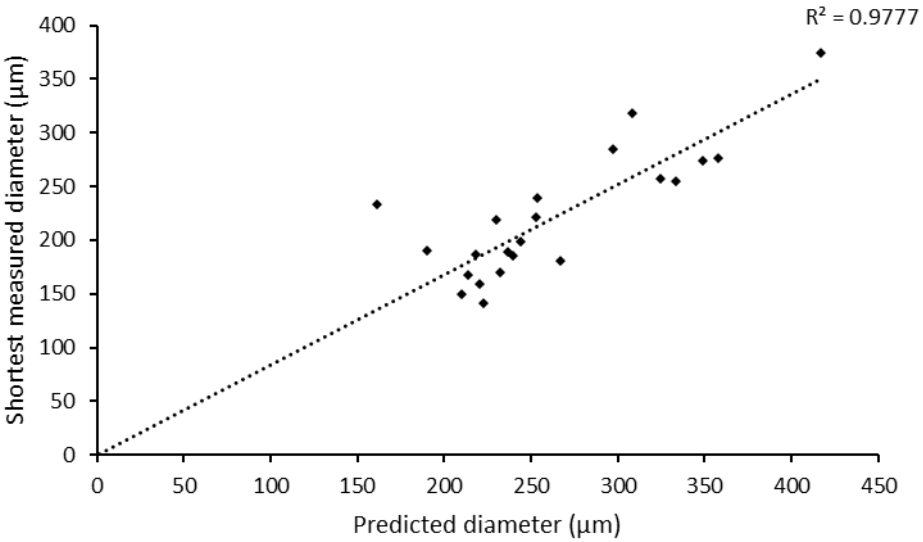

Supplementary figure 1. Spheroid diameter measured in IMARIS plotted against diameter predicted from their volume measured in IMARIS.

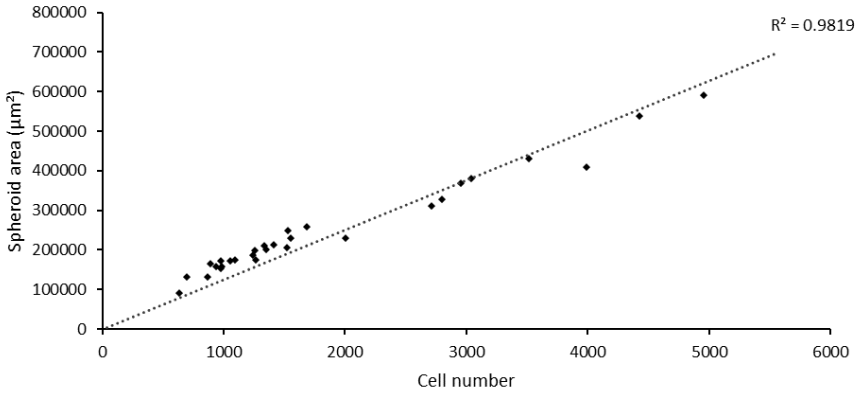

Supplementary figure 2. Spheroid area calculated using IMARIS.

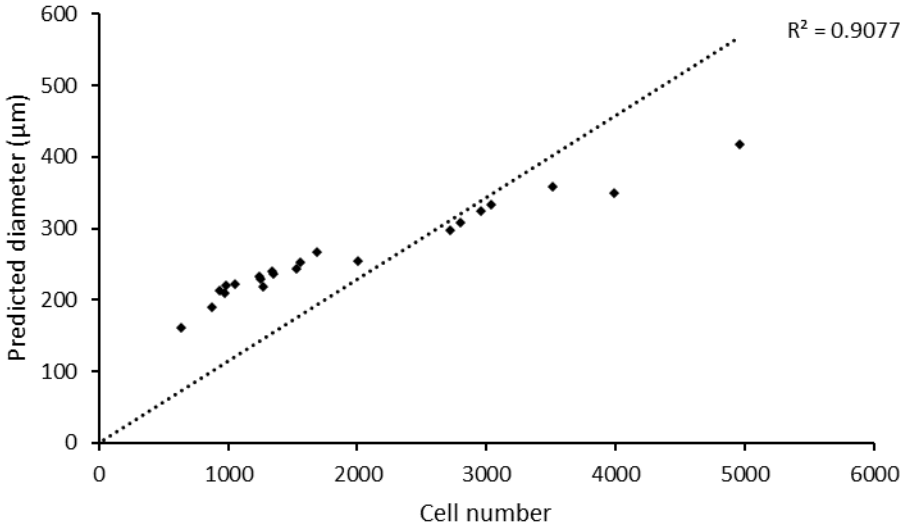

Supplementary figure 3. Spheroid diameter predicted from the spheroid volume plotted against cell number counted using light-sheet microscopy. The same effect of compaction can be seen as in Figure 4.7.

Bibliography

Adcock, A. F. (2015). Three-Dimensional (3D) Cell Cultures in Cell-based Assays for in-vitro Evaluation of Anticancer Drugs. *Journal of Analytical & Bioanalytical Techniques*, *06*(03). https://doi.org/10.4172/2155-9872.1000249

Adcock, A. F., Trivedi, G., Edmondson, R., Spearman, C., & Yang, L. (2015). Three-Dimensional (3D) Cell Cultures in Cell-based Assays for in-vitro Evaluation of Anticancer Drugs. *Journal of Analytical & Bioanalytical Techniques 2015 6:3*, *6*(3), 1–12. https://doi.org/10.4172/2155-9872.1000249

Aldridge, G. M., Podrebarac, D. M., Greenough, W. T., & Weiler, I. J. (2008). The use of total protein stains as loading controls: An alternative to high-abundance single-protein controls in semi-quantitative immunoblotting. *Journal of Neuroscience Methods*, *172*(2), 250–254. https://doi.org/10.1016/j.jneumeth.2008.05.003

Aninat, C., Piton, A., Glaise, D., Le Charpentier, T., Langouët, S., Morel, F., Guguen-Guillouzo, C., & Guillouzo, A. (2006). Expression of cytochromes P450, conjugating enzymes and nuclear receptors in human hepatoma HepaRG cells. *Drug Metabolism and Disposition: The Biological Fate of Chemicals*, *34*(1), 75–83. https://doi.org/10.1124/DMD.105.006759

Ash, C., Dubec, M., Donne, K., & Bashford, T. (2017). Effect of wavelength and beam width on penetration in light-tissue interaction using computational methods. *Lasers in Medical Science*, *32*(8), 1909–1918. https://doi.org/10.1007/s10103-017-2317-4

Asthana, A., & Kisaalita, W. S. (2012). Microtissue size and hypoxia in HTS with 3D cultures. *Drug Discovery Today*, *17*(15–16), 810–817. https://doi.org/10.1016/j.drudis.2012.03.004

Asthana, A., Mcrae White, C., Douglass, M., Kisaalita, W. S., & Library, W. O. (2018). Evaluation of Cellular Adhesion and Organization in Different Microporous Polymeric Scaffolds. *Ameri-Can Institute of Chemical Engineers Biotechnol. Prog*, *34*, 505–514. https://doi.org/10.1002/btpr.2627

Bacon, B. R., O'Grady, J. G., Di Bisceglie, A. M., & Lake, J. R. (2006). Comprehensive Clinical Hepatology. *Comprehensive Clinical Hepatology*. https://doi.org/10.1016/B978-0-323-03675-7.X5001-X

Bassim, N. D., De Gregorio, B. T., Kilcoyne, A. L. D., Scott, K., Chou, T., Wirick, S., Cody, G., & Stroud, R. M. (2012). Minimizing damage during FIB sample preparation of soft materials. *Journal of Microscopy*, *245*(3), 288–301. https://doi.org/10.1111/j.1365-2818.2011.03570.x

Basu, A., Dydowiczová, A., Čtveráčková, L., Jaša, L., Trosko, J. E., Bláha, L., & Babica, P. (2018). Assessment of Hepatotoxic Potential of Cyanobacterial Toxins Using 3D In Vitro Model of Adult Human Liver Stem Cells. *Environmental Science & Technology*, *52*(17), 10078–10088. https://doi.org/10.1021/acs.est.8b02291

Bate, T. S. R., Gadd, V. L., Forbes, S. J., & Callanan, A. (2021). Response differences of HepG2 and Primary Mouse Hepatocytes to morphological changes in electrospun PCL scaffolds. *Scientific Reports 2021 11:1*, *11*(1), 1–13. https://doi.org/10.1038/s41598-021-81761-z

Baze, A., Parmentier, C., Hendriks, D. F. G., Hurrell, T., Heyd, B., Bachellier, P., Schuster, C., Ingelman-Sundberg, M., & Richert, L. (2018). Three-Dimensional Spheroid Primary Human Hepatocytes in Monoculture and Coculture with Nonparenchymal Cells. *Tissue Engineering - Part C: Methods*, *24*(9), 534–545. https://doi.org/10.1089/ten.tec.2018.0134

Bell, C. C., Dankers, A. C. A., Lauschke, V. M., Sison-Young, R., Jenkins, R., Rowe, C., Goldring, C. E., Park, K., Regan, S. L., Walker, T., Schofield, C., Baze, A., Foster, A. J., Williams, D. P., van de Ven, A. W. M., Jacobs, F., van Houdt, J., Lahteenmaki, T., Snoeys, J., … Ingelman-Sundberg, M. (2018). Comparison of Hepatic 2D Sandwich Cultures and 3D Spheroids for Long-term Toxicity Applications: A Multicenter Study. *TOXICOLOGICAL SCIENCES*, *162*(2), 655–666. https://doi.org/10.1093/toxsci/kfx289

Bell, C. C., Dankers, A. C. A., Lauschke, V. M., Sison-Young, R., Jenkins, R., Rowe, C., Goldring, C. E., Park, K., Regan, S. L., Walker, T., Schofield, C., Baze, A., Foster, A. J., Williams, D. P., van de Ven, A. W. M., Jacobs, F., van Houdt, J., Lähteenmäki, T., Snoeys, J., … Ingelman-Sundberg, M. (2018). Comparison of Hepatic 2D Sandwich Cultures and 3D Spheroids for Long-term Toxicity Applications: A Multicenter Study. *Toxicological Sciences*, *162*(2), 655–666. https://doi.org/10.1093/TOXSCI/KFX289

Bell, C. C., Hendriks, D. F. G., Moro, S. M. L., Ellis, E., Walsh, J., Renblom, A., Fredriksson Puigvert, L., Dankers, A. C. A., Jacobs, F., Snoeys, J., Sison-Young, R. L., Jenkins, R. E., Nordling, Å., Mkrtchian, S., Park, B. K., Kitteringham, N. R., Goldring, C. E. P., Lauschke, V. M., & Ingelman-Sundberg, M. (2016). Characterization of primary human hepatocyte spheroids as a model system for drug-induced liver injury, liver function and disease. *Scientific Reports 2016 6:1*, *6*(1), 1–13. https://doi.org/10.1038/srep25187

Bell, C. C., Hendriks, D. F. G., Moro, S. M. L., Ellis, E., Walsh, J., Renblom, A., Puigvert, L. F., Dankers, A. C. A., Jacobs, F., Snoeys, J., Sison-Young, R. L., Jenkins, R. E., Nordling, A., Mkrtchian, S., Park, B. K., Kitteringham, N. R., Goldring, C. E. P., Lauschke, V. M., & Ingelman-Sundberg, M. (2016). Characterization of primary human hepatocyte spheroids as a model system for drug-induced liver injury, liver function and disease. *SCIENTIFIC REPORTS*, *6*. https://doi.org/10.1038/srep25187

Bellani, C. F., Yue, K., Flaig, F., Hébraud, A., Ray, P., Annabi, N., Selistre De Araújo, H. S., Branciforti, M. C., Minarelli Gaspar, A. M., Shin, S. R., Khademhosseini, A., & Schlatter, G. (2021). Suturable elastomeric tubular grafts with patterned porosity for rapid vascularization of 3D constructs. *Biofabrication*, *13*(3), 035020. https://doi.org/10.1088/1758-5090/ABDF1D

Berger, B., Donzelli, M., Maseneni, S., Boess, F., Roth, A., Krähenbühl, S., & Haschke, M. (2016). Comparison of Liver Cell Models Using the Basel Phenotyping Cocktail. *Frontiers in Pharmacology*, *7*(NOV), 443. https://doi.org/10.3389/FPHAR.2016.00443/BIBTEX

Bernardello, M., Gualda, E. J., & Loza-Alvarez, P. (2022). Modular multimodal platform for classical and high throughput light sheet microscopy. *Scientific Reports 2022 12:1*, *12*(1), 1–14. https://doi.org/10.1038/s41598-022-05940-2

Bircsak, K. M., DeBiasio, R., Miedel, M., Alsebahi, A., Reddinger, R., Saleh, A., Shun, T., Vernetti, L. A., & Gough, A. (2021). A 3D microfluidic liver model for high throughput compound toxicity screening in the OrganoPlate®. *Toxicology*, *450*, 152667. https://doi.org/10.1016/J.TOX.2020.152667

Bissell, M. J., Hall, H. G., & Parry, G. (1982). How does the extracellular matrix direct gene expression? *Journal of Theoretical Biology*, *99*(1), 31–68. https://doi.org/10.1016/0022-5193(82)90388-5

Bissell, M. J., Radisky, D. C., Rizki, A., Weaver, V. M., & Petersen, O. W. (2002). The organizing principle: microenvironmental influences in the normal and malignant breast. *Differentiation; Research in Biological Diversity*, *70*(9–10), 537. https://doi.org/10.1046/J.1432-0436.2002.700907.X

Bokhari, M., Carnachan, R. J., Cameron, N. R., & Przyborski, S. A. (2007a). *Novel cell culture device*

enabling three-dimensional cell growth and improved cell function. https://doi.org/10.1016/j.bbrc.2007.01.105

Bokhari, M., Carnachan, R. J., Cameron, N. R., & Przyborski, S. A. (2007b). Culture of HepG2 liver cells on three dimensional polystyrene scaffolds enhances cell structure and function during toxicological challenge. *Journal of Anatomy*, *0*(0), 070816212604002-??? https://doi.org/10.1111/j.1469-7580.2007.00778.x

Böttcher, B., Pflieger, A., Schumacher, J., Jungnickel, B., & Feller, K. H. (2022). 3D Bioprinting of Prevascularized Full-Thickness Gelatin-Alginate Structures with Embedded Co-Cultures. *Bioengineering*, *9*(6), 242. https://doi.org/10.3390/BIOENGINEERING9060242/S1

Brown, J. H., Das, P., DiVito, M. D., Ivancic, D., Tan, L. P., & Wertheim, J. A. (2018a). Nanofibrous PLGA electrospun scaffolds modified with type I collagen influence hepatocyte function and support viability in vitro. *Acta Biomaterialia*, *73*, 217–227. https://doi.org/10.1016/j.actbio.2018.02.009

Brown, J. H., Das, P., DiVito, M. D., Ivancic, D., Tan, L. P., & Wertheim, J. A. (2018b). Nanofibrous PLGA electrospun scaffolds modified with type I collagen influence hepatocyte function and support viability in vitro. *Acta Biomaterialia*, *73*, 217–227. https://doi.org/10.1016/J.ACTBIO.2018.02.009

Burdick, J. A., & Vunjak-Novakovic, G. (2009). Engineered microenvironments for controlled stem cell differentiation. *Tissue Engineering. Part A*, *15*(2), 205–219. https://doi.org/10.1089/ten.tea.2008.0131

Bustin, S. A. (2000). Absolute quantification of mRNA using real-time reverse transcription polymerase chain reaction assays. *Journal of Molecular Endocrinology*, *25*(2), 169–193. http://www.ncbi.nlm.nih.gov/pubmed/11013345

Carletti, E., Motta, A., & Migliaresi, C. (2011). Scaffolds for tissue engineering and 3D cell culture. *Methods in Molecular Biology (Clifton, N.J.)*, *695*, 17–39. https://doi.org/10.1007/978-1-60761-984-0_2/COVER

Carragher, N., Piccinini, F., Tesei, A., Trask, O. J., Bickle, M., & Horvath, P. (2018). Concerns, challenges and promises of high-content analysis of 3D cellular models. *Nature Reviews Drug Discovery 2018 17:8*, *17*(8), 606–606. https://doi.org/10.1038/nrd.2018.99

Chao, P., Maguire, T., Novik, E., Cheng, K. C., & Yarmush, M. L. (2009). Evaluation of a microfluidic based cell culture platform with primary human hepatocytes for the prediction of hepatic clearance in human. *Biochemical Pharmacology*, *78*(6), 625–632. https://doi.org/10.1016/j.bcp.2009.05.013

Chatterjee, S., Richert, L., Augustijns, P., & Annaert, P. (2014). Hepatocyte-based in vitro model for assessment of drug-induced cholestasis. *Toxicology and Applied Pharmacology*, *274*(1), 124–136. https://doi.org/10.1016/J.TAAP.2013.10.032

Chim, L. K., & Mikos, A. G. (2018). Biomechanical forces in tissue engineered tumor models. In *Current Opinion in Biomedical Engineering* (Vol. 6, pp. 42–50). Elsevier B.V. https://doi.org/10.1016/j.cobme.2018.03.004

Chitrangi, S., Nair, P., & Khanna, A. (2017). 3D engineered In vitro hepatospheroids for studying drug toxicity and metabolism. *Toxicology in Vitro*, *38*, 8–18. https://doi.org/10.1016/J.TIV.2016.10.009

Cho, C. H., Berthiaume, F., Tilles, A. W., & Yarmush, M. L. (2008). A new technique for primary hepatocyte expansion in vitro. *Biotechnology and Bioengineering*, *101*(2), 345–356.

https://doi.org/10.1002/BIT.21911

Choi, S.-W., Yeh, Y.-C., Zhang, Y., Sung, H.-W., & Xia, Y. (2010). Uniform beads with controllable pore sizes for biomedical applications. *Small (Weinheim an Der Bergstrasse, Germany)*, *6*(14), 1492–1498. https://doi.org/10.1002/smll.201000544

Christoffersson, J., Bergström, G., Schwanke, K., Kempf, H., Zweigerdt, R., & Mandenius, C.-F. (2016). A Microfluidic Bioreactor for Toxicity Testing of Stem Cell Derived 3D Cardiac Bodies. In *Methods in Molecular Biology* (Vol. 1502, pp. 159–168). Humana Press Inc. https://doi.org/10.1007/7651_2016_340

Chumduri, C., Gurumurthy, R. K., Berger, H., Dietrich, O., Kumar, N., Koster, S., Brinkmann, V., Hoffmann, K., Drabkina, M., Arampatzi, P., Son, D., Klemm, U., Mollenkopf, H. J., Herbst, H., Mangler, M., Vogel, J., Saliba, A. E., & Meyer, T. F. (2021). Opposing Wnt signals regulate cervical squamocolumnar homeostasis and emergence of metaplasia. *Nature Cell Biology 2021 23:2*, *23*(2), 184–197. https://doi.org/10.1038/s41556-020-00619-0

Chung, C. A., Yang, C. W., & Chen, C. W. (2006). Analysis of cell growth and diffusion in a scaffold for cartilage tissue engineering. *Biotechnology and Bioengineering*, *94*(6), 1138–1146. https://doi.org/10.1002/bit.20944

Cimetta, E., Figallo, E., Cannizzaro, C., Elvassore, N., & Vunjak-Novakovic, G. (2009). Micro-bioreactor arrays for controlling cellular environments: design principles for human embryonic stem cell applications. *Methods (San Diego, Calif.)*, *47*(2), 81–89. https://doi.org/10.1016/j.ymeth.2008.10.015

Clevers, H. (2016). Modeling Development and Disease with Organoids. In *Cell* (Vol. 165, Issue 7, pp. 1586–1597). Cell. https://doi.org/10.1016/j.cell.2016.05.082

Costa, E. C., Silva, D. N., Moreira, A. F., & Correia, I. J. (2019). Optical clearing methods: An overview of the techniques used for the imaging of 3D spheroids. *Biotechnology and Bioengineering*, *116*(10), 2742–2763. https://doi.org/10.1002/BIT.27105

Cox, C. R., Lynch, S., Goldring, C., & Sharma, P. (2020). Current Perspective: 3D Spheroid Models Utilizing Human-Based Cells for Investigating Metabolism-Dependent Drug-Induced Liver Injury. *Frontiers in Medical Technology*, *0*, 14. https://doi.org/10.3389/FMEDT.2020.611913

Cox, M. C., Mendes, R., Silva, F., Mendes, T. F., Zelaya-Lazo, A., Halwachs, K., Purkal, J. J., Isidro, I. A., Félix, A., Boghaert, E. R., & Brito, C. (2021). Application of LDH assay for therapeutic efficacy evaluation of ex vivo tumor models. *Scientific Reports 2021 11:1*, *11*(1), 1–14. https://doi.org/10.1038/s41598-021-97894-0

Cox, M. E., & Dunn, B. (1986). Oxygen diffusion in poly(dimethyl siloxane) using fluorescence quenching. I. Measurement technique and analysis. *Journal of Polymer Science Part A: Polymer Chemistry*, *24*(4), 621–636. https://doi.org/10.1002/POLA.1986.080240405

Cussler, E. (2009). *Diffusion: Mass Transfer in Fluid Systems* (Issue 3). Cambridge University Press.

Danti, S., Serino, L. P., D'Alessandro, D., Moscato, S., Danti, S., Trombi, L., Dinucci, D., Chiellini, F., Pietrabissa, A., Lisanti, M., Berrettini, S., & Petrini, M. (2013). Growing Bone Tissue-Engineered Niches with Graded Osteogenicity: An *In Vitro* Method for Biomimetic Construct Assembly. *Tissue Engineering Part C: Methods*, *19*(12), 911–924. https://doi.org/10.1089/ten.tec.2012.0445

Das, P., DiVito, M. D., Wertheim, J. A., & Tan, L. P. (2020). Collagen-I and fibronectin modified three-dimensional electrospun PLGA scaffolds for long-term in vitro maintenance of functional hepatocytes. *Materials Science and Engineering: C*, *111*, 110723.

https://doi.org/10.1016/J.MSEC.2020.110723

Das, V., Fürst, T., Gurská, S., Džubák, P., & Hajdúch, M. (2016). Reproducibility of Uniform Spheroid Formation in 384-Well Plates. *Journal of Biomolecular Screening*, *21*(9), 923–930. https://doi.org/10.1177/1087057116651867

Dehili, C., Lee, P., Shakesheff, K. M., & Alexander, M. R. (2006). Comparison of Primary Rat Hepatocyte Attachment to Collagen and Plasma-Polymerised Allylamine on Glass. *Plasma Processes and Polymers*, *3*(6–7), 474–484. https://doi.org/10.1002/PPAP.200500169

Del Duca, D., Werbowetski, T., & Del Maestro, R. F. (2004). Spheroid Preparation from Hanging Drops: Characterization of a Model of Brain Tumor Invasion. *Journal of Neuro-Oncology*, *67*(3), 295–303. https://doi.org/10.1023/B:NEON.0000024220.07063.70

Doi, A., Oketani, R., Nawa, Y., & Fujita, K. (2018). High-resolution imaging in two-photon excitation microscopy using in situ estimations of the point spread function. *Biomedical Optics Express*, *9*(1), 202. https://doi.org/10.1364/BOE.9.000202

Dubiak-Szepietowska, M., Karczmarczyk, A., Joensson-Niedziolka, M., Winckler, T., & Feller, K.-H. (2016). Development of complex-shaped liver multicellular spheroids as a human-based model for nanoparticle toxicity assessment in vitro. *TOXICOLOGY AND APPLIED PHARMACOLOGY*, *294*, 78–85. https://doi.org/10.1016/j.taap.2016.01.016

Dunn, J. C., Tompkins, R. G., & Yarmush, M. L. (1992). Hepatocytes in collagen sandwich: evidence for transcriptional and translational regulation. *The Journal of Cell Biology*, *116*(4), 1043–1053. https://doi.org/10.1083/jcb.116.4.1043

Dunn, J. C. Y., Yarmush, M. L., Koebe, H. G., & Tompkins, R. G. (1989). Hepatocyte function and extracellular matrix geometry: Long-term culture in a sandwich configuration. *FASEB Journal*, *3*(2), 174–177. https://pdfs.semanticscholar.org/11fd/0f4f2e7fabbb7e65cb9cc6138030fb0d8564.pdf

Eaton, S. L., Roche, S. L., Llavero Hurtado, M., Oldknow, K. J., Farquharson, C., Gillingwater, T. H., & Wishart, T. M. (2013). Total Protein Analysis as a Reliable Loading Control for Quantitative Fluorescent Western Blotting. *PLoS ONE*, *8*(8), e72457. https://doi.org/10.1371/journal.pone.0072457

Edmondson, R., Broglie, J. J., Adcock, A. F., & Yang, L. (2014). Three-Dimensional Cell Culture Systems and Their Applications in Drug Discovery and Cell-Based Biosensors. *Assay and Drug Development Technologies*, *12*(4), 207. https://doi.org/10.1089/ADT.2014.573

Edwards, I. R., & Aronson, J. K. (2000). Adverse drug reactions: definitions, diagnosis, and management. *Lancet (London, England)*, *356*(9237), 1255–1259. https://doi.org/10.1016/S0140-6736(00)02799-9

Engel, R. M., Chan, W. H., Nickless, D., Hlavca, S., Richards, E., Kerr, G., Oliva, K., McMurrick, P. J., Jardé, T., & Abud, H. E. (2020). Patient-derived colorectal cancer organoids upregulate revival stem cell marker genes following chemotherapeutic treatment. *Journal of Clinical Medicine*, *9*(1). https://doi.org/10.3390/jcm9010128

Fang, Y., & Eglen, R. M. (2017). Three-Dimensional Cell Cultures in Drug Discovery and Development. *SLAS Discovery : Advancing Life Sciences R & D*, *22*(5), 456–472. https://doi.org/10.1177/1087057117696795

Feng, J., Lu, P. zhi, Zhu, G. zhi, Hooi, S. C., Wu, Y., Huang, X. wei, Dai, H. qi, Chen, P. hong, Li, Z. jie, Su, W. jing, Han, C. ye, Ye, X. ping, Peng, T., Zhou, J., & Lu, G. dong. (2021). ACSL4 is a predictive biomarker of sorafenib sensitivity in hepatocellular carcinoma. *Acta Pharmacologica Sinica*,

42(1), 160–170. https://doi.org/10.1038/S41401-020-0439-X

Feng, Z.-Q., Chu, X.-H., Huang, N.-P., Leach, M. K., Wang, G., Wang, Y.-C., Ding, Y.-T., & Gu, Z.-Z. (2010). Rat hepatocyte aggregate formation on discrete aligned nanofibers of type-I collagen-coated poly(l-lactic acid). *Biomaterials*, *31*(13), 3604–3612. https://doi.org/10.1016/j.biomaterials.2010.01.080

Fernando, J., Sancho, P., Fernández-Rodriguez, C. M., Lledó, J. L., Caja, L., Campbell, J. S., Fausto, N., & Fabregat, I. (2012). SORAFENIB SENSITIZES HEPATOCELLULAR CARCINOMA CELLS TO PHYSIOLOGICAL APOPTOTIC STIMULI. *Journal of Cellular Physiology*, *227*(4), 1319. https://doi.org/10.1002/JCP.22843

Fierz, F. C., Beckmann, F., Huser, M., Irsen, S. H., Leukers, B., Witte, F., Degistirici, Ö., Andronache, A., Thie, M., & Müller, B. (2008). The morphology of anisotropic 3D-printed hydroxyapatite scaffolds. *Biomaterials*, *29*(28), 3799–3806. https://doi.org/10.1016/j.biomaterials.2008.06.012

Figallo, E., Cannizzaro, C., Gerecht, S., Burdick, J. A., Langer, R., Elvassore, N., & Vunjak-Novakovic, G. (2007). Micro-bioreactor array for controlling cellular microenvironments. *Lab on a Chip*, *7*(6), 710–719. https://doi.org/10.1039/b700063d

Fink, S. L., & Cookson, B. T. (2005). Apoptosis, Pyroptosis, and Necrosis: Mechanistic Description of Dead and Dying Eukaryotic Cells. *Infection and Immunity*, *73*(4), 1907. https://doi.org/10.1128/IAI.73.4.1907-1916.2005

Flanagan, D. J., Pentinmikko, N., Luopajärvi, K., Willis, N. J., Gilroy, K., Raven, A. P., Mcgarry, L., Englund, J. I., Webb, A. T., Scharaw, S., Nasreddin, N., Hodder, M. C., Ridgway, R. A., Minnee, E., Sphyris, N., Gilchrist, E., Najumudeen, A. K., Romagnolo, B., Perret, C., … Sansom, O. J. (2021). NOTUM from Apc-mutant cells biases clonal competition to initiate cancer. *Nature 2021 594:7863*, *594*(7863), 430–435. https://doi.org/10.1038/s41586-021-03525-z

Foster, A. J., Chouhan, B., Regan, S. L., Rollison, H., Amberntsson, S., Andersson, L. C., Srivastava, A., Darnell, M., Cairns, J., Lazic, S. E., Jang, K.-J., Petropolis, D. B., Kodella, K., Rubins, J. E., Williams, D., Hamilton, G. A., Ewart, L., & Morgan, P. (2019). Integrated in vitro models for hepatic safety and metabolism: evaluation of a human Liver-Chip and liver spheroid. *Archives of Toxicology*, *93*(4), 1021–1037. https://doi.org/10.1007/s00204-019-02427-4

Freyer, N., Greuel, S., Knöspel, F., Gerstmann, F., Storch, L., Damm, G., Seehofer, D., Harris, J. F., Iyer, R., Schubert, F., & Zeilinger, K. (2018). Microscale 3D liver bioreactor for in vitro hepatotoxicity testing under perfusion conditions. *Bioengineering*, *5*(1). https://doi.org/10.3390/bioengineering5010024

Fusco, P., Parisatto, B., Rampazzo, E., Persano, L., Frasson, C., Di Meglio, A., Leslz, A., Santoro, L., Cafferata, B., Zin, A., Cimetta, E., Basso, G., Esposito, M. R., & Tonini, G. P. (2019). Patient-derived organoids (PDOs) as a novel in vitro model for neuroblastoma tumours. *BMC Cancer*, *19*(1), 1–11. https://doi.org/10.1186/s12885-019-6149-4

Gao, X., & Liu, Y. (2017). A transcriptomic study suggesting human iPSC-derived hepatocytes potentially offer a better in vitro model of hepatotoxicity than most hepatoma cell lines. *Cell Biology and Toxicology*, *33*(4), 407–421. https://doi.org/10.1007/S10565-017-9383-Z

Gaskell, H., Sharma, P., Colley, H. E., Murdoch, C., Williams, D. P., & Webb, S. D. (2016). Characterization of a functional C3A liver spheroid model. *Toxicology Research*, *5*(4), 1053. https://doi.org/10.1039/C6TX00101G

Gerets, H. H. J., Tilmant, K., Gerin, B., Chanteux, H., Depelchin, B. O., Dhalluin, S., & Atienzar, F. A. (2012a). Characterization of primary human hepatocytes, HepG2 cells, and HepaRG cells at the

mRNA level and CYP activity in response to inducers and their predictivity for the detection of human hepatotoxins. *Cell Biology and Toxicology*, *28*(2), 69–87. https://doi.org/10.1007/S10565-011-9208-4

Gerets, H. H. J., Tilmant, K., Gerin, B., Chanteux, H., Depelchin, B. O., Dhalluin, S., & Atienzar, F. A. (2012b). Characterization of primary human hepatocytes, HepG2 cells, and HepaRG cells at the mRNA level and CYP activity in response to inducers and their predictivity for the detection of human hepatotoxins. *Cell Biology and Toxicology*, *28*(2), 69–87. https://doi.org/10.1007/S10565-011-9208-4/FIGURES/2

German, C. L., & Madihally, S. V. (2019a). Type of endothelial cells affects HepaRG cell acetaminophen metabolism in both 2D and 3D porous scaffold cultures. *Journal of Applied Toxicology*, *39*(3), 461–472. https://doi.org/10.1002/JAT.3737

German, C. L., & Madihally, S. V. (2019b). Type of endothelial cells affects HepaRG cell acetaminophen metabolism in both 2D and 3D porous scaffold cultures. *Journal of Applied Toxicology*, *39*(3), 461–472. https://doi.org/10.1002/jat.3737

Gissen, P., & Arias, I. M. (2015). Structural and functional hepatocyte polarity and liver disease. *Journal of Hepatology*, *63*(4), 1023–1037. https://doi.org/10.1016/J.JHEP.2015.06.015

Godoy, P., Hewitt, N. J., Albrecht, U., Andersen, M. E., Ansari, N., Bhattacharya, S., Bode, J. G., Bolleyn, J., Borner, C., Böttger, J., Braeuning, A., Budinsky, R. A., Burkhardt, B., Cameron, N. R., Camussi, G., Cho, C. S., Choi, Y. J., Craig Rowlands, J., Dahmen, U., … Hengstler, J. G. (2013). Recent advances in 2D and 3D in vitro systems using primary hepatocytes, alternative hepatocyte sources and non-parenchymal liver cells and their use in investigating mechanisms of hepatotoxicity, cell signaling and ADME. *Archives of Toxicology*, *87*(8), 1315–1530. https://doi.org/10.1007/S00204-013-1078-5

Gomez-Lechon, M., Donato, M., Lahoz, A., & Castell, J. (2008). Cell Lines: A Tool for In Vitro Drug Metabolism Studies. *Current Drug Metabolism*, *9*(1), 1–11. https://doi.org/10.2174/138920008783331086

Gong, L., Petchakup, C., Shi, P., Tan, P. L., Tan, L. P., Tay, C. Y., & Hou, H. W. (2021). Direct and Label-Free Cell Status Monitoring of Spheroids and Microcarriers Using Microfluidic Impedance Cytometry. *Small*, *17*(21), 2007500. https://doi.org/10.1002/SMLL.202007500

Graf, B. W., & Boppart, S. A. (2010). Imaging and Analysis of Three-Dimensional Cell Culture Models. *Methods in Molecular Biology (Clifton, N.J.)*, *591*, 211. https://doi.org/10.1007/978-1-60761-404-3_13

Griffith, L. G., & Swartz, M. A. (2006). Capturing complex 3D tissue physiology in vitro. *Nature Reviews Molecular Cell Biology*, *7*(3), 211–224. https://doi.org/10.1038/nrm1858

Gu, X., Albrecht, W., Edlund, K., Kappenberg, F., Rahnenfuehrer, J., Leist, M., Moritz, W., Godoy, P., Cadenas, C., Marchan, R., Brecklinghaus, T., Tolosa Pardo, L., Castell, J. V, Gardner, I., Han, B., Hengstler, J. G., & Stoeber, R. (2018). Relevance of the incubation period in cytotoxicity testing with primary human hepatocytes. *ARCHIVES OF TOXICOLOGY*, *92*(12), 3505–3515. https://doi.org/10.1007/s00204-018-2302-0

Guguen-Guillouzo, C., Corlu, A., & Guillouzo, A. (2010). Stem cell-derived hepatocytes and their use in toxicology. *Toxicology*, *270*(1), 3–9. https://doi.org/10.1016/J.TOX.2009.09.019

Guo, L., Dial, S., Shi, L., Branham, W., Liu, J., Fang, J. L., Green, B., Deng, H., Kaput, J., & Ning, B. (2011). Similarities and differences in the expression of drug-metabolizing enzymes between human hepatic cell lines and primary human hepatocytes. *Drug Metabolism and Disposition:*

The Biological Fate of Chemicals, *39*(3), 528–538. https://doi.org/10.1124/DMD.110.035873

Gupta, P., Totti, S., Pérez-Mancera, P. A., Dyke, E., Nisbet, A., Schettino, G., Webb, R., & Velliou, E. G. (2019). Chemoradiotherapy screening in a novel biomimetic polymer based pancreatic cancer model. *RSC Advances*, *9*(71), 41649–41663. https://doi.org/10.1039/c9ra09123h

Gutierrez, R. A., & Crumpler, E. T. (2008). Potential Effect of Geometry on Wall Shear Stress Distribution Across Scaffold Surfaces. *Annals of Biomedical Engineering*, *36*(1), 77–85. https://doi.org/10.1007/s10439-007-9396-5

Hama, H., Kurokawa, H., Kawano, H., Ando, R., Shimogori, T., Noda, H., Fukami, K., Sakaue-Sawano, A., & Miyawaki, A. (2011). Scale: a chemical approach for fluorescence imaging and reconstruction of transparent mouse brain. *Nature Neuroscience*, *14*(11), 1481–1488. https://doi.org/10.1038/nn.2928

Hamdi, D. H., Barbieri, S., Chevalier, F., Groetz, J.-E., Legendre, F., Demoor, M., Galera, P., Lefaix, J.-L., & Saintigny, Y. (2015). In vitro engineering of human 3D chondrosarcoma: a preclinical model relevant for investigations of radiation quality impact. *BMC Cancer*, *15*(1), 579. https://doi.org/10.1186/s12885-015-1590-5

Hay, D. C., Zhao, D., Fletcher, J., Hewitt, Z. A., McLean, D., Urruticoechea-Uriguen, A., Black, J. R., Elcombe, C., Ross, J. A., Wolf, R., & Cui, W. (2008). Efficient differentiation of hepatocytes from human embryonic stem cells exhibiting markers recapitulating liver development in vivo. *Stem Cells (Dayton, Ohio)*, *26*(4), 894–902. https://doi.org/10.1634/STEMCELLS.2007-0718

Haycock, J. W. (2011). 3D cell culture: a review of current approaches and techniques. In *Methods in molecular biology (Clifton, N.J.)* (Vol. 695, pp. 1–15). https://doi.org/10.1007/978-1-60761-984-0_1

Huang, Q., Garrett, A., Bose, S., Blocker, S., Rios, A. C., Clevers, H., & Shen, X. (2021). The frontier of live tissue imaging across space and time. *Cell Stem Cell*, *28*(4), 603–622. https://doi.org/10.1016/J.STEM.2021.02.010

Huch, M., & Koo, B. K. (2015). Modeling mouse and human development using organoid cultures. In *Development (Cambridge)* (Vol. 142, Issue 18, pp. 3113–3125). Development. https://doi.org/10.1242/dev.118570

Hughes, C. S., Postovit, L. M., & Lajoie, G. A. (2010). Matrigel: a complex protein mixture required for optimal growth of cell culture. *Proteomics*, *10*(9), 1886–1890. https://doi.org/10.1002/pmic.200900758

InSphero. (2015). *GravityPLUS™ Hanging Drop System Gravity Manual*. www.insphero.com.

Jensen, C., & Teng, Y. (2020). Is It Time to Start Transitioning From 2D to 3D Cell Culture? *Frontiers in Molecular Biosciences*, *7*, 33. https://doi.org/10.3389/FMOLB.2020.00033/XML/NLM

Jones, H. M., Barton, H. A., Lai, Y., Bi, Y. -a., Kimoto, E., Kempshall, S., Tate, S. C., El-Kattan, A., Houston, J. B., Galetin, A., & Fenner, K. S. (2012). Mechanistic Pharmacokinetic Modeling for the Prediction of Transporter-Mediated Disposition in Humans from Sandwich Culture Human Hepatocyte Data. *Drug Metabolism and Disposition*, *40*(5), 1007–1017. https://doi.org/10.1124/dmd.111.042994

Jorand, R., Le Corre, G., Andilla, J., Maandhui, A., Frongia, C., Lobjois, V., Ducommun, B., & Lorenzo, C. (2012). Deep and Clear Optical Imaging of Thick Inhomogeneous Samples. *PLOS ONE*, *7*(4), e35795. https://doi.org/10.1371/JOURNAL.PONE.0035795

Kaja, S., Payne, A. J., Naumchuk, Y., & Koulen, P. (2017). Quantification of lactate dehydrogenase for

cell viability testing using cell lines and primary cultured astrocytes. *Current Protocols in Toxicology*, *72*, 2.26.1. https://doi.org/10.1002/CPTX.21

Kallepitis, C., Bergholt, M. S., Mazo, M. M., Leonardo, V., Skaalure, S. C., Maynard, S. A., & Stevens, M. M. (2017). Quantitative volumetric Raman imaging of three dimensional cell cultures. *Nature Communications 2017 8:1*, *8*(1), 1–9. https://doi.org/10.1038/ncomms14843

Kammerer, S. (2021). Three-Dimensional Liver Culture Systems to Maintain Primary Hepatic Properties for Toxicological Analysis In Vitro. *International Journal of Molecular Sciences*, *22*(19). https://doi.org/10.3390/IJMS221910214

Kanebratt, K. P., & Andersson, T. B. (2008). Evaluation of HepaRG cells as an in vitro model for human drug metabolism studies. *Drug Metabolism and Disposition: The Biological Fate of Chemicals*, *36*(7), 1444–1452. https://doi.org/10.1124/DMD.107.020016

Khodabakhshaghdam, S., Khoshfetrat, A. B., & Rahbarghazi, R. (2021). Alginate-chitosan core-shell microcapsule cultures of hepatic cells in a small scale stirred bioreactor: impact of shear forces and microcapsule core composition. *Journal of Biological Engineering*, *15*(1), 1–12. https://doi.org/10.1186/S13036-021-00265-6/TABLES/2

Kim, Y. E., Jeon, H. J., Kim, D., Lee, S. Y., Kim, K. Y., Hong, J., Maeng, P. J., Kim, K. R., & Kang, D. (2018). Quantitative Proteomic Analysis of 2D and 3D Cultured Colorectal Cancer Cells: Profiling of Tankyrase Inhibitor XAV939-Induced Proteome. *Scientific Reports*, *8*(1). https://doi.org/10.1038/s41598-018-31564-6

Klein, S., Mueller, D., Schevchenko, V., & Noor, F. (2014). Long-term maintenance of HepaRG cells in serum-free conditions and application in a repeated dose study. *Journal of Applied Toxicology : JAT*, *34*(10), 1078–1086. https://doi.org/10.1002/JAT.2929

Kleinman, H. K., & Martin, G. R. (2005). Matrigel: Basement membrane matrix with biological activity. *Seminars in Cancer Biology*, *15*(5), 378–386. https://doi.org/10.1016/j.semcancer.2005.05.004

Kleinman, H. K., Philp, D., & Hoffman, M. P. (2003). Role of the extracellular matrix in morphogenesis. *Current Opinion in Biotechnology*, *14*(5), 526–532. https://doi.org/10.1016/J.COPBIO.2003.08.002

Kloxin, A. M., Kasko, A. M., Salinas, C. N., & Anseth, K. S. (2009). Photodegradable Hydrogels for Dynamic Tuning of Physical and Chemical Properties. *Science*, *324*(5923), 59–63. https://doi.org/10.1126/science.1169494

Kmieć, Z. (2001). Cooperation of liver cells in health and disease. *Advances in Anatomy, Embryology, and Cell Biology*, *161*. https://doi.org/10.1007/978-3-642-56553-3

Knight, E., & Przyborski, S. (2015). Advances in 3D cell culture technologies enabling tissue-like structures to be created *in vitro*. *Journal of Anatomy*, *227*(6), 746–756. https://doi.org/10.1111/joa.12257

Kordes, C., Sawitza, I., & Häussinger, D. (2009). Hepatic and pancreatic stellate cells in focus. *Biological Chemistry*, *390*(10), 1003–1012. https://doi.org/10.1515/BC.2009.121

Kostadinova, R., Boess, F., Applegate, D., Suter, L., Weiser, T., Singer, T., Naughton, B., & Roth, A. (2013). A long-term three dimensional liver co-culture system for improved prediction of clinically relevant drug-induced hepatotoxicity. *Toxicology and Applied Pharmacology*, *268*(1), 1–16. https://doi.org/10.1016/J.TAAP.2013.01.012

Krishna, M. (2013). Microscopic anatomy of the liver. *Clinical Liver Disease*, *2*(S1), S4–S7.

https://doi.org/10.1002/CLD.147

Kuang, J., Yan, X., Genders, A. J., Granata, C., & Bishop, D. J. (2018). An overview of technical considerations when using quantitative real-time PCR analysis of gene expression in human exercise research. *PLOS ONE*, *13*(5), e0196438. https://doi.org/10.1371/journal.pone.0196438

Kumar, H. R., Zhong, X., Hoelz, D. J., Rescorla, F. J., Hickey, R. J., Malkas, L. H., & Sandoval, J. A. (2008). Three-dimensional neuroblastoma cell culture: proteomic analysis between monolayer and multicellular tumor spheroids. *Pediatric Surgery International*, *24*(11), 1229–1234. https://doi.org/10.1007/s00383-008-2245-2

Kumari, J., Karande, A. A., & Kumar, A. (2016). Combined Effect of Cryogel Matrix and Temperature-Reversible Soluble-Insoluble Polymer for the Development of in Vitro Human Liver Tissue. *ACS Applied Materials and Interfaces*, *8*(1), 264–277. https://doi.org/10.1021/acsami.5b08607

Kuntz, E., & Kuntz, H.-D. (2008). *Hepatology : textbook and atlas : history, morphology, biochemistry, diagnostics, clinic, therapy*. 937. https://books.google.com/books/about/Hepatology.html?id=oL6d9KuVqLQC

Kuss, M., Kim, J., Qi, D., Wu, S., Lei, Y., Chung, S., & Duan, B. (2018). Effects of tunable, 3D-bioprinted hydrogels on human brown adipocyte behavior and metabolic function. *Acta Biomaterialia*, *71*, 486–495. https://doi.org/10.1016/J.ACTBIO.2018.03.021

Kutner, R. H., Zhang, X. Y., & Reiser, J. (2009). Production, concentration and titration of pseudotyped HIV-1-based lentiviral vectors. *Nature Protocols*, *4*(4), 495–505. https://doi.org/10.1038/NPROT.2009.22

Kyffin, J. A., Sharma, P., Leedale, J., Colley, H. E., Murdoch, C., Harding, A. L., Mistry, P., & Webb, S. D. (2019). Characterisation of a functional rat hepatocyte spheroid model. *Toxicology in Vitro*, *55*, 160–172. https://doi.org/10.1016/j.tiv.2018.12.014

Lan, S. F., Safiejko-Mroczka, B., & Starly, B. (2010). Long-term cultivation of HepG2 liver cells encapsulated in alginate hydrogels: A study of cell viability, morphology and drug metabolism. *Toxicology in Vitro*, *24*(4), 1314–1323. https://doi.org/10.1016/j.tiv.2010.02.015

Lancaster, M. A., & Knoblich, J. A. (2014). Organogenesisin a dish: Modeling development and disease using organoid technologies. In *Science* (Vol. 345, Issue 6194). American Association for the Advancement of Science. https://doi.org/10.1126/science.1247125

Lauschke, V. M., Hendriks, D. F. G., Bell, C. C., Andersson, T. B., & Ingelman-Sundberg, M. (2016). Novel 3D Culture Systems for Studies of Human Liver Function and Assessments of the Hepatotoxicity of Drugs and Drug Candidates. *Chemical Research in Toxicology*, *29*(12), 1936–1955. https://doi.org/10.1021/ACS.CHEMRESTOX.6B00150/ASSET/IMAGES/LARGE/TX-2016-00150F_0006.JPEG

Lazar, A., Mann, H. J., Remmel, R. P., Shatford, R. A., Cerra, F. B., & Hu, W.-S. (1995). Extended Liver-Specific Functions of Porcine Hepatocyte Spheroids Entrapped in Collagen. In *Source: In Vitro Cellular & Developmental Biology. Animal* (Vol. 31, Issue 5). https://www.jstor.org/stable/pdf/4294423.pdf?refreqid=excelsior%3Ab39c73cca7953513171758b724a886c0

Lazzari, G., Nicolas, V., Matsusaki, M., Akashi, M., Couvreur, P., & Mura, S. (2018). Multicellular spheroid based on a triple co-culture: A novel 3D model to mimic pancreatic tumor complexity. *Acta Biomaterialia*, *78*, 296–307. https://doi.org/10.1016/j.actbio.2018.08.008

Le Vee, M., Noel, G., Jouan, E., Stieger, B., & Fardel, O. (2013). Polarized expression of drug transporters in differentiated human hepatoma HepaRG cells. *Toxicology in Vitro : An*

International Journal Published in Association with BIBRA, *27*(6), 1979–1986. https://doi.org/10.1016/J.TIV.2013.07.003

LeCluyse, E. L., Audus, K. L., & Hochman, J. H. (1994). Formation of extensive canalicular networks by rat hepatocytes cultured in collagen-sandwich configuration. *American Journal of Physiology-Cell Physiology*, *266*(6), C1764–C1774. https://doi.org/10.1152/ajpcell.1994.266.6.C1764

Lee, J., Cuddihy, M. J., & Kotov, N. A. (2008). Three-Dimensional Cell Culture Matrices: State of the Art. *Tissue Engineering Part B: Reviews*, *14*(1), 61–86. https://doi.org/10.1089/teb.2007.0150

Leise, M. D., Poterucha, J. J., & Talwalkar, J. A. (2014). Drug-Induced Liver Injury. *Mayo Clinic Proceedings*, *89*(1), 95–106. https://doi.org/10.1016/J.MAYOCP.2013.09.016

Leite, S. B., Roosens, T., El Taghdouini, A., Mannaerts, I., Smout, A. J., Najimi, M., Sokal, E., Noor, F., Chesne, C., & van Grunsven, L. A. (2016a). Novel human hepatic organoid model enables testing of drug-induced liver fibrosis in vitro. *Biomaterials*, *78*, 1–10. https://doi.org/10.1016/J.BIOMATERIALS.2015.11.026

Leite, S. B., Roosens, T., El Taghdouini, A., Mannaerts, I., Smout, A. J., Najimi, M., Sokal, E., Noor, F., Chesne, C., & van Grunsven, L. A. (2016b). Novel human hepatic organoid model enables testing of drug-induced liver fibrosis in vitro. *Biomaterials*, *78*, 1–10. https://doi.org/10.1016/J.BIOMATERIALS.2015.11.026

Lewis, P. L., Green, R. M., & Shah, R. N. (2018). 3D-Printed Gelatin Scaffolds of Differing Pore Geometry Modulate Hepatocyte Function and Gene Expression. *Acta Biomaterialia*, *69*, 63. https://doi.org/10.1016/J.ACTBIO.2017.12.042

Li, C.-L., Tian, T., Nan, K.-J., Zhao, N., Guo, Y.-H., Cui, J., Wang, J., & Zhang, W.-G. (2008). Survival advantages of multicellular spheroids vs. monolayers of HepG2 cells in vitro. *Oncology Reports*, *20*(6), 1465–1471. https://doi.org/10.3892/or_00000167

Limmer, A., & Knolle, P. A. (2001). Liver sinusoidal endothelial cells: a new type of organ-resident antigen-presenting cell. *Archivum Immunologiae et Therapiae Experimentalis*, *49 Suppl 1*(SUPPL. 1), S7-11. https://europepmc.org/article/med/11603871

Liu, H., Ye, Z., Kim, Y., Sharkis, S., & Jang, Y. Y. (2010). Generation of endoderm-derived human induced pluripotent stem cells from primary hepatocytes. *Hepatology (Baltimore, Md.)*, *51*(5), 1810–1819. https://doi.org/10.1002/HEP.23626

Liu, Y., Hu, K., & Wang, Y. (2017). Primary Hepatocytes Cultured on a Fiber-Embedded PDMS Chip to Study Drug Metabolism. *Polymers*, *9*(6), 215. https://doi.org/10.3390/polym9060215

Liu, Y., Wang, S., & Wang, Y. (2016). Patterned Fibers Embedded Microfluidic Chips Based on PLA and PDMS for Ag Nanoparticle Safety Testing. *Polymers*, *8*(11), 402. https://doi.org/10.3390/polym8110402

Liu, Y., Wei, J., Lu, J., Lei, D., Yan, S., & Li, X. (2016). Micropatterned coculture of hepatocytes on electrospun fibers as a potential in vitro model for predictive drug metabolism. *MATERIALS SCIENCE & ENGINEERING C-MATERIALS FOR BIOLOGICAL APPLICATIONS*, *63*, 475–484. https://doi.org/10.1016/j.msec.2016.03.025

Logan, S. L., Dudley, C., Baker, R. P., Taormina, M. J., Hay, E. A., & Parthasarathy, R. (2018). Automated high-throughput light-sheet fluorescence microscopy of larval zebrafish. *PLoS ONE*, *13*(11). https://doi.org/10.1371/JOURNAL.PONE.0198705

Lőrincz, T., Deák, V., Makk-Merczel, K., Varga, D., Hajdinák, P., & Szarka, A. (2021). The Performance of HepG2 and HepaRG Systems through the Glass of Acetaminophen-Induced Toxicity. *Life*,

11(8). https://doi.org/10.3390/LIFE11080856

Luckert, C., Schulz, C., Lehmann, N., Thomas, M., Hofmann, U., Hammad, S., Hengstler, J. G., Braeuning, A., Lampen, A., & Hessel, S. (2017). Comparative analysis of 3D culture methods on human HepG2 cells. *Archives of Toxicology*, *91*(1), 393–406. https://doi.org/10.1007/s00204-016-1677-z

Mandon, M., Huet, S., Dubreil, E., Fessard, V., & Le Hégarat, L. (2019). Three-dimensional HepaRG spheroids as a liver model to study human genotoxicity in vitro with the single cell gel electrophoresis assay. *Scientific Reports 2019 9:1*, *9*(1), 1–9. https://doi.org/10.1038/s41598-019-47114-7

Maruyama, M., Matsunaga, T., Harada, E., & Ohmori, S. (2007). Comparison of basal gene expression and induction of CYP3As in HepG2 and human fetal liver cells. *Biological & Pharmaceutical Bulletin*, *30*(11), 2091–2097. https://doi.org/10.1248/BPB.30.2091

Marzi, J., Fuhrmann, E., Brauchle, E., Singer, V., Pfannstiel, J., Schmidt, I., & Hartmann, H. (2022). Non-Invasive Three-Dimensional Cell Analysis in Bioinks by Raman Imaging. *ACS Applied Materials & Interfaces*, *14*(27), 30455–30465. https://doi.org/10.1021/ACSAMI.1C24463

Medine, C. N., Lucendo-Villarin, B., Storck, C., Wang, F., Szkolnicka, D., Khan, F., Pernagallo, S., Black, J. R., Marriage, H. M., Ross, J. A., Bradley, M., Iredale, J. P., Flint, O., & Hay, D. C. (2013). Developing high-fidelity hepatotoxicity models from pluripotent stem cells. *Stem Cells Translational Medicine*, *2*(7), 505–509. https://doi.org/10.5966/SCTM.2012-0138

Mehesz, A. N., Brown, J., Hajdu, Z., Beaver, W., da Silva, J. V. L., Visconti, R. P., Markwald, R. R., & Mironov, V. (2011). Scalable robotic biofabrication of tissue spheroids. *Biofabrication*, *3*(2), 025002. https://doi.org/10.1088/1758-5082/3/2/025002

Messner, S., Agarkova, I., Moritz, W., & Kelm, J. M. (2013). Multi-cell type human liver microtissues for hepatotoxicity testing. *Archives of Toxicology*, *87*(1), 209–213. https://doi.org/10.1007/S00204-012-0968-2

Messner, Simon, Fredriksson, L., Lauschke, V. M., Roessger, K., Escher, C., Bober, M., Kelm, J. M., Ingelman-Sundberg, M., & Moritz, W. (2018). Transcriptomic, Proteomic, and Functional Long-Term Characterization of Multicellular Three-Dimensional Human Liver Microtissues. *Applied In Vitro Toxicology*, *4*(1), 1–12. https://doi.org/10.1089/aivt.2017.0022

Miller, D. R., Jarrett, J. W., Hassan, A. M., & Dunn, A. K. (2017). Deep Tissue Imaging with Multiphoton Fluorescence Microscopy. *Current Opinion in Biomedical Engineering*, *4*, 32. https://doi.org/10.1016/J.COBME.2017.09.004

Modulevsky, D. J., Lefebvre, C., Haase, K., Al-Rekabi, Z., & Pelling, A. E. (2014). Apple Derived Cellulose Scaffolds for 3D Mammalian Cell Culture. *PLOS ONE*, *9*(5), e97835. https://doi.org/10.1371/JOURNAL.PONE.0097835

Montesanto, S., Smithers, N. P., Bucchieri, F., Brucato, V., Carrubba, V. La, Davies, D. E., & Conforti, F. (2019). Establishment of a pulmonary epithelial barrier on biodegradable poly-L-lactic-acid membranes. *PLOS ONE*, *14*(1), e0210830. https://doi.org/10.1371/JOURNAL.PONE.0210830

Munaz, A., Vadivelu, R. K., St. John, J., Barton, M., Kamble, H., & Nguyen, N.-T. (2016). Three-dimensional printing of biological matters. *Journal of Science: Advanced Materials and Devices*, *1*(1), 1–17. https://doi.org/10.1016/J.JSAMD.2016.04.001

Murphy, C. M., Haugh, M. G., & O'Brien, F. J. (2010). The effect of mean pore size on cell attachment, proliferation and migration in collagen–glycosaminoglycan scaffolds for bone tissue engineering. *Biomaterials*, *31*(3), 461–466.

https://doi.org/10.1016/J.BIOMATERIALS.2009.09.063

Nahmias, Y., Schwartz, R. E., Hu, W.-S., Verfaillie, C. M., & Odde, D. J. (2006). Endothelium-Mediated Hepatocyte Recruitment in the Establishment of Liver-like Tissue *In Vitro*. *Tissue Engineering*, *12*(6), 1627–1638. https://doi.org/10.1089/ten.2006.12.1627

Nature methods. (2015). Method of the Year 2014. In *Nature methods* (Vol. 12, Issue 1, p. 1). Nature Publishing Group. https://doi.org/10.1038/nmeth.3251

Norris, W., Paredes, A. H., & Lewis, J. H. (2008). Drug-induced liver injury in 2007. *Current Opinion in Gastroenterology*, *24*(3), 287–297. https://doi.org/10.1097/MOG.0B013E3282F9764B

Novik, E., Maguire, T. J., Chao, P., Cheng, K. C., & Yarmush, M. L. (2010). A microfluidic hepatic coculture platform for cell-based drug metabolism studies. *Biochemical Pharmacology*, *79*(7), 1036. https://doi.org/10.1016/J.BCP.2009.11.010

Ogihara, T., Arakawa, H., Jomura, T., Idota, Y., Koyama, S., Yano, K., & Kojima, H. (2017a). Utility of human hepatocyte spheroids without feeder cells for evaluation of hepatotoxicity. In *Journal of Toxicological Sciences* (Vol. 42, Issue 4, pp. 499–507). https://doi.org/10.2131/jts.42.499

Ogihara, T., Arakawa, H., Jomura, T., Idota, Y., Koyama, S., Yano, K., & Kojima, H. (2017b). Utility of human hepatocyte spheroids without feeder cells for evaluation of hepatotoxicity. *JOURNAL OF TOXICOLOGICAL SCIENCES*, *42*(4), 499–507. https://doi.org/10.2131/jts.42.499

Olsen, A. K., & Whalen, M. D. (2009). Public perceptions of the pharmaceutical industry and drug safety: implications for the pharmacovigilance professional and the culture of safety. *Drug Safety*, *32*(10), 805–810. https://doi.org/10.2165/11316620-000000000-00000

Ott, L. M., Ramachandran, K., & Stehno-Bittel, L. (2017). An Automated Multiplexed Hepatotoxicity and CYP Induction Assay Using HepaRG Cells in 2D and 3D. *SLAS DISCOVERY: Advancing Life Sciences R&D*, *22*(5), 614–625. https://doi.org/10.1177/2472555217701058

Ou, D. L., Shen, Y. C., Yu, S. L., Chen, K. F., Yeh, P. Y., Fan, H. H., Feng, W. C., Wang, C. T., Lin, L. I., Hsu, C., & Cheng, A. L. (2010). Induction of DNA damage-inducible gene GADD45beta contributes to sorafenib-induced apoptosis in hepatocellular carcinoma cells. *Cancer Research*, *70*(22), 9309–9318. https://doi.org/10.1158/0008-5472.CAN-10-1033

Ounkomol, C., Seshamani, S., Maleckar, M. M., Collman, F., & Johnson, G. R. (2018). Label-free prediction of three-dimensional fluorescence images from transmitted-light microscopy. *Nature Methods*, *15*(11), 917–920. https://doi.org/10.1038/s41592-018-0111-2

Paul, J. (1970). Cell and tissue culture. In *Cell and tissue culture.* (Issue 4th Edition). London: E. & S. Livingstone Ltd. https://www.cabdirect.org/cabdirect/abstract/19712701883

Paul, John. (1970). *Cell and tissue culture*. 430. https://books.google.com/books/about/Cell_and_Tissue_Culture.html?id=zFlIAAAAMAAJ

Paulsen, S. J., & Miller, J. S. (2015). Tissue vascularization through 3D printing: Will technology bring us flow? *Developmental Dynamics*, *244*(5), 629–640. https://doi.org/10.1002/DVDY.24254

Pelham, R. J., & Wang, Y. (1997). Cell locomotion and focal adhesions are regulated by substrate flexibility. *Proceedings of the National Academy of Sciences*, *94*(25), 13661–13665. https://doi.org/10.1073/PNAS.94.25.13661

Phelps, E. A., Enemchukwu, N. O., Fiore, V. F., Sy, J. C., Murthy, N., Sulchek, T. A., Barker, T. H., & García, A. J. (2012). Maleimide Cross-Linked Bioactive PEG Hydrogel Exhibits Improved Reaction Kinetics and Cross-Linking for Cell Encapsulation and In Situ Delivery. *Advanced Materials*, *24*(1), 64–70. https://doi.org/10.1002/adma.201103574

Pineda, E. T., Nerem, R. M., & Ahsan, T. (2013). Differentiation patterns of embryonic stem cells in two- versus three-dimensional culture. *Cells, Tissues, Organs*, *197*(5), 399–410. https://doi.org/10.1159/000346166

Pitaktong, I., Lui, C., Lowenthal, J., Mattson, G., Jung, W. H., Bai, Y., Yeung, E., Ong, C. S., Chen, Y., Gerecht, S., & Hibino, N. (2020). Early Vascular Cells Improve Microvascularization Within 3D Cardiac Spheroids. *Tissue Engineering - Part C: Methods*, *26*(2), 80–90. https://doi.org/10.1089/TEN.TEC.2019.0228/ASSET/IMAGES/LARGE/TEN.TEC.2019.0228_FIGURE4.JPEG

Polonchuk, L., Chabria, M., Badi, L., Hoflack, J. C., Figtree, G., Davies, M. J., & Gentile, C. (2017). Cardiac spheroids as promising in vitro models to study the human heart microenvironment. *Scientific Reports*, *7*(1), 1–12. https://doi.org/10.1038/s41598-017-06385-8

Preibisch, S., Amat, F., Stamataki, E., Sarov, M., Singer, R. H., Myers, E., & Tomancak, P. (2014). Efficient Bayesian-based multiview deconvolution. *Nature Methods 2014 11:6*, *11*(6), 645–648. https://doi.org/10.1038/nmeth.2929

Preibisch, S., Saalfeld, S., Schindelin, J., & Tomancak, P. (2010). Software for bead-based registration of selective plane illumination microscopy data. *Nature Methods 2010 7:6*, *7*(6), 418–419. https://doi.org/10.1038/nmeth0610-418

Proctor, W. R., Foster, A. J., Vogt, J., Summers, C., Middleton, B., Pilling, M. A., Shienson, D., Kijanska, M., Stroebel, S., Kelm, J. M., Morgan, P., Messner, S., & Williams, D. (2017). Utility of spherical human liver microtissues for prediction of clinical drug-induced liver injury. *ARCHIVES OF TOXICOLOGY*, *91*(8), 2849–2863. https://doi.org/10.1007/s00204-017-2002-1

Promega. (2022). *CellTiter-Glo® 3D Cell Viability Assay | 3D Cell Culture*. https://www.promega.co.uk/products/cell-health-assays/cell-viability-and-cytotoxicity-assays/celltiter-glo-3d-cell-viability-assay/?catNum=G9681&gclid=CjwKCAjw6raYBhB7EiwABge5KvC1d1YNEzYbQfDa-H3Uh_Jjlc72nBKIq9QbNN4Jdh3Ap5HO79TG9RoCY1EQAvD_BwE

ProteinSimple. (2023). *Jess - Chemiluminescent & Fluorescent Western Blotting*. https://www.bio-techne.com/p/simple-western/jess_004-650

Pruksakorn, D., Lirdprapamongkol, K., Chokchaichamnankit, D., Subhasitanont, P., Chiablaem, K., Svasti, J., & Srisomsap, C. (2010). Metabolic alteration of HepG2 in scaffold-based 3-D culture: Proteomic approach. *Proteomics*, *10*(21), 3896–3904. https://doi.org/10.1002/pmic.201000137

Qiao, S., Feng, S., Wu, Z., He, T., Ma, C., Peng, Z., Tian, E., & Pan, G. (2021). Functional Proliferating Human Hepatocytes: In Vitro Hepatocyte Model for Drug Metabolism, Excretion, and Toxicity. *Drug Metabolism and Disposition*, *49*(4), 305–313. https://doi.org/10.1124/DMD.120.000275

Raghavan, S., Mehta, P., Horst, E. N., Ward, M. R., Rowley, K. R., & Mehta, G. (2016). Comparative analysis of tumor spheroid generation techniques for differential in vitro drug toxicity. *Oncotarget*, *7*(13), 16948–16961. https://doi.org/10.18632/oncotarget.7659

Rajendran, D., Hussain, A., Yip, D., Parekh, A., Shrirao, A., & Cho, C. H. (2017). Long-term liver-specific functions of hepatocytes in electrospun chitosan nanofiber scaffolds coated with fibronectin. *Journal of Biomedical Materials Research Part A*, *105*(8), 2119–2128. https://doi.org/10.1002/jbm.a.36072

Ramaiahgari, S. C., Den Braver, M. W., Herpers, B., Terpstra, V., Commandeur, J. N. M., Van De Water, B., & Price, L. S. (2014). A 3D in vitro model of differentiated HepG2 cell spheroids with improved liver-like properties for repeated dose high-throughput toxicity studies. *Archives of*

Toxicology, *88*(5), 1083–1095. https://doi.org/10.1007/S00204-014-1215-9

Reis, L. A., Chiu, L. L. Y., Liang, Y., Hyunh, K., Momen, A., & Radisic, M. (2012). A peptide-modified chitosan–collagen hydrogel for cardiac cell culture and delivery. *Acta Biomaterialia*, *8*(3), 1022–1036. https://doi.org/10.1016/J.ACTBIO.2011.11.030

Riss, T. L., Moravec, R. A., Niles, A. L., Duellman, S., Benink, H. A., Worzella, T. J., & Minor, L. (2016). Cell Viability Assays. *Assay Guidance Manual*. https://www.ncbi.nlm.nih.gov/books/NBK144065/

Riss, T., & Trask, O. J. (2021). Factors to consider when interrogating 3D culture models with plate readers or automated microscopes. *In Vitro Cellular and Developmental Biology - Animal*, *57*(2), 238–256. https://doi.org/10.1007/S11626-020-00537-3/FIGURES/10

Ruoß, M., Häussling, V., Schügner, F., Damink, L. H. H. O., Lee, S. M. L., Ge, L., Ehnert, S., & Nussler, A. K. (2018). A Standardized Collagen-Based Scaffold Improves Human Hepatocyte Shipment and Allows Metabolic Studies over 10 Days. *Bioengineering*, *5*(4). https://doi.org/10.3390/BIOENGINEERING5040086

Ruoß, M., Kieber, V., Rebholz, S., Linnemann, C., Rinderknecht, H., Häussling, V., Häcker, M., Damink, L. H. H. O., Ehnert, S., & Nussler, A. K. (2019). Cell-Type-Specific Quantification of a Scaffold-Based 3D Liver Co-Culture. *Methods and Protocols 2020, Vol. 3, Page 1*, *3*(1), 1. https://doi.org/10.3390/MPS3010001

Salerno, A., Guarnieri, D., Iannone, M., Zeppetelli, S., & Netti, P. A. (2010). Effect of Micro- and Macroporosity of Bone Tissue Three-Dimensional-Poly(ε-Caprolactone) Scaffold on Human Mesenchymal Stem Cells Invasion, Proliferation, and Differentiation *In Vitro*. *Tissue Engineering Part A*, *16*(8), 2661–2673. https://doi.org/10.1089/ten.tea.2009.0494

Samimi, H., Sohi, A. N., Irani, S., Arefian, E., Mahdiannasser, M., Fallah, P., & Haghpanah, V. (2021). Alginate-based 3D cell culture technique to evaluate the half-maximal inhibitory concentration: an in vitro model of anticancer drug study for anaplastic thyroid carcinoma. *Thyroid Research*, *14*(1), 1–9. https://doi.org/10.1186/S13044-021-00118-W/FIGURES/5

Sampaziotis, F., Segeritz, C. P., & Vallier, L. (2015). Potential of human induced pluripotent stem cells in studies of liver disease. *Hepatology (Baltimore, Md.)*, *62*(1), 303–311. https://doi.org/10.1002/HEP.27651

Sarkar, J., Kumari, J., Tonello, J. M., Kamihira, M., & Kumar, A. (2017a). Enhanced Hepatic Functions of Genetically Modified Mouse Hepatoma Cells by Spheroid Culture for Drug Toxicity Screening. *Biotechnology Journal*, *12*(10), 1700274. https://doi.org/10.1002/biot.201700274

Sarkar, J., Kumari, J., Tonello, J. M., Kamihira, M., & Kumar, A. (2017b). Enhanced Hepatic Functions of Genetically Modified Mouse Hepatoma Cells by Spheroid Culture for Drug Toxicity Screening. *Biotechnology Journal*, *12*(10). https://doi.org/10.1002/BIOT.201700274

Sato, T., Vries, R. G., Snippert, H. J., Van De Wetering, M., Barker, N., Stange, D. E., Van Es, J. H., Abo, A., Kujala, P., Peters, P. J., & Clevers, H. (2009). Single Lgr5 stem cells build crypt-villus structures in vitro without a mesenchymal niche. *Nature*, *459*(7244), 262–265. https://doi.org/10.1038/NATURE07935

Schutte, M., Fox, B., Baradez, M. O., Devonshire, A., Minguez, J., Bokhari, M., Przyborski, S., & Marshall, D. (2011). Rat primary hepatocytes show enhanced performance and sensitivity to acetaminophen during three-dimensional culture on a polystyrene scaffold designed for routine use. *Assay and Drug Development Technologies*, *9*(5), 475–486. https://doi.org/10.1089/ADT.2011.0371/ASSET/IMAGES/LARGE/FIGURE7.JPEG

Sellaro, T. L., Ranade, A., Faulk, D. M., McCabe, G. P., Dorko, K., Badylak, S. F., & Strom, S. C. (2010). Maintenance of human hepatocyte function in vitro by liver-derived extracellular matrix gels. *Tissue Engineering - Part A*, *16*(3), 1075–1082. https://doi.org/10.1089/ten.tea.2008.0587

Seo, J. E., Tryndyak, V., Wu, Q., Dreval, K., Pogribny, I., Bryant, M., Zhou, T., Robison, T. W., Mei, N., & Guo, X. (2019). Quantitative comparison of in vitro genotoxicity between metabolically competent HepaRG cells and HepG2 cells using the high-throughput high-content CometChip assay. *Archives of Toxicology*, *93*(5), 1433–1448. https://doi.org/10.1007/S00204-019-02406-9/FIGURES/5

Serras, A. S., Rodrigues, J. S., Cipriano, M., Rodrigues, A. V., Oliveira, N. G., & Miranda, J. P. (2021). A Critical Perspective on 3D Liver Models for Drug Metabolism and Toxicology Studies. *Frontiers in Cell and Developmental Biology*, *9*, 203. https://doi.org/10.3389/FCELL.2021.626805/BIBTEX

Shah, U. K., Mallia, J. de O., Singh, N., Chapman, K. E., Doak, S. H., & Jenkins, G. J. S. (2018). A three-dimensional in vitro HepG2 cells liver spheroid model for genotoxicity studies. *Mutation Research - Genetic Toxicology and Environmental Mutagenesis*, *825*, 51–58. https://doi.org/10.1016/j.mrgentox.2017.12.005

Shanbhag, S., Woolee, J., & Kotov, N. (2005). Diffusion in three-dimensionally ordered scaffolds with inverted colloidal crystal geometry. *Biomaterials*, *26*(27), 5581–5585. https://doi.org/10.1016/j.biomaterials.2005.01.059

Shearer, T., Bradley, R. S., Hidalgo-Bastida, L. A., Sherratt, M. J., & Cartmell, S. H. (2016). Three-dimensional visualisation of soft biological structures by X-ray computed micro-tomography. In *Journal of Cell Science* (Vol. 129, Issue 13, pp. 2483–2492). https://doi.org/10.1242/jcs.179077

Shen, H., Cai, S., Wu, C., Yang, W., Yu, H., & Liu, L. (2021). Recent Advances in Three-Dimensional Multicellular Spheroid Culture and Future Development. *Micromachines*, *12*(1), 1–21. https://doi.org/10.3390/MI12010096

Shin, D.-S., Seo, H., Yang, J. Y., Joo, J., Im, S. H., Kim, S. S., Kim, S. K., & Bae, M. A. (2018). Quantitative Evaluation of Cytochrome P450 3A4 Inhibition and Hepatotoxicity in HepaRG 3-D Spheroids. *International Journal of Toxicology*, *37*(5), 393–403. https://doi.org/10.1177/1091581818780149

Shinozawa, T., Kimura, M., Cai, Y., Saiki, N., Yoneyama, Y., Ouchi, R., Koike, H., Maezawa, M., Zhang, R. R., Dunn, A., Ferguson, A., Togo, S., Lewis, K., Thompson, W. L., Asai, A., & Takebe, T. (2021). High-Fidelity Drug-Induced Liver Injury Screen Using Human Pluripotent Stem Cell-Derived Organoids. *Gastroenterology*, *160*(3), 831–846. https://doi.org/10.1053/J.GASTRO.2020.10.002

Sibulesky, L. (2013). Normal liver anatomy. *Clinical Liver Disease*, *2*(S1), S1–S3. https://doi.org/10.1002/CLD.124

Simian, M., & Bissell, M. J. (2017). Organoids: A historical perspective of thinking in three dimensions. *Journal of Cell Biology*, *216*(1), 31–40. https://doi.org/10.1083/jcb.201610056

Sirenko, O., Hancock, M. K., Hesley, J., Hong, D., Cohen, A., Gentry, J., Carlson, C. B., & Mann, D. A. (2016). Phenotypic characterization of toxic compound effects on liver spheroids derived from ipsc using confocal imaging and three-dimensional image analysis. *Assay and Drug Development Technologies*, *14*(7), 381–394. https://doi.org/10.1089/adt.2016.729

Sirenko, O., Mitlo, T., Hesley, J., Luke, S., Owens, W., & Cromwell, E. F. (2015). High-Content Assays for Characterizing the Viability and Morphology of 3D Cancer Spheroid Cultures. *Assay and Drug Development Technologies*, *13*(7), 402–414. https://doi.org/10.1089/adt.2015.655

Soldatow, V. Y., Lecluyse, E. L., Griffith, L. G., & Rusyn, I. (2013). In vitro models for liver toxicity

testing. In *Toxicology Research* (Vol. 2, Issue 1, pp. 23–39). https://doi.org/10.1039/c2tx20051a

Štampar, M., Breznik, B., Filipič, M., & Žegura, B. (2020). Characterization of In Vitro 3D Cell Model Developed from Human Hepatocellular Carcinoma (HepG2) Cell Line. *Cells 2020, Vol. 9, Page 2557*, *9*(12), 2557. https://doi.org/10.3390/CELLS9122557

Stanley, L. A., & Wolf, C. R. (2022). Through a glass, darkly? HepaRG and HepG2 cells as models of human phase I drug metabolism. *Https://Doi.Org/10.1080/03602532.2022.2039688*, *54*(1), 46–62. https://doi.org/10.1080/03602532.2022.2039688

Stefaniuk, M., Gualda, E. J., Pawlowska, M., Legutko, D., Matryba, P., Koza, P., Konopka, W., Owczarek, D., Wawrzyniak, M., Loza-Alvarez, P., & Kaczmarek, L. (2016). Light-sheet microscopy imaging of a whole cleared rat brain with Thy1-GFP transgene. *Scientific Reports 2016 6:1*, *6*(1), 1–9. https://doi.org/10.1038/srep28209

Strowitzki, M. J., Cummins, E. P., & Taylor, C. T. (2019). Protein Hydroxylation by Hypoxia-Inducible Factor (HIF) Hydroxylases: Unique or Ubiquitous? *Cells*, *8*(5). https://doi.org/10.3390/CELLS8050384

Suparna, S. (2014). 3D culture: Culture and Assay Systems Used for 3D Cell Culture. *Corning*, *9*, 1–18.

Suzuki, T., Higgins, P. J., & Crawford, D. R. (2000). Control Selection for RNA Quantitation. *BioTechniques*, *29*(2), 332–337. https://doi.org/10.2144/00292rv02

Takahashi, Y., Hori, Y., Yamamoto, T., Urashima, T., Ohara, Y., & Tanaka, H. (2015a). 3D spheroid cultures improve the metabolic gene expression profiles of HepaRG cells. *Bioscience Reports*, *35*(3), 1–7. https://doi.org/10.1042/BSR20150034

Takahashi, Y., Hori, Y., Yamamoto, T., Urashima, T., Ohara, Y., & Tanaka, H. (2015b). 3D spheroid cultures improve the metabolic gene expression profiles of HepaRG cells. *Bioscience Reports*, *35*(3), 1–7. https://doi.org/10.1042/BSR20150034

Takayama, K., Morisaki, Y., Kuno, S., Nagamoto, Y., Harada, K., Furukawa, N., Ohtaka, M., Nishimura, K., Imagawa, K., Sakurai, F., Tachibana, M., Sumazaki, R., Noguchi, E., Nakanishi, M., Hirata, K., Kawabata, K., & Mizuguchi, H. (2014). Prediction of interindividual differences in hepatic functions and drug sensitivity by using human iPS-derived hepatocytes. *Proceedings of the National Academy of Sciences of the United States of America*, *111*(47), 16772–16777. https://doi.org/10.1073/PNAS.1413481111/SUPPL_FILE/PNAS.1413481111.SAPP.PDF

Tasnim, F., Toh, Y. C., Qu, Y., Li, H., Phan, D., Narmada, B. C., Ananthanarayanan, A., Mittal, N., Meng, R. Q., & Yu, H. (2016). Functionally Enhanced Human Stem Cell Derived Hepatocytes in Galactosylated Cellulosic Sponges for Hepatotoxicity Testing. *Molecular Pharmaceutics*, *13*(6), 1947–1957. https://doi.org/10.1021/acs.molpharmaceut.6b00119

Temple, J., Velliou, E., Shehata, M., & Lévy, R. (2022). Current strategies with implementation of three-dimensional cell culture: the challenge of quantification. *Interface Focus*, *12*(5). https://doi.org/10.1098/RSFS.2022.0019

Thyng, F. W. (1914). The anatomy of a 17.8 mm. human embryo. *American Journal of Anatomy*, *17*(1), 31–112. https://doi.org/10.1002/aja.1000170103

Tong, J. Z., Bernard, O., & Alvarez, F. (1990). Long-term culture of rat liver cell spheroids in hormonally defined media. *Experimental Cell Research*, *189*(1), 87–92. https://doi.org/10.1016/0014-4827(90)90260-H

Tostões, R. M., Leite, S. B., Serra, M., Jensen, J., Björquist, P., Carrondo, M. J. T., Brito, C., & Alves, P. M. (2012). Human liver cell spheroids in extended perfusion bioreactor culture for repeated-

dose drug testing. *Hepatology (Baltimore, Md.)*, *55*(4), 1227–1236. https://doi.org/10.1002/HEP.24760

Totti, S., Allenby, M. C., Dos Santos, S. B., Mantalaris, A., & Velliou, E. G. (2018). A 3D bioinspired highly porous polymeric scaffolding system for: In vitro simulation of pancreatic ductal adenocarcinoma. *RSC Advances*, *8*(37), 20928–20940. https://doi.org/10.1039/c8ra02633e

Totti, S., Vernardis, S. I., Meira, L., Pérez-Mancera, P. A., Costello, E., Greenhalf, W., Palmer, D., Neoptolemos, J., Mantalaris, A., & Velliou, E. G. (2017). Designing a bio-inspired biomimetic in vitro system for the optimization of ex vivo studies of pancreatic cancer. In *Drug Discovery Today* (Vol. 22, Issue 4, pp. 690–701). Elsevier Ltd. https://doi.org/10.1016/j.drudis.2017.01.012

Tung, Y.-C., Hsiao, A. Y., Allen, S. G., Torisawa, Y., Ho, M., & Takayama, S. (2011). High-throughput 3D spheroid culture and drug testing using a 384 hanging drop array. *The Analyst*, *136*(3), 473–478. https://doi.org/10.1039/C0AN00609B

Underhill, G. H., & Khetani, S. R. (2018). Advances in Engineered Human Liver Platforms for Drug Metabolism Studies. *DRUG METABOLISM AND DISPOSITION*, *46*(11), 1626–1637. https://doi.org/10.1124/dmd.118.083295

Usui, H., Nishiwaki, A., Landiev, L., Kacza, J., Eichler, W., Wako, R., Kato, A., Takase, N., Kuwayama, S., Ohashi, K., Yafai, Y., Bringmann, A., Kubota, A., Ogura, Y., Seeger, J., Wiedemann, P., & Yasukawa, T. (2018). *In vitro drusen model-three-dimensional spheroid culture of retinal pigment epithelial cells*. https://doi.org/10.1242/jcs.215798

van Neerven, S. M., de Groot, N. E., Nijman, L. E., Scicluna, B. P., van Driel, M. S., Lecca, M. C., Warmerdam, D. O., Kakkar, V., Moreno, L. F., Vieira Braga, F. A., Sanches, D. R., Ramesh, P., ten Hoorn, S., Aelvoet, A. S., van Boxel, M. F., Koens, L., Krawczyk, P. M., Koster, J., Dekker, E., … Vermeulen, L. (2021). Apc-mutant cells act as supercompetitors in intestinal tumour initiation. *Nature 2021 594:7863*, *594*(7863), 436–441. https://doi.org/10.1038/s41586-021-03558-4

Vantage Market Research. (2021). *3D Cell Culture Market Size USD 2,051.5 Million by 2028*. https://www.vantagemarketresearch.com/industry-report/3d-cell-culture-market-1286

Verhertbruggen, Y., Walker, J. L., Guillon, F., & Scheller, H. V. (2017). A comparative study of sample preparation for staining and immunodetection of plant cell walls by light microscopy. *Frontiers in Plant Science*, *8*. https://doi.org/10.3389/fpls.2017.01505

Vorrink, S. U., Zhou, Y., Ingelman-Sundberg, M., & Lauschke, V. M. (2018). Prediction of Drug-Induced Hepatotoxicity Using Long-Term Stable Primary Hepatic 3D Spheroid Cultures in Chemically Defined Conditions. *Toxicological Sciences : An Official Journal of the Society of Toxicology*, *163*(2), 655–665. https://doi.org/10.1093/TOXSCI/KFY058

Vu, L. T., Orbach, S. M., Ray, W. K., Cassin, M. E., Rajagopalan, P., & Helm, R. F. (2016). The hepatocyte proteome in organotypic rat liver models and the influence of the local microenvironment. *Proteome Science*, *15*(1), 12. https://doi.org/10.1186/s12953-017-0120-6

Walker, M., Rizzuto, P., Godin, M., & Pelling, A. E. (2020). Structural and mechanical remodeling of the cytoskeleton maintains tensional homeostasis in 3D microtissues under acute dynamic stretch. *Scientific Reports*, *10*(1), 7696. https://doi.org/10.1038/s41598-020-64725-7

Wang, J., Chen, F., Liu, L., Qi, C., Wang, B., Yan, X., Huang, C., Hou, W., Zhang, M. Q., Chen, Y., & Du, Y. (2016). Engineering EMT using 3D micro-scaffold to promote hepatic functions for drug hepatotoxicity evaluation. *Biomaterials*, *91*, 11–22. https://doi.org/10.1016/j.biomaterials.2016.03.001

Wang, Yan, Kim, M. H., Shirahama, H., Lee, J. H., Ng, S. S., Glenn, J. S., & Cho, N. J. (2016). ECM proteins in a microporous scaffold influence hepatocyte morphology, function, and gene expression. *Scientific Reports*, *6*. https://doi.org/10.1038/SREP37427

Wang, Yaqing, Su, W., Wang, L., Jiang, L., Liu, Y., Hui, L., & Qin, J. (2018a). Paper supported long-term 3D liver co-culture model for the assessment of hepatotoxic drugs. *Toxicology Research*, *7*(1), 13–21. https://doi.org/10.1039/C7TX00209B

Wang, Yaqing, Su, W., Wang, L., Jiang, L., Liu, Y., Hui, L., & Qin, J. (2018b). Paper supported long-term 3D liver co-culture model for the assessment of hepatotoxic drugs. *Toxicology Research*, *7*(1), 13–21. https://doi.org/10.1039/C7TX00209B

Wang, Z., Luo, X., Anene-Nzelu, C., Yu, Y., Hong, X., Singh, N. H., Xia, L., Liu, S., & Yu, H. (2015). HepaRG culture in tethered spheroids as an in vitro three-dimensional model for drug safety screening. *JOURNAL OF APPLIED TOXICOLOGY*, *35*(8), 909–917. https://doi.org/10.1002/jat.3090

Wardwell-Swanson, J., Greve, F., & Frey, O. (2021). *Three PRACTICAL STEPS to transform 3D cell culture White Paper What does it take to achieve high-quality results with in vitro 3D cell culture experiments?*

Ware, B. R., Liu, J. S., Monckton, C. P., Ballinger, K. R., & Khetani, S. R. (2021). Micropatterned Coculture With 3T3-J2 Fibroblasts Enhances Hepatic Functions and Drug Screening Utility of HepaRG Cells. *Toxicological Sciences*, *181*(1), 90–104. https://doi.org/10.1093/TOXSCI/KFAB018

Wen, J. H., Vincent, L. G., Fuhrmann, A., Choi, Y. S., Hribar, K. C., Taylor-Weiner, H., Chen, S., & Engler, A. J. (2014). Interplay of matrix stiffness and protein tethering in stem cell differentiation. *Nature Materials*, *13*(10), 979–987. https://doi.org/10.1038/nmat4051

Westerink, W. M. A., & Schoonen, W. G. E. J. (2007). Cytochrome P450 enzyme levels in HepG2 cells and cryopreserved primary human hepatocytes and their induction in HepG2 cells. *Toxicology in Vitro*, *21*(8), 1581–1591. https://doi.org/10.1016/J.TIV.2007.05.014

Wheeler, M. D. (2003). Endotoxin and kupffer cell activation in alcoholic liver disease. In *Alcohol Research and Health* (Vol. 27, Issue 4, pp. 300–306).

Wishart, G., Gupta, P., Schettino, G., Nisbet, A., & Velliou, E. (2021). 3d tissue models as tools for radiotherapy screening for pancreatic cancer. *British Journal of Radiology*, *94*(1120), 20201397. https://doi.org/10.1259/BJR.20201397

Wong, M. W., Pridgeon, C. S., Schlott, C., Park, B. K., & Goldring, C. E. P. (2018). Status and use of induced pluripotent stem cells (iPSCs) in toxicity testing. *Methods in Pharmacology and Toxicology*, *9781493976768*, 199–212. https://doi.org/10.1007/978-1-4939-7677-5_10/FIGURES/2

Wu, L., Ferracci, G., Wang, Y., Fan, T. F., Cho, N.-J., & Chow, P. K. H. (2019a). Porcine hepatocytes culture on biofunctionalized 3D inverted colloidal crystal scaffolds as an in vitro model for predicting drug hepatotoxicity. *RSC ADVANCES*, *9*(31), 17995–18007. https://doi.org/10.1039/c9ra03225h

Wu, L., Ferracci, G., Wang, Y., Fan, T. F., Cho, N.-J., & Chow, P. K. H. (2019b). Porcine hepatocytes culture on biofunctionalized 3D inverted colloidal crystal scaffolds as an *in vitro* model for predicting drug hepatotoxicity. *RSC Advances*, *9*(31), 17995–18007. https://doi.org/10.1039/C9RA03225H

Wu, Y., Geng, X. chao, Wang, J. feng, Miao, Y. fa, Lu, Y. li, & Li, B. (2016). The HepaRG cell line, a superior in vitro model to L-02, HepG2 and hiHeps cell lines for assessing drug-induced liver

injury. *Cell Biology and Toxicology*, *32*(1), 37–59. https://doi.org/10.1007/S10565-016-9316-2

Xu, J. J., Henstock, P. V., Dunn, M. C., Smith, A. R., Chabot, J. R., & de Graaf, D. (2008). Cellular imaging predictions of clinical drug-induced liver injury. *Toxicological Sciences : An Official Journal of the Society of Toxicology*, *105*(1), 97–105. https://doi.org/10.1093/TOXSCI/KFN109

Yan, S., Wei, J., Liu, Y., Zhang, H., Chen, J., & Li, X. (2015). Hepatocyte spheroid culture on fibrous scaffolds with grafted functional ligands as an in vitro model for predicting drug metabolism and hepatotoxicity. *Acta Biomaterialia*, *28*, 138–148. https://doi.org/10.1016/j.actbio.2015.09.027

Yang, K., Guo, C., Woodhead, J. L., St Claire, R. L., Watkins, P. B., Siler, S. Q., Howell, B. A., & Brouwer, K. L. R. (2016). Sandwich-Cultured Hepatocytes as a Tool to Study Drug Disposition and Drug-Induced Liver Injury. *Journal of Pharmaceutical Sciences*, *105*(2), 443–459. https://doi.org/10.1016/J.XPHS.2015.11.008

You, S., Tu, H., Chaney, E. J., Sun, Y., Zhao, Y., Bower, A. J., Liu, Y. Z., Marjanovic, M., Sinha, S., Pu, Y., & Boppart, S. A. (2018). Intravital imaging by simultaneous label-free autofluorescence-multiharmonic microscopy. *Nature Communications*, *9*(1). https://doi.org/10.1038/s41467-018-04470-8

Zeigerer, A., Wuttke, A., Marsico, G., Seifert, S., Kalaidzidis, Y., & Zerial, M. (2017). Functional properties of hepatocytes in vitro are correlated with cell polarity maintenance. *Experimental Cell Research*, *350*(1), 242–252. https://doi.org/10.1016/J.YEXCR.2016.11.027

Zeiss. (2022). *Light Sheet Microscope to Image Live or Cleared Samples*. https://www.zeiss.com/microscopy/int/products/imaging-systems/light-sheet-microscope-for-lsfm-imaging-of-live-and-cleared-samples-lightsheet-7.html?vaURL=www.zeiss.com/microscopy/int/cmp/lsc/20/light-sheet-microscopy/new-zeiss-lightsheet-7.html&utm_medium

Zhao, Z., & Fairchild, P. W. (1998). Dependence of light transmission through human skin on incident beam diameter at different wavelengths. In S. L. Jacques (Ed.), *Laser-Tissue Interaction IX* (Vol. 3254, p. 354). https://doi.org/10.1117/12.308184

Zhou, Y., Chen, H., Li, H., & Wu, Y. (2017). 3D culture increases pluripotent gene expression in mesenchymal stem cells through relaxation of cytoskeleton tension. *Journal of Cellular and Molecular Medicine*, *21*(6), 1073–1084. https://doi.org/10.1111/jcmm.12946

Zustiak, S. P., Boukari, H., & Leach, J. B. (2010). Solute diffusion and interactions in cross-linked poly(ethylene glycol) hydrogels studied by Fluorescence Correlation Spectroscopy. *Soft Matter*, *6*(15), 3609. https://doi.org/10.1039/c0sm00111b